ICLIAD 65 (4), 403-497, 2024

p-ISSN 0535-5133
e-ISSN 2477-9393

Volumen 65
No. 4
Diciembre
2024

Investigación Clínica

Universidad del Zulia
Facultad de Medicina
Instituto de Investigaciones Clínicas
"Dr. Américo Negrette"
Maracaibo, Venezuela

Investigación Clínica

https://sites.google.com/site/revistainvestigacionesclinicas

Revista arbitrada dedicada a estudios humanos, animales y de laboratorio relacionados con la investigación clínica y asuntos conexos.

La Revista es de Acceso Abierto, publicada trimestralmente por el Instituto de Investigaciones Clínicas "Dr. Américo Negrette", de la Facultad de Medicina, de la Universidad del Zulia, Maracaibo, Venezuela.

Investigación Clínica está indizada en Science Citation Index Expanded (USA), Excerpta Medica/EMBASE y Scopus (Holanda), Tropical Diseases Bulletin y Global Health (UK), Biblioteca Regional de Medicina/BIREME (Brasil), Ulrich's Periodicals, Journal Citation Reports (USA), Index Copernicus (Polonia), SIIEC Data Bases, Sección Iberoamérica (Argentina) e Infobase Index (India), Redalyc y las bases de datos: SciELO (www.Scielo.org.ve), Revencyt, LILACS, LIVECS, PERIODICA y web de LUZ: http://www.produccioncientificaluz.org/revistas

Para cualquier otra información dirigir su correspondencia a:

Dra. Elena Ryder, Editora
Instituto de Investigaciones Clínicas "Dr. Américo Negrette"
Facultad de Medicina, Universidad del Zulia
Maracaibo, Venezuela.

Teléfono:
+58-0414-6305451

Correos electrónicos:
elenaryder@gmail.com
riclinicas@gmail.com

Páginas web:
https://sites.google.com/site/revistainvestigacionesclinicas

http://www.produccioncientificaluz.org/revistas

For any information please address correspondence to:

Dr. Elena Ryder, Editor
Instituto de Investigaciones Clínicas "Dr. Américo Negrette"
Facultad de Medicina, Universidad del Zulia
Maracaibo, Venezuela.

Phone:
+58-0414-6305451

E-mails:
elenaryder@gmail.com
riclinicas@gmail.com

Web pages:
https://sites.google.com/site/revistainvestigacionesclinicas

http://www.produccioncientificaluz.org/revistas

Universidad del Zulia
Publicación auspiciada por el
Vicerrectorado Académico
Serbiluz-CONDES

CODEN: ICLIAD
Versión impresa ISSN: 0535-5133
Depósito legal pp 196002ZU37
Versión electrónica ISSN: 2477-9393 Depósito legal ppi 201502ZU4667

Artes finales:
Lisbeny Valencia
lisbenyvalencia@gmail.com

Invest Clin 65(4): 403 - 405, 2024 https://doi.org/10.54817/IC.v65n4a00

EDITORIAL
Sesenta y cinco aniversario del Instituto de Investigaciones Clínicas "Dr. Américo Negrette". Ícono de la ciencia en el Zulia.

El Instituto de Investigaciones Clínicas "Dr. Américo Negrette", arriba a su LXV aniversario. Esta institución constituye una dependencia de la Facultad de Medicina de la Universidad del Zulia, fundada el 4 de diciembre de 1959, gracias a la iniciativa y constancia de un insigne profesor e investigador, Dr. Américo Negrette, acompañado de un pequeño grupo de entusiastas estudiantes. En esa época no se vislumbraba aún el desarrollo de verdaderas políticas que conllevaran a inculcar la cultura de investigación en la población venezolana. Inicialmente, funcionó como un Departamento de Investigación, que posteriormente, en 1963, se convirtió en Centro de Investigaciones y, finalmente, el 24 de septiembre de 1965, fue elevado a la categoría de Instituto por resolución del Consejo Nacional de Universidades. Desde 1984 ocupa su sede propia y en 1988, por decisión unánime del Consejo Técnico del Instituto, se le asigna el nombre de su fundador el Dr. Américo Negrette, como un merecido homenaje, considerando su exitosa y dilatada trayectoria.

Actualmente, siete secciones son las encargadas de ejecutar los proyectos de investigación enmarcados en las diversas líneas de investigación biomédica básica y aplicada al estudio y resolución de los principales problemas de salud a nivel regional, nacional e internacional; estas secciones son: Bioquímica, Inmunología y Biología Celular, Investigaciones Hematológicas, Neurofarmacología y Neurociencias, Neuroquímica Clínica, Parasitología y Virología.

La extensa productividad científica de este Instituto, se ha visto materializada a través de miles de publicaciones en revistas indexadas y comunicaciones a congresos tanto nacionales como internacionales cuya excelencia ha sido digna de un justo reconocimiento de la comunidad científica. Toda esta actividad científica ha sido producto del esfuerzo, capacitación, dedicación, ética, pasión y altruismo de todo el personal que laboró o que labora en él, conformando un conjunto con un engranaje perfecto para la generación de conocimiento. Desde su creación, esta dependencia universitaria ha contribuido, de manera destacada, al avance de la ciencia en el área de la Biomedicina, no solo a nivel regional y nacional, sino también a nivel internacional, con investigaciones de gran impacto y pertinencia social, que se reflejan tanto en el desarrollo de la región y del país como en el incremento de la calidad de vida de los venezolanos.

En sesenta y cinco años, son innumerables los investigadores que se han formado en el Instituto de Investigaciones Clínicas y que han logrado desarrollar una fructífera carrera profesional, gracias a su talento y preparación. Algunos de ellos, ocupan actualmente o han ocupado, importantes cargos en instituciones universitarias y no universitarias, tanto nacionales como internacionales, y gozan de un notorio reconocimiento mundial. Fiel a sus objetivos y a su misión, nuestra institución constituye un pilar fundamental no solo de la investigación científica, sino también de la docencia de pregrado y postgrado, incluyendo maestrías, especializaciones y doctorados. Asimismo, en lo referente a actividades de extensión hacia la comunidad, brindando atención médica y de laboratorio especializada, de excelente calidad,

oportuna y permanente y sin costo alguno, para favorecer de esta manera a los diversos sectores de la población, especialmente a los de escasos recursos económicos.

El Instituto además cuenta con su órgano de divulgación científica, la Revista Investigación Clínica, cuya primera edición se realizó el 26 de julio de 1960. Esta revista se encuentra registrada en algunos de los índices de referencia internacional más importantes; posee un gran prestigio en Venezuela y renombre a nivel internacional. La frecuencia trimestral y la comprobada calidad de los trabajos que en ella se publican, como consecuencia directa de la minuciosa actuación del Comité Editorial en cuanto a la selección de árbitros idóneos, tanto nacionales como extranjeros, para la revisión de los trabajos, le ha permitido posicionarse como una de las mejores revistas científicas nacionales.

Este año, nuestra celebración aniversaria se tiñe de un matiz especial al coincidir con el centenario del natalicio de su fundador, el Dr. Américo Negrette. Este brillante, pero a la vez, humilde médico e investigador, considerado el pionero de la investigación biomédica en la región, nació en La Cañada de Urdaneta, el día 13 de diciembre de 1924. En sus estudios clínicos iniciales, el Dr. Negrette demostró la presencia del asentamiento más numeroso de pacientes con Corea de Huntington en Venezuela, específicamente en la población de San Francisco. Posteriormente, sus observaciones permitieron el aislamiento del gen relacionado con esta enfermedad por un equipo de investigadores norteamericanos. Su tenaz necesidad de estudiar y tratar de resolver los principales problemas de la región, lo llevó a describir la primera epidemia de Encefalitis Equina Venezolana e introducir por primera vez la terapia antiviral basada en antibióticos como la tetraciclina, concepto muy novedoso para la década de los años setenta. Su labor incansable como investigador, docente y formador de varias generaciones de investigadores, con altos valores éticos y morales, la ejerció hasta los últimos momentos de su vida. Tal actividad fue compartida con otras que realizaba con extrema pasión y destreza, como la autoría de varios libros y poemarios, la pintura artística e incluso con participación destacada en el ámbito deportivo. El principal legado del Dr. Negrette a nuestra ilustre Universidad del Zulia y a la sociedad en general, está plasmado en la creación del Instituto de Investigaciones Clínicas y de la revista Investigación Clínica. Esta gran obra, logró materializarse soslayando múltiples obstáculos, y solo la visión, la persistencia y el ímpetu de su fundador pudieron sentar las bases sólidas para su consolidación. Su obra representó su vida y con vibrante orgullo podemos decir que después de muchos años y de varias tempestades, aún se mantiene y perdurará en el tiempo como su innegable huella imborrable. Todos estos innumerables logros que representan apenas una pequeña muestra de la productividad del Instituto a lo largo de toda su historia, se han desarrollado en medio de un entorno cambiante y de escenarios complejos que hoy en día están enmarcados por una gran incertidumbre que, lamentablemente ha caracterizado al ámbito de la educación superior venezolana. Sin embargo, a pesar de la aciaga situación actual en la que se sumerge nuestra Universidad, debemos ser capaces de estar por encima de las contingencias y proyectarnos con optimismo hacia nuevos rumbos que nos permitan mantener un elevado nivel científico y ético, como siempre se ha caracterizado la investigación realizada en nuestros espacios.

Sesenta y cinco años después de su fundación, el Instituto de Investigaciones Clínicas “Dr. Américo Negrette” brilla con luz propia, una luz que hoy se ha esparcido por decenas de países y que perdurará en el tiempo como una fuente inagotable de sabiduría, convirtiéndose en un ícono de la ciencia en el Zulia y en todos los rincones de Venezuela.

Jesús Alberto Quintero González
ORCID 0000-0001-5677-8821

Sixty-fifth anniversary of the Instituto de Investigaciones Clínicas "Dr. Américo Negrette". Icon of science in Zulia.

The Instituto de Investigaciones Clínicas "Dr. Américo Negrette", created on December 4, 1959, reaches its 65th anniversary, a celebration with a particular nuance coinciding with the centenary of the birth of its founder, Dr. Américo Negrette. This distinguished but humble doctor, professor and researcher, considered the pioneer of Biomedical research in the Zulia region, managed to consolidate his work, and over the years, the Institute has become an obligatory reference in many areas of scientific work. Its contribution to the development of science in Biomedicine, both regionally and nationally, has been its primary mission. Thousands of publications and communications to national and international conferences support its scientific productivity. Several generations of national researchers have been trained in this institution following the ideals and principles instilled by its founder. The main legacy of Dr. Negrette to the University of Zulia and society is embodied in the creation of the Instituto de Investigaciones Clínicas and the journal Investigación Clínica. Sixty-five years after its founding, this university department shines with its own light, a light that has now spread to dozens of countries and will endure over time as an inexhaustible source of wisdom, establishing itself as a true icon of science in Zulia and every corner of Venezuela.

Invest Clin 65(4): 406 - 417, 2024 https://doi.org/10.54817/IC.v65n4a01

Rehabilitation training effect guided by cardiopulmonary fitness assessment on NT-proBNP levels in patients with chronic heart failure.

Huamei Yang

Department of Cardiovascular, Lujiang County Hospital of Traditional Chinese Medicine, Hefei, China.

Keywords: cardiopulmonary fitness assessment; cardiopulmonary function; chronic heart failure; plasma N-terminal B-type pronatriuretic peptide; rehabilitation training.

Abstract. This study explored the impact of rehabilitation training guided by cardiopulmonary fitness assessment on NT-proBNP levels in patients with chronic heart failure (CHF). It was conducted on 220 chronic heart failure (CHF) patients from March 2020 to February 2022. They were divided into a control and observation group. The control group received routine nursing, while the an observation group underwent rehabilitation guided by a cardiopulmonary fitness assessment. Changes in NT-proBNP levels, vascular endothelial function, and cardiopulmonary function were compared between the groups at admission, eight, and 12 weeks later. Upon admission, the two groups had no statistically significant difference in NT-proBNP levels ($p>0.05$). However, after eight and 12 weeks of intervention, both groups showed decreased NT-proBNP levels, with the observation group exhibiting significantly lower levels than the control group ($p<0.05$). Similarly, there was no significant difference between the groups initially ($p>0.05$) in endothelial function comparison. However, after eight and 12 weeks, ET-1 and Ang-II levels decreased in both groups, with the observation group showing significantly lower levels than the control group ($p<0.05$). In terms of cardiopulmonary function, there was no significant difference initially. However, after eight and 12 weeks, Peak VO_2, VO_2 AT, and maximum exercise power increased in both groups compared to before the intervention, with the observation group showing significantly higher values than the control group ($p<0.05$). Additionally, the VE/VCO_2 slope decreased in both groups post-intervention, with the observation group having a lower slope than the control group ($p<0.05$). Cardiopulmonary fitness-guided rehabilitation objectively evaluates patients, formulates precise plans, reduces NT-proBNP levels and inflammation, improves vascular endothelial function, and is vital in secondary chronic heart failure prevention.

Corresponding author: Huamei Yang. Department of Cardiovascular, Lujiang County Hospital of Traditional Chinese Medicine, Hefei, China. E-mail: 13943475960@163.com

Efecto del entrenamiento de rehabilitación guiado por la evaluación de la aptitud cardiorrespiratoria en los niveles de NT-proBNP en pacientes con insuficiencia cardíaca crónica.

Invest Clin 2024; 65 (4): 406 – 417

Palabras clave: evaluación de la aptitud cardiorrespiratoria; función cardiorrespiratoria; insuficiencia cardíaca crónica; péptido natriurético tipo B terminal plasmático; entrenamiento de rehabilitación.

Resumen. Este estudio tuvo como objetivo explorar el impacto del entrenamiento de rehabilitación guiado por la evaluación de la aptitud cardiorrespiratoria en los niveles de NT-proBNP en pacientes con insuficiencia cardíaca crónica (ICC). El estudio se llevó a cabo con 220 pacientes de ICC desde marzo de 2020 hasta febrero de 2022. Estos se dividieron en un grupo de control y un grupo de observación. El grupo de control recibió cuidados rutinarios, mientras que el grupo de observación se sometió a rehabilitación guiada por una evaluación de la aptitud cardiorrespiratoria. Se compararon los cambios en los niveles de NT-proBNP, la función endotelial vascular y la función cardiorrespiratoria entre los grupos al ingreso, a las 8 y a las 12 semanas. Al ingreso, no hubo diferencias estadísticamente significativas en el nivel de NT-proBNP entre los dos grupos ($p>0,05$). Sin embargo, después de 8 y 12 semanas de intervención, ambos grupos mostraron niveles disminuidos de NT-proBNP en comparación con antes de la intervención, con el grupo de observación exhibiendo niveles significativamente más bajos que el grupo de control ($p<0,05$). De manera similar, en la comparación de la función endotelial, no hubo diferencias significativas entre los grupos inicialmente ($p>0,05$), pero después de 8 y 12 semanas, los niveles tanto de ET-1 como de Ang-II disminuyeron en ambos grupos, con el grupo de observación mostrando niveles significativamente menores que el grupo de control ($p<0,05$). En términos de función cardiorrespiratoria, no hubo diferencia significativa inicialmente, pero después de 8 y 12 semanas, el pico de VO_2, VO_2 AT y la potencia máxima de ejercicio aumentaron en ambos grupos en comparación con antes de la intervención, con el grupo de observación mostrando valores significativamente más altos que el grupo de control ($p<0,05$). Además, la pendiente VE/VCO_2 disminuyó en ambos grupos después de la intervención, con el grupo de observación teniendo una pendiente más baja que el grupo de control ($p<0,05$). La rehabilitación guiada por la aptitud cardiorrespiratoria evalúa objetivamente a los pacientes, formula planes precisos, reduce los niveles de NT-proBNP y la inflamación, mejora la función endotelial vascular y es vital en la prevención secundaria de la insuficiencia cardíaca crónica.

Received: 10-12-2023 Accepted: 15-04-2024

INTRODUCTION

Chronic heart failure (CHF) is a series of compensatory reactive diseases caused by weakened myocardial contraction caused by myocardial disease and the inability of cardiac output to meet the metabolic needs of the body [1, 2]. The prevalence of CHF varies globally, with an estimated 64 million people affected worldwide [3]. The condition is more

common in older adults, with a higher prevalence in men than women [4].

Patients with CHF typically present with signs and symptoms such as dyspnea, fatigue, reduced exercise tolerance, and fluid retention, manifesting as pulmonary congestion and peripheral edema. As the condition progresses, it can lead to a decline in quality of life and functional capacity [1].

The diagnosis of CHF relies on a combination of clinical assessment, biomarkers, and imaging techniques [5]. N-terminal pro-b-type natriuretic peptide (NT-proBNP) is an essential biomarker in the diagnosis and management of CHF, reflecting the degree of ventricular stress and providing prognostic information [6, 7]. Echocardiography remains the primary imaging modality for assessing cardiac function and structure [8].

Cardiopulmonary exercise testing (CPET) is valuable in evaluating cardiopulmonary fitness and functional capacity in CHF patients. It assists in the precise assessment of the severity of CHF, prognosis prediction, and tailoring individualized treatment strategies, including rehabilitation programs [9]. CPET measures various parameters, including oxygen consumption (VO_2), carbon dioxide production, and ventilatory efficiency, providing a comprehensive evaluation of the cardiovascular, pulmonary, and muscular systems during exercises [10, 11].

Rehabilitation training in the context of CHF has emerged as a necessary adjunctive therapy to improve functional capacity and quality of life, and potentially reduce hospital readmission rates. Rehabilitation programs are tailored to the individual and often involve aerobic exercise, resistance training, and respiratory exercises guided by cardiopulmonary fitness assessments [12]. These assessments, which include cardiopulmonary exercise testing (CPET), provide valuable information on the patient's functional limitations and responses to physical stress [13].

A study by Bozkurt *et al*. showed that cardiac rehabilitation (CR) is beneficial in patients with HF and is recommended as a Class 1A indication in HF practice guidelines [12] Another study conducted by Wang *et al*. showed that CPET for patients with CHF increases heart and lung function, improves exercise endurance, decreases NT-proBNP and hscTnT levels, and improves patients' quality of life [14].

The necessity of conducting the present study stems from the need to understand better the relationship between rehabilitation training and NT-proBNP levels in patients with CHF. Since few studies have been conducted in this field, it is necessary to conduct the present study to investigate the effect of rehabilitation exercise guided by assessment of cardiopulmonary fitness on NT-proBNP levels in patients with CHF.

MATERIALS AND METHODS

General information

Two hundred twenty patients with CHF treated in our hospital from March 2020 to February 2022 were chosen as samples. The sample size calculation formula is $n1=n2=2[(\mu_\alpha+\mu_\beta)\ \sigma/\delta]^2$, of which σ denotes the overall standard deviation, δ is the mean difference between the two samples, and n1=n2 represents the sample size of the control group (C) and the observation group (O), respectively, α= 0.05, β= 0.10. According to the t-limit table, $\mu_\alpha=1.96$, $\mu_\beta=1.28$, the sample size n1=n2=92 was calculated, taking into account the 20% loss of follow-up rate, and the required sample size was at least $(92+92)/(1+20\%)\approx220$. Finally, the sample size n1=n2=110 was determined. There were no statistically significant differences between the data in both groups of patients, as shown in Table 1. This study obtained the consent of patients and their families and was approved by the Ethics Committee.

Inclusion and exclusion criteria

Inclusion criteria: ① Patients meeting the relevant diagnostic criteria in the 2018 NICE Guidelines for the Diagnosis and Man-

Table 1
General information comparison.

Project	Gender		Age (Years)	Left ventricular Ejection Fraction (%)	Complications			New York Heart Function Classification	
	M	F			Hyperlipidemia	Diabetes	Hypertension	I	II
Group C (n=110)	61(55.45)	49(44.55)*	63.67±9.26**	42.79±2.09	26(23.64)	38(34.55)	46(41.82)	63(57.27)	47(42.73)
Group O (n=110)	65(59.09)	45(40.91)*	62.95±8.55**	43.14±2.36	22(20.00)	43(39.09)	45(40.91)	68(61.82)	42(38.18)
χ^2/t	0.297		0.641	1.181	0.653			0.472	
$p^{\#}$	0.586		0.522	0.239	0.721			0.492	

C: control group, O: observation group. Data are expressed as *frequency (%), ** mean ± SD: # p t-test (Independent Samples t-test) and chi-square χ^2.

agement of Adult Chronic Heart Failure[15]; ② Patients showing fatigue dyspnea, upright breathing, anorexia, epigastrium pain, pleural effusion or ascites in severe cases[16]; ③ New York Heart Association Cardiac Function Classification I-II; ④ Patients with stable condition for ≥ 1 month; ⑤ First onset; ⑥ Age from 30 to 85 years old.

Exclusion criteria: ① Patients having myocardial infarction, hypertrophic obstructive cardiomyopathy, aortic valve stenosis and acute myocarditis in recent three months; ② Patients with substantial lesions of essential organs, such as heart, lungs, and kidneys; ③ Patients with chronic obstructive pulmonary disease or pulmonary heart disease; ④ Patients with intermittent claudication, limb dysfunction, or inability to take care of themselves; ⑤ Patients with malignant arrhythmia and unstable angina pectoris; ⑥ Patients with electrolyte disorders; ⑦ Patients with a high degree of atrioventricular block. The two groups of general data were balanced with no statistically significant difference ($p>0.05$), as shown below.

Research method

Group C implemented routine nursing measures: (1) Exercise: The amount of exercise was determined based on the patient's heart function grading. It was generally recommended that patients with heart function level II should appropriately limit physical activity, not affect physical labor and household chores, and increase nap time. Strict physical activity restrictions were required for patients with heart function level III. Patients can get out of bed and move around, but general physical labor was limited. (2) Diet: Low salt and low-fat diet, with a sodium intake of less than 2.5 g/d, and strict restrictions on foods, such as sausages, canned goods, and seafood. Patients with severe heart failure had a daily fluid volume of 1.5-2.0 liters. (3) Medication care: When patients take diuretics, their blood potassium content should be monitored to avoid hypokalemia. For digitalis preparations, attention should be paid to observing the patient's appetite, palpitations, and vision. If the patient's pulse was less than 60 beats per minute, administration was discontinued and reported to the doctor. Group O implemented rehabilitation training under the guidance of cardiopulmonary fitness assessment with the following steps.

Cardiopulmonary fitness assessment

Cardiopulmonary function testing was performed using the MasterScreen CPX pulmonary function testing system (CEPT). The first choice was to complete a full set of static pulmonary function tests in the sitting position, guide the patient to sit on the power bike and record non-invasive blood, 12 lead ECG, oxygen saturation, gas exchange, and other indicators. Patients should rest for 3

minutes first, then warm up without load at a cycling rate of 60 r/min for 3 minutes. Based on the patient's gender, age, and functional status, the bicycle power increase rate was set to 20-30 W/min, so the patient could reach the symptom-limiting maximum exercise target within 10 minutes. The patient's maximum motor power and Peak VO2, VO2 AT, maximum exercise time, and VE/VCO2 sleep were recorded during the recovery period.

A high-load intensity exercise prescription was accurately formulated based on CEPT results: 50% power=[(anaerobic threshold measurement power - power increase rate) × 0.75)/2], and medical-grade precision power waste trucks were selected for training tools. (1) Stretching exercise: The patient performed muscle stretching exercises before using the bike trainer. Neck extension: Hands were placed on hips, waist and back were straightened, and the head was slightly extended upwards. Neck stretching left and right: Seated in a sitting position, the patient's head was tilted left and right to the left, repeated 3 times. Baby position: Assume a kneeling and standing position with legs spread wider than shoulder-width apart, then sit the hips towards the heels, lean the body forward, and touch the ground with their upper limbs from the front to the forehead. Maintain this stance for five seconds and repeat the exercise five times. Baby hugging posture: Patient sitting position: Keep the waist and back straight, stretch one thigh to the chest, keep the knee level with the same elbow socket, and the foot level with the opposite elbow socket. Maintain this position for 10 seconds and complete two sides into a group of 5 groups. (2) Car riding exercise: Warm up without power for 2 minutes, exercise for 30 minutes at 50% power intensity, with a speed of 60 revolutions per minute. If the speed cannot be maintained during the exercise, it is necessary to reverse without power and rest for 1 minute before continuing the exercise. After completing 30 minutes of exercise, enter the recovery period and run the car without power for 5 minutes. The exercise frequency is 5d/week for 8 weeks (2 months).

Exercise precautions: During exercise, relevant vital indicator monitoring instruments were equipped, such as blood pressure, heart rate, and pulse oxygen saturation.

Indication of exercise termination: ① The target heart rate was achieved; ② Patients having difficulty breathing, noticeable shortness of breath, pale complexion, as well as damp and cold skin; ③ Patients having central nervous system symptoms, such as dizziness, sensory abnormalities, ataxia, and visual impairments occur; ④ As the power increased, blood pressure decreased by>10mmHg or continuous baseline blood pressure or systolic blood pressure>220mmHg, diastolic blood pressure>115mmHg; ⑤ Patients having severe arrhythmia, persistent ventricular tachycardia, and rapid atrial fibrillation; ⑥ Patients requested to stop exercising.

Outcome measures

NT-proBNP: 5mL of patients' venous blood was collected upon admission, and after 8 weeks and 12 weeks. After centrifugation, serum was stored at -80°C, and the NT-proBNP level was determined by automatic electrochemiluminescence immunoassay. The reagent kits were all purchased from Shanghai Zhenma Industrial Co., Ltd., and the operation process was strictly carried out following the instructions.

Vascular endothelial function: 10mL of fasting venous blood was collected from patients upon admission, 8 weeks later, and 12 weeks later. After centrifugation, the serum was stored in a refrigerator at -80°C. The serum levels of endothelin-1 (ET-1) and angiopoietin-II (Ang-II) were measured using ELISA. The reagent kits were all purchased from Shanghai Hengyuan Biotechnology Co., Ltd, and the operation process followed the instructions.

Cardiopulmonary function: CPET was conducted using the MasterScreen CPX pulmonary function testing system produced by company Yeger (German) upon admission, 8

weeks later, and 12 weeks later. Basic patient information was collected, and the patient was asked to wear a mask after 5 minutes of rest. The electrocardiogram lead wire and electrode were connected, and the cuff was tied. Then, the patient started the measurement and the results were recorded. This included 50% peak oxygen consumption (Peak VO_2), anaerobic threshold oxygen consumption (VO_2 AT), maximum exercise power, and carbon dioxide ventilation equivalent slope (VE/VCO_2 slope) [17].

Statistical methods

EpiData software was applied to establish a database, and two people ensured the accuracy of data input through parallel input. The research collected data was statistically analyzed using the IBM® SPSS software (version 26.0), $\bar{x}\pm SD$ represents data, and inter-group comparisons were conducted using sample t-tests. The counting data is expressed as frequency or percentage, using c^2. Multiple data sets were analyzed using repeated variance measures, with $p<0.05$ indicating statistical differences.

Ethical considerations

Ethical approval was obtained before the commencement of the study. Informed consent was obtained from all participants before their inclusion in the study. The study protocol ensured the privacy and confidentiality of patient information. The study complied with relevant data protection regulations and the Declaration of Helsinki.

RESULTS

NT-proBNP comparison of two groups

Upon admission, there was no statistically significant difference in the levels of NT-proBNP between the two groups ($p>0.05$). After 8 and 12 weeks of intervention, the levels of NT-proBNP in the two groups were lower than those before the intervention, and those of the observation group were lower than those of the control group ($p<0.05$) (Table 2). The two groups' change curves of NT-proBNP levels showed a downward trend.

Endothelial function levels comparison between the two groups of blood vessels

Upon admission, there was no statistically significant difference in endothelial function levels between the two groups ($p>0.05$). After 8 and 12 weeks of intervention, the levels of ET-1 and Ang-II in both groups were lower than those before the intervention, and those of the observation group were lower than those of the control group ($p<0.05$) (Table 3). The levels of ET-1 and Ang-II in the two groups showed a downward trend.

Cardiopulmonary function comparison of the two groups

Upon admission, there was no statistically significant difference in cardiopulmonary function between the two groups ($p>0.05$). After 8 and 12 weeks of intervention, peak VO_2, VO_2 AT, and maximum exercise power in both groups were higher than those before the intervention, and those of the observation group were higher than those of the control group ($p<0.05$) (Table 4). The VE/VCO_2 slope in both groups was low-

Table 2
NT-proBNP Comparison of two groups.

Group	NT-proBNP(ng/mL)		
	Upon admission	8 Weeks	12 Weeks
C* (n=110)	380.41±39.56**	357.31±41.74	316.15±38.63
O* (n=110)	383.49±42.07	322.65±38.96	292.51±35.34
t	0.559	6.389	4.736
p#	0.577	<0.001	<0.001

N-terminal pro-b-type natriuretic peptide (NT-proBNP) *C: control group, O: observational group. **Mean±SD, # p t-test (Independent Samples t Test).

Table 3
Endothelial function levels comparison

Group	ET-1 (ng/L)		
	Upon admission	8 Weeks	12 Weeks
C* (n=110)	23.82±4.07**	22.18±3.44	19.77±4.23
O* (n=110)	23.92±3.99	20.28±4.05	18.03±3.49
t	0.184	3.750	3.328
pP#	0.854	<0.001	0.001
Group	Ang -II (ng/L)		
	Upon admission	8 Weeks	12 Weeks
C* (n=110)	109.70±12.24**	104.29±12.37	99.12±11.55
O* (n=110)	107.09±11.50	98.61±12.49	91.30±12.79
t	1.630	3.389	4.759
p#	0.105	0.001	<0.001

ET-1: endothelin-1 , Ang-II: angiotensin II *C: control group, O: observational group. **Mean±SD, # p t-test (Independent Samples t Test).

Table 4
Cardiopulmonary function comparison of the two groups.

Group	Peak VO_2[mL/(min·kg)]		
	Upon admission	8 Weeks	12 Weeks
C* (n=110)	17.24±1.34**	17.72±1.57	18.35±1.43
O* (n=110)	17.15±1.39	18.69±1.72	19.09±1.54
t	0.489	4.369	3.691
p#	0.625	0.001	<0.001
Group	VO_2 AT[mL/(min·kg)]		
	Upon admission	8 Weeks	12 Weeks
C* (n=110)	9.25±1.15**	9.90±1.37	10.47±1.49
O* (n=110)	9.45±1.47	10.47±1.25	11.09±1.68
t	1.124	3.224	2.896
p#	0.262	0.002	0.004

*C: control group, O: observational group. **Mean±SD, # p t-test (Independent Samples t Test).

er than that before the intervention, and that of the observation group was lower than that of the control group ($p<0.05$) (Table 5). The peak VO_2, VO_2 AT, and maximum exercise power of the two groups showed an upward trend, while the VE/VCO_2 slope showed a downward trend.

DISCUSSION

NT-proBNP, as an important biochemical CHF marker, predicts CFH development and progression and can accurately determine its severity [18]. Results showed no sta-

Table 5
Cardiopulmonary function comparison of the two groups.

Group	Maximum Motion Power		
	Upon admission	8 Weeks	12 Weeks
C* (n=110)	104.87±13.73**	108.84±13.49	112.64±12.92
O* (n=110)	103.83±13.26	113.94±12.19	120.34±12.28
t	0.572	2.942	4.531
$p^{\#}$	0.568	0.004	<0.001
Group	VE/VCO_2 slop (%)		
	Upon admission	8 Weeks	12 Weeks
C (n=110)	33.70±3.64**	31.23±3.53	30.32±3.37
O (n=110)	33.28±3.45	29.91±3.37	28.50±3.15
t	0.878	2.837	4.138
$p^{\#}$	0.381	0.005	<0.001

*C: control group, O: observational group. **Mean±SD, # p-value t test (Independent Samples t Test).

tistically significant difference in NT-proBNP level upon admission (p>0.05). After 8 and 12 weeks of intervention, NT-proBNP levels were lower than before and much lower in Group O (p<0.05). The repeated analysis of variance results showed group, time, and interaction effects between the two groups (p<0.05). Rehabilitation training guided by cardiopulmonary fitness assessment reduces NT-proBNP levels in CHF patients. The reason is that as an essential part of secondary prevention of heart failure, exercise rehabilitation is recommended as Class 1 in the management guidelines of the American Heart Association and is valued by patients and clinicians [19]. High-intensity exercise is the core of rehabilitation training, and exercise intensity is related to patient safety and treatment effects. The conventional exercise intensity system is determined based on the patient's heart rate; however, currently, the commonly used drugs in clinical practice for heart failure patients are β Receptor blockers. Therefore, determining exercise intensity based on heart rate poses significant safety risks, so it is imperative to develop reasonable intensity exercise rehabilitation training based on the patient's exercise endurance [20,21]. After the stimulation of the synthesis of brain natriuretic peptide precursor by myocardial cells, the brain natriuretic peptide precursor protease decomposes into NT-proBNP and the bioactive hormone brain natriuretic peptide, which then enters the bloodstream, leading to an increase in the content of NT-proBNP in the blood. Rehabilitation training guided by cardiopulmonary fitness assessment can increase glucose oxidation, improve substrate utilization and mitochondrial respiratory oxidation ability, reduce oxidative stress, delay myocardial fibrosis, stabilize myocardial cell contraction rhythm, reduce myocardial cell stimulation, and lower blood NT-proBNP levels.

Results showed no statistically significant difference in endothelial function level upon admission (p>0.05). After 8 and 12 weeks of intervention, the ET-1 and Ang II levels in both groups were lower than before the intervention and much lower in Group O (p<0.05). Repeated analysis of variance results showed group, time, and interaction effects between the two groups (p<0.05). This is similar to the research results of Papathanasiou *et al.* [22,23]. CHF may cause an increase in the excitability of renin-angiotensin-aldosterone and the sympathetic nervous system, stimulate inflammation and oxida-

tive stress reactions, and subsequently cause dysfunction of vascular endothelial function. Meanwhile, vascular endothelial dysfunction can lead to increased cardiac load, myocardial ischemia exacerbation, and vicious cycle formation [24,25]. ET-1 is mainly synthesized and secreted by endothelial cells. When myocardial cells are damaged, endothelial cells accelerate the synthesis of a large amount of ET-1. This may be related to the fact that rehabilitation training guided by cardiopulmonary fitness assessment can reduce the concentration of catecholamines in the blood, reduce the stimulation of inflammatory and oxidative stress reactions on vascular endothelium, and protect vascular endothelial function [26,27].

The research results also showed no statistically significant difference in cardiopulmonary function upon admission ($p>0.05$). After 8 and 12 weeks of intervention, Peak VO_2, VO_2 AT, and maximum exercise power in both groups were higher than before and much higher in Group O ($p<0.05$). The VE/VCO_2 slope was lower than before the intervention and much lower in Group O ($p<0.05$). Repeated analysis of variance results showed group, time, and interaction effects between the two groups ($p<0.05$). This is similar to the research results of Turri Silva and others [28]. Rehabilitation training guided by cardiopulmonary fitness assessment can help improve the cardiovascular function of CHF patients. CPET can accurately evaluate the exercise ability of subjects, objectively evaluate their exercise endurance and cardiac reserve function, and provide a reliable basis for developing rehabilitation training for heart failure patients. CPET evaluated this study, and a 50% anaerobic threshold exercise intensity was selected to avoid lactic acid accumulation caused by prolonged aerobic metabolism and systemic muscle soreness. Moderate and mild exercise can inhibit excessive vasoconstriction, improve the elastic reserve capacity of blood vessels, regulate myocardial metabolism, improve cardiac contractile function, and improve cardiopulmonary function.

In conclusion, the findings of this study demonstrate significant improvements in NT-proBNP levels, endothelial function, and cardiopulmonary function. The results revealed a notable decrease in NT-proBNP levels after 8 and 12 weeks of intervention, particularly in the observation group, indicating the effectiveness of rehabilitation training in reducing NT-proBNP levels in CHF patients. Furthermore, improvements in endothelial function, as evidenced by lower levels of ET-1 and Ang II after the intervention period, suggest that rehabilitation training guided by cardiopulmonary fitness assessment can mitigate vascular endothelial dysfunction associated with CHF. Additionally, enhancements in cardiopulmonary function, including increased Peak VO_2, VO_2 AT, maximum exercise power, and decreased VE/VCO_2 slope, highlight the positive impact of this intervention on cardiovascular function. These results underscore the importance of tailored rehabilitation programs based on cardiopulmonary fitness assessment for improving outcomes in CHF patients by enhancing NT-proBNP levels, endothelial function, and cardiopulmonary performance.

Limitations

The study encountered several limitations. Firstly, the sample size of 220 patients may not adequately represent the general population, potentially limiting the robustness of the results. Secondly, including patients with chronic heart failure could introduce selection bias, thus challenging the study's applicability to the broader population. Additionally, 8 to 12 weeks might not have been sufficiently long to observe significant changes in specific outcomes. Finally, the study focused on NT-proBNP levels, endothelial function, and cardiopulmonary function, but other relevant outcomes could have been included to provide a more comprehensive understanding of the effects of the intervention.

ACKNOWLEDGMENTS

None.

Authors' ORCID number

- Huamei Yang: 0009-0000-3737-8419

Contributions of authors

The author was involved in data collection, article design, interpretation of results, review, and manuscript preparation.

Conflict of competence

The author declares no conflict of interest.

Funding

None.

REFERENCES

1. **Malik A, Brito D, Vaqar S, Chhabra L**. Congestive Heart Failure. StatPearls. Treasure Island (FL) ineligible companies. Disclosure: Lovely Chhabra declares no relevant financial relationships with ineligible companies: StatPearls Publishing, Copyright © 2024, StatPearls Publishing LLC.; 2024.
2. **Holden S, Lyng K, Graven-Nielsen T, Riel H, Olesen JL, Larsen LH, Rathleff MS**. Isometric exercise and pain in patellar tendinopathy: A randomized crossover trial. J Sci Med Sport. 2020;23(3):208-214. *https://doi.org/10.1016/j.jsams.2019.09.015*
3. **Savarese G, Becher PM, Lund LH, Seferovic P, Rosano GMC, Coats AJS**. Global burden of heart failure: a comprehensive and updated review of epidemiology. Cardiovasc Res. 2023;118(17):3272-3287. *https://doi.org/10.1093/cvr/cvac013*
4. **Metra M, Tomasoni D, Adamo M, Bayes-Genis A, Filippatos G, Abdelhamid M, Adamopoulos S, Anker SD, Antohi L, Böhm M, Braunschweig F, Gal TB, Butler J, Cleland JGF, Cohen-Solal A, Damman K, Gustafsson F, Hill L, Jankowska EA, Lainscak M, Lund LH, McDonagh T, Mebazaa A, Moura B, Mullens W, Piepoli M, Ponikowski P, Rakisheva A, Ristic A, Savarese G, Seferovic P, Sharma R, Tocchetti CG, Yilmaz MB, Vitale C, Volterrani M, von Haehling S, Chioncel O, Coats AJS, Rosano G.** Worsening of chronic heart failure: definition, epidemiology, management and prevention. A clinical consensus statement by the Heart Failure Association of the European Society of Cardiology. Eur J Heart Fail. 2023;25(6):776-791. *https://doi.org/10.1002/ejhf.2874*
5. **Shrivastava A, Haase T, Zeller T, Schulte C**. Biomarkers for heart failure prognosis: proteins, genetic scores and non-coding RNAs. Front Cardiovasc Med 2020;7(1):1-20. *https://doi.org/10.3389/fcvm.2020.601364*
6. **Welsh P, Campbell RT, Mooney L, Kimenai DM, Hayward C, Campbell A, Porteous D, Mills NL, Lang NN, Petrie MC, Januzzi JL, McMurray JJV, Sattar N.** Reference ranges for NT-proBNP (N-Terminal Pro-B-Type Natriuretic Peptide) and risk factors for higher NT-proBNP concentrations in a large general population cohort. Circulation: Heart Failure. 2022;15(10):e009427. *https://doi.org/10.1161/CIRCHEARTFAILURE.121.009427*
7. **Mallick A, Januzzi JL, Jr.** Biomarkers in acute heart failure. Rev Esp Cardiol (Engl Ed). 2015;68(6):514-525. *https://doi.org/10.1016/j.rec.2015.02.009*
8. **Lowry MTH, Gibson PH**. Echocardiography. Medicine. 2022;50(6):357-362. *https://doi.org/10.1016/j.mpmed.2022.03.008*
9. **Juarez M, Castillo-Rodriguez C, Soliman D, Del Rio-Pertuz G, Nugent K**. Cardiopulmonary exercise testing in heart failure. J Cardiovasc Dev Dis 2024;11(3):70. *https://doi.org/10.3390/jcdd11030070*
10. **Razvi Y, Ladie DE**. Cardiopulmonary Exercise Testing. StatPearls. Treasure Island (FL) ineligible companies. Disclosure: Danielle Ladie declares no relevant financial relationships with ineligible companies.: StatPearls Publishing, Copyright © 2024, StatPearls Publishing LLC.; 2024.
11. **Leclerc K**. Cardiopulmonary exercise testing: A contemporary and versatile clinical tool. Cleve Clin J Med. 2017;84(2):161-168. *https://doi.org/10.3949/ccjm.84a.15013*
12. **Bozkurt B, Fonarow G, Goldberg L, Guglin M, Josephson R, Forman D, Lin G,**

Lindenfeld J, O'Connor C, Panjrath G, Piña I, Shah T, Sinha S, Wolfel E. Cardiac rehabilitation for patients with heart failure. J Am Coll Cardiol 2021;77(11):1454-1469. *http://dx.doi.org/10.1016/j.jacc.2021.01.030*

13. **Morris JH, Chen L**. Exercise training and heart failure: a review of the literature. Card Fail Rev. 2019;5(1):57-61. *https://doi.org/10.15420%2Fcfr.2018.31.1*
14. **Wang Y, Cao J, Kong X, Wang S, Meng L, Wang Y**. The effects of CPET-guided cardiac rehabilitation on the cardiopulmonary function, the exercise endurance, and the NT-proBNP and hscTnT levels in CHF patients. Am J Transl Res. 2021;13(6):7104-114.
15. **Xu D, Ma Z**. Interpretation of the Updates in 2018 NICE Guideline for the Diagnosis and Management of Chronic Heart Failure in Adults. Chinese General Practice. 2019;22(17):2015. *https://doi.org/10.12114/j.issn.1007-9572.2019.00.065*
16. **Ngue H, Ngue M, Lee I, Chang C-F, Baydur A**. Dead space breathing in patients with malignancies: determination by cardiopulmonary exercise testing. Open J Resp Dis 2022;12(1):15-36. *https://doi.org/10.4236/ojrd.2022.121002*
17. **Mueller C, McDonald K, de Boer RA, Maisel A, Cleland JGF, Kozhuharov N, Coats AJS, Metra M, Mebazaa A, Ruschitzka F, Lainscak M, Filippatos G, Seferovic PM, Meijers WC, Bayes-Genis A, Mueller T, Richards M, Januzzi JL, Jr.** Heart Failure Association of the European Society of Cardiology practical guidance on the use of natriuretic peptide concentrations. Eur J Heart Fail. 2019;21(6):715-731. *https://doi.org/10.1002/ejhf.1494*
18. **Ma L, Zhang Y, Liu P, Li S, Li Y, Ji T, Zhang L, Chhetri JK, Li Y**. Plasma N-Terminal Pro-B-Type Natriuretic Peptide is associated with intrinsic capacity decline in an older population. J Nutr Health Aging 2021;25(2):271-277. *https://doi.org/10.1007/s12603-020-1468-3*
19. **Tucker WJ, Fegers-Wustrow I, Halle M, Haykowsky MJ, Chung EH, Kovacic JC**. Exercise for Primary and Secondary Prevention of Cardiovascular Disease: JACC Focus Seminar 1/4. J Am Coll Cardiol. 2022;80(11):1091-1106. *https://doi.org/10.1016/j.jacc.2022.07.004*
20. **Sherrington C, Fairhall NJ, Wallbank GK, Tiedemann A, Michaleff ZA, Howard K, Clemson L, Hopewell S, Lamb SE**. Exercise for preventing falls in older people living in the community. Cochrane Database Syst Rev. 2019;1(1):Cd012424. *https://doi.org/10.1002/14651858.cd012424.pub2*
21. **Liu-Ambrose T, Davis JC, Best JR, Dian L, Madden K, Cook W, Hsu CL, Khan KM**. Effect of a home-based exercise program on subsequent falls among community-dwelling high-risk older adults after a fall: a randomized clinical trial. JAMA 2019;321(21):2092-2100. *https://doi.org/10.1001/jama.2019.5795*
22. **Papathanasiou JV, Petrov I, Tsekoura D, Dionyssiotis Y, Ferreira AS, Lopes AJ, Ljoka C, Foti C**. Does group-based high-intensity aerobic interval training improve the inflammatory status in patients with chronic heart failure? Eur J Phys Rehabil Med. 2022;58(2):242-250. *https://doi.org/10.23736/s1973-9087.21.06894-5*
23. **Leddy JJ, Haider MN, Ellis MJ, Mannix R, Darling SR, Freitas MS, Suffoletto HN, Leiter J, Cordingley DM, Willer B**. Early subthreshold aerobic exercise for sport-related concussion: a randomized clinical trial. JAMA Pediatr. 2019;173(4):319-325. *https://doi.org/10.1001/jamapediatrics.2018.4397*
24. **Alem MM**. Endothelial dysfunction in chronic heart failure: assessment, findings, significance, and potential therapeutic targets. Int J Mol Sci. 2019;20(13):3198. *https://doi.org/10.3390/ijms20133198*
25. **Nakamura M**. Pharmacological modulations of the renin-angiotensin-aldosterone system in human congestive heart failure: effects on peripheral vascular endothelial function. Curr Vasc Pharmacol. 2004;2(1):65-70. *https://doi.org/10.2174/1570161043476537*
26. **Parnell MM, Holst DP, Kaye DM**. Augmentation of endothelial function following

exercise training is associated with increased L-arginine transport in human heart failure. Clin Sci (Lond). 2005;109(6):523-530. *https://doi.org/10.1042/cs20050171*

27. **Kourek C, Alshamari M, Mitsiou G, Psarra K, Delis D, Linardatou V, Pittaras T, Ntalianis A, Papadopoulos C, Panagopoulou N, Vasileiadis I, Nanas S, Karatzanos E**. The acute and long-term effects of a cardiac rehabilitation program on endothelial progenitor cells in chronic heart failure patients: Comparing two different exercise training protocols. Int J Cardiol Heart Vasc. 2021;32:100702. *https://doi.org/10.1016/j.ijcha.2020.100702*

28. **Turri-Silva N, Vale-Lira A, Verboven K, Quaglioti Durigan JL, Hansen D, Ciprianо G.** High-intensity interval training versus progressive high-intensity circuit resistance training on endothelial function and cardiorespiratory fitness in heart failure: A preliminary randomized controlled trial. PloS one. 2021;16(10):e0257607. *https://doi.org/10.1371/journal.pone.0257607*

Invest Clin 65(4): 418 - 425, 2024 https://doi.org/10.54817/IC.v65n4a02

Escala CHA_2DS_2-VASc como predictor de severidad de ictus en pacientes con fibrilación auricular.

Miguel López-Hidalgo[1, 2], Luis Pinto-Longart[3], Antonio Eblen-Zajjur[4], Euler Regis[5], José Reina[5], Ignacio Poggioli[5] y José Ramírez[5]

[1]Postgrado de Cardiología, Ciudad Hospitalaria "Dr. Enrique Tejera". Valencia, Venezuela.
[2]Programa de Doctorado en Ciencias Médicas, Universidad de Carabobo, Valencia, Venezuela.
[3]Postgrado de Neurología, Ciudad Hospitalaria "Dr. Enrique Tejera", Valencia, Venezuela.
[4]Laboratorio de Neurociencia Traslacional, Facultad de Medicina, Universidad Diego Portales, Santiago, Chile.
[5]Facultad de Medicina, Universidad de Carabobo, Valencia, Venezuela.

Palabras clave: ictus; fibrilación auricular; $CHADS_2DS_2VASc$; escala 6S de severidad de ictus.

Resumen. La escala CHA_2DS_2-VASc se creó como instrumento predictivo del riesgo de presentación de ictus isquémico embolico, en pacientes con fibrilación auricular (FA) y para toma de decisión terapéutica. Esta no fue creada como instrumento para predecir la severidad de ictus isquémico, a pesar de que sus componentes tienen relación con la formación, tamaño y crecimiento del trombo en atrio izquierdo. Basado en esto, se evaluó la posible utilidad de la escala CHA_2DS_2-VASc como predictor de severidad de ictus isquémicos de origen tromboembólico, en los pacientes que ingresan con ictus y FA. Se realizó un estudio observacional prospectivo, de corte transversal donde se evaluó el puntaje de la escala CHA_2DS_2-VASc en relación con el grado de severidad de ictus isquémico. Se utilizó la escala 6S como referencia para su correlación en pacientes que ingresaron con ictus y FA, en la emergencia de la Ciudad Hospitalaria "Dr. Enrique Tejera", durante el periodo enero-septiembre 2022. Se evaluaron 85 pacientes, con una mediana de edad de 71 [64-76] años, siendo 55,3% femeninos; de ellos, 85,9% tenían hipertensión arterial, 40% diabetes; 7% ictus previo, 14% insuficiencia cardiaca y 16,5% FA previa. Solo el 5,9% de los pacientes recibían anticoagulación cuando ingresaron. La mediana y [p25-p75] para las escalas CHA_2DS_2VASc: 5 [4-6] y para la 6S: 11[8-11] puntos. Ambas escalas se asociaron significativamente (19,2%; R=0,19; p<0,001). Este estudio, utilizando la escala 6S de severidad neurológica como comparador, muestra que la CHA_2DS_2-VASc puede ser una herramienta clínica útil para predecir la severidad de ictus.

Autor de Correspondencia: Miguel López-Hidalgo. Ciudad Hospitalaria "Dr. Enrique Tejera", Servicio de Cardiología. Ave. Lisandro Alvarado, Valencia, Venezuela. Correo electrónico: lopezh900@hotmail.com. @drmiguellopez. X: @m_lopezh

CHA_2DS_2-VASc score as a predictor of stroke severity in patients with atrial fibrillation.

Invest Clin 2024; 65 (4): 418 – 425

Key words: stroke, atrial fibrillation, CHA_2DS_2-VASc score, 6S stroke severity score.

Abstract. The CHA_2DS_2-VASc score was created as a predictive instrument of risk of embolic stroke occurrence in patients with atrial fibrillation (AF), for therapeutic decisions. This score was not created as a tool to assess ischemic stroke severity in patients with AF, although the components of the score are associated with the formation, size, and growth of thrombus in the left atrium. Based on this, we assessed the possible utility of CHA_2DS_2-VASc score as a predictor of ischemic stroke severity in patients with stroke and AF, using the simplified 6S score as an indicator. Observational, prospective, and cross-sectional study, in which the CHA_2DS_2-VASc score was evaluated concerning the degree of ischemic stroke severity, using the 6S score as a reference for correlation analysis in patients hospitalized with stroke and AF in the emergency room of the Ciudad Hospitalaria "Dr. Enrique Tejera", from January- September 2022. The median age was 71 [41-76] years, 55.3% were female, 85.9% had hypertension; 42.4% diabetes, 31.8% previous stroke; 14% heart failure and 16.5% had previous AF. Only 5.9% of the patients received anticoagulation when admitted. The median [p25-p75] was 5 [4-6] points for the CHA_2DS_2-VASc score and 11 [8-11] points for 6S score. Both scores had a significant association (19.2%, $R = 0.19$, $p < 0.001$. This study using the 6S severity score as an indicator, showed that CHA_2DS_2-VASc, could be a useful clinical tool to predict stroke severity.

Recibido: 05-03-2024 Aceptado: 12-09-2024

INTRODUCCIÓN

La fibrilación auricular (FA) es la arritmia cardíaca más común en adultos a nivel mundial. Esta entidad desarrolla un estado protrombótico dado por modificaciones funcionales y estructurales de la aurícula izquierda, tales como: la disfunción miocítica, estasis sanguínea y activación de los factores de coagulación. La complicación más temida de este cuadro clínico es el ictus de origen tromboembólico, siendo esta la principal causa de discapacidad en personas mayores de 60 años [1,2].

Las guías europeas de diagnóstico y tratamiento de FA del 2020 estiman su prevalencia entre 1,5 a 2,0% en la población general. La presencia de FA representa un incremento de 4 a 5 veces mayor riesgo de presentar ictus, 2 a 3 veces mayor riesgo de insuficiencia cardiaca, disminución de la calidad de vida y el doble de mortalidad [3]. La tasa de ictus cardioembólico atribuible a la FA se ha triplicado durante las últimas dos décadas y se proyecta su continuo aumento en las próximas décadas con el envejecimiento de la población [4].

Debido al riesgo que representa la FA en los pacientes de padecer un ictus, se han desarrollado diferentes escalas para valorar la necesidad de terapia anticoagulante que disminuya la probabilidad de éste. La escala con mayor validación y, por lo tanto, la más utilizada en la actualidad es la CHA_2DS_2-

VASc, basada en los siguientes parámetros: insuficiencia cardiaca, hipertensión, rango de edad, diabetes, ictus previo, enfermedad vascular y sexo femenino parámetros (**C**ongestive Heart Failure, **H**ypertension, **A**ge, **D**iabetes, **S**troke**, V**ascular disease and female **S**ex) [4-6].

Se sabe que los factores de riesgo presentes en la escala CHA_2DS_2-VASc para predecir la ocurrencia del ictus cardioembólico, también están asociados a la formación, crecimiento y tamaño del trombo, por lo que, desde el punto de vista fisiopatológico, tiene sentido considerar que estos también pudieran tener incidencia en el grado de severidad de la lesión neuronal que provocan [6]. Ante esto, sería interesante evaluar la posibilidad de usar la propia escala CHA_2DS_2-VASc para determinar la severidad del ictus en pacientes con FA [6,7].

En la actualidad, la escala mayormente utilizada para la evaluación de la severidad de ictus, es la NIHSS (National Institute of Health Stroke Scale) o Escala de Ictus del Instituto Nacional de Salud de Estados Unidos [8-10]. Sin embargo, debido a su complejidad para aplicarla en la emergencia en nuestro medio, se decidió utilizar como alternativa más práctica la escala 6S (six symptoms severity score) o escala de severidad de 6 síntomas, desarrollada recientemente, para la valoración de funciones neurológicas básicas en la fase aguda del ictus [11, 12].

El objetivo de este estudio fue evaluar la capacidad predictiva de la escala CHA_2DS_2VASc, en la estratificación de riesgo de severidad de ictus cardioembólico por FA, en los pacientes ingresados en la emergencia de la Ciudad Hospitalaria "Dr. Enrique Tejera", utilizando como escala de comparación la escala 6S [11].

PACIENTES Y MÉTODOS

El diseño del estudio fue observacional, prospectivo y de corte transversal.

La población estuvo conformada por pacientes mayores de 45 años que ingresaron a la emergencia de adultos de la Ciudad Hospitalaria "Dr. Enrique Tejera", Valencia, Venezuela durante el periodo comprendido entre enero y diciembre de 2022 con diagnóstico de ictus en presencia de arritmia supraventricular tipo fibrilación auricular (FA) aguda o historia clínica de FA crónica documentada.

La información obtenida se registró en el instrumento de recolección de datos elaborado para tal fin, que incluyo datos demográficos, factores de riesgo cardiovascular y factores de riesgo de presentar ictus en presencia de FA. Se registraron los parámetros de la escala CHA_2DS_2-VASc, que evalúa el riesgo de tener un ictus en pacientes con FA no valvular [7] y los de la escala 6S, la cual se utilizó como parámetro comparador para evaluar el grado de severidad del ictus. [11,12].

La escala CHA_2DS_2-VASc define como riesgo bajo pacientes con 0 puntos, riesgo intermedio de 1 a 2 puntos y riesgo alto >= 3 puntos [6-8]. En la escala de los 6 síntomas o 6S score, el grado de severidad se define como bajo, de 2 a 4 puntos; moderado, de 5 a 9 puntos y alto, un puntaje igual o mayor a 10 puntos, teniendo esta escala un máximo puntaje de 15 [11,12].

El Comité de Bioética del departamento de investigación y docencia general de la Ciudad Hospitalaria "Dr. Enrique Tejera", otorgó la autorización de este estudio bajo el No 001026, el 22/11/2021, garantizando el anonimato de los pacientes. El estudio se realizó respetando las recomendaciones internacionales para investigación clínica, de acuerdo con la declaración de Helsinki.

Con la información recolectada se realizó una base de datos en Excel de Microsoft. Las variables categóricas se expresaron en valores absolutos y porcentuales y las variables continuas en medianas y percentiles [25-75]. El análisis estadístico se realizó con el programa de libre acceso, Epi-Info™ del CDC (Center for Disease Control) de Atlanta, v.7.1. Las variables categóricas se analizaron con tablas 2 x 2 utilizando la prueba Chi^2 y para las variables continuas, se utilizó

estadística no-paramétrica, con la prueba de Mann-Whitney U. Se consideró como significancia estadística valores de p <0,05.

Se realizó un análisis de correlación y regresión entre las 2 escalas evaluadas (CHA_2DS_2-VASc y 6S score) con un modelo polinomial; para las comparaciones se usó la prueba de Spearman, calculándose los coeficientes de correlación/regresión (r); de determinación (R^2); y el % de intensidad de asociación de escalas (R^2 x 100), se estableció como significancia p <0,05. Se seleccionó la regresión con la ecuación correspondiente a la de 1° orden, ya que cumplía los requisitos adecuados.

RESULTADOS

Se estudiaron un total de 85 pacientes con ictus y fibrilación auricular asociada, de los cuales 55,3% fueron femeninos, con una mediana de edad de 71 años [64-76]. Los factores de riesgo cardiovasculares y factores predictores de riesgo de ictus están representados en la Tabla 1 y Fig. 1.

Se observó que estos pacientes recibían al ingreso los siguientes medicamentos: inhibidores de la enzima convertidora de angiotensina I/Antagonista de los receptores de angiotensina 2 (IECA/ARA2): 65,8%; betabloqueantes: 27%; calcio-antagonistas: 17,7%; aspirina: 12,9%; clopidogrel: 8,2%; y warfarina: 5,9% (Tabla 2).

En cuanto a los estudios de neuroimagen, 38 pacientes (44,7%) contaban con tomografía de cráneo, realizados en una mediana de 5 [3-7] días desde su ingreso; los patrones imagenológicos se distribuyeron de la siguiente manera: 76,3% mostraron lesiones neurológicas isquémicas focales y 24% multifocales; de estas últimas, 66% fueron unilaterales, 30% bilaterales y 4% indeterminadas.

La mediana del puntaje obtenido para los pacientes en la escala CHA_2DS_2-VASc fue de 5 [4-6] y en la escala 6S fue de 11 [8-11]. El análisis de regresión polinomial mostró un coeficiente de determinación, R^2 = 0,19

Tabla 1
Características basales de los pacientes con ictus y fibrilación auricular asociada.

Variables	n (%)
Edad, mediana [25-75]	71 [64-76]
Sexo Femenino	47 (55,3)
Hipertensión	73 (85,9)
Sedentarismo	38 (44,7)
Tabaquismo	36(42,4)
Diabetes mellitus	34(40,0)
Alcohol	28 (33,3)
Ataque isquémico transitorio	27 (31,8)
Ictus	6 (7,1)
Dislipidemia	23 (27,0)
Infarto de miocardio	16 (18,8)
Fibrilación auricular previa	14 (16,5)
Insuficiencia Cardiaca	12 (14,1)
Enfermedad Arterial Periférica	10 (11,2)
COVID-19	9 (10,6%)
PAS, mediana [25-75]	146 [138-160]
PAD, mediana [25-75]	90 [80-100]
FC, mediana [25-75]	91 [80-100]
FR, mediana [25-75]	18 [16-20]
S. O_2%, mediana [25-75]	97 [95-98]
CHA_2DS_2VASC, mediana [25-75]	5 [4-6]
6S score [25-75]	11 [8-11]

[25-75]: percentil 25 -75, PAS: Presión arterial sistólica, PAD: Presión arterial diastólica, FC: Frecuencia Cardíaca, FR: Frecuencia Respiratoria, S. O_2%: Saturación de Oxígeno.

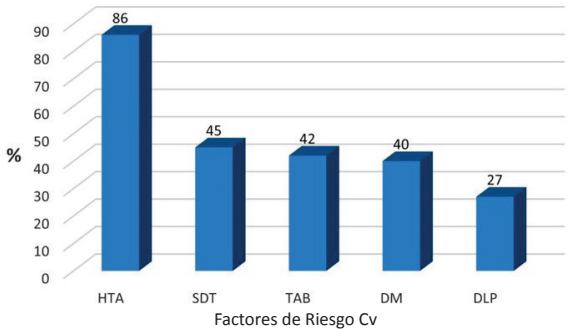

Fig. 1. Características basales de los pacientes. HTA: Hipertensión Arterial, SDT: Sedentarismo, TAB: Tabaquismo, DM: Diabetes, DLP: Dislipidemia.

e intensidad de asociación entre ambas escalas de 19%, siendo esto altamente significativo con una p <0,0001 (Fig. 2).

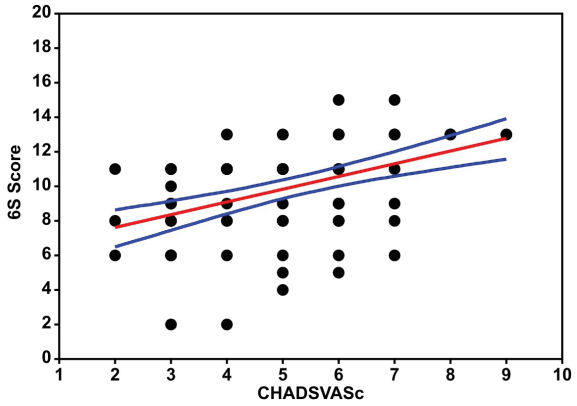

Fig. 2. Correlación entre las escalas CHA_2DS_2-VASc y 6S score en pacientes con ictus y FA, (6S Score: escala de severidad de 6 síntomas). Análisis de regresión polinomial. r=0,433 (p< 0,0001). Ecuación: y=0,737x/6,145.

DISCUSIÓN

En el presente estudio se evaluó, por primera vez, la potencial correlación entre la escala CHA_2DS_2-VASc de riesgo de aparición de ictus agudos en pacientes con FA, frente a la escala 6S de grado severidad de ictus, con la finalidad de determinar si existe una asociación para predecir la severidad de ictus isquémico cardioembólico con la escala CHA_2DS_2-VASc.

En la muestra se evidenció una mediana de edad de 71 años, similar a la registrada en otros estudios relacionados al tema [12, 13]. En cuanto a los factores de riesgo cardiovascular y de riesgo de ictus en pacientes con FA, se encontró la hipertensión arterial como el más frecuente (85,9%); esto coincide de otros estudios publicados [12-14], incluyendo el estudio ICTUSCARE [14], con una muestra de 975 pacientes. De igual forma, la presencia de otros factores de riesgo como la diabetes, dislipidemia, cardiopatía isquémica e insuficiencia cardiaca, fueron similares en los estudios ya referidos; sin embargo, en el presente estudio el tabaquismo fue más elevado que el observado en otros estudios con muestras similares (42,4% vs 22 a 26%) [12-14]. La presencia de FA previa como importante predictor de ictus en el presente estudio fue de 16,5%, mientras que, en el realizado por González Hernández y col, fue de 25% [13]

En relación con el tratamiento de base, que recibían estos pacientes al momento de ingreso, Tabla 2, se observa que la mayoría estaban sub-tratados cuando fueron comparados con otros estudios (González Hernández y col. y el ICTUSCARE [13,14]). Es importante resaltar, el bajísimo porcentaje de pacientes que recibían tratamiento anticoagulante, solo un 5,9% recibían warfarina y ninguno recibía inhibidores del factor Xa o inhibidores directos de trombina; de los 14 pacientes con FA previa, con alto riesgo para ictus cardioembólico, solo 2 (14,3%) recibían warfarina. Esto probablemente se deba - en gran medida- a razones económicas, por tratarse de una institución pública; otra posibilidad pudiera ser, la pasividad de la indicación de anticoagulantes.

Tabla 2
Medicación de los pacientes previo a su ingreso.

Fármaco	n (%)
IECA/ARA-2	56 (65,9)
B-Bloqueantes	23 (27,0)
Estatinas	16 (18,8)
Calcio-antagonistas	15 (17,8)
Diuréticos	8 (9,4)
Amiodarona	5 (5,9)
Aspirina	23 (27,0)
Clopidogrel	11 (12,9)
Warfarina	5 (5,9)
Rivaroxaban	0
Dabigatran	0

IECA/ARA-2: inhibidores de la enzima convertidora de angiotensina I/Antagonista de los receptores de angiotensina 2.

En la actualidad, no existe una escala ideal para predecir el pronóstico de severi-

dad de los ictus isquémicos en pacientes con FA. Se han realizado algunas aproximaciones con las escalas de CHA_2DS_2-VASc en cuanto a desenlaces, como fueron los estudios de Vitturi BK y col. y el de Tanaka y col.[8,9], quienes determinaron que las escalas de $CHADS_2$ y CHA_2DS_2-VASc se asociaron con la severidad del ictus al inicio y el resultado clínico funcional en los pacientes con ictus isquémico agudo y FA concomitante. El estudio de Deguchi y col. [16] y el de Acciarresi y col. [17], encontraron que la gravedad del ictus cardioembólico inicial, inducido por una fibrilación auricular no valvular, aumentó con puntuaciones más elevadas de CHA_2DS_2-VASc, y los resultados clínicos fueron más desfavorables, con aumento de la mortalidad en el seguimiento. Todos estos estudios utilizaron la escala de NIHSS como comparador de severidad de ictus [8,9,16-19].

El presente estudio pretende mostrar que los puntajes más elevados en la escala CHA_2DS_2-VASc se correlacionan con mayor daño neuronal y, por lo tanto, con puntajes más elevados en la escala 6 S score. En los resultados obtenidos de los pacientes que llegan a la emergencia con FA e ictus, se observó que las medianas de los puntajes de las escalas analizadas, CHA_2DS_2-VASc y 6S-Stroke, fueron elevadas en ambas, ubicándolos en las categorías de alto riesgo. El análisis de correlación mostró un nivel bajo, con una intensidad de asociación del 19% entre ambas escalas, pero altamente significativo ($p < 0,0001$), particularmente en los extremos mayores de las escalas. Esto se puede interpretar de la siguiente manera. La mediana de los pacientes para la escala 6S de severidad de ictus fue de 11 [8-11] puntos, por lo que la mayoría de los pacientes que ingresaron estuvieron en el rango de elevada severidad de lesión cerebral, ya que el punto de corte de severidad mayor para la escala 6S es de 10 puntos. En cuanto a la escala CHA_2DS_2-VASc el punto de corte para alto riesgo de presentar ictus cardioembólico en pacientes con FA es igual o mayor a 3 puntos y en la muestra estudiada la mediana fue de 5 [4-6] puntos; por lo tanto, la mayor proporción de pacientes se encontraban en el extremo de alto riesgo cardioembólico y de mayor severidad para lesión neuronal. Este predominio de valores en el extremo de las escalas de mayor riesgo y severidad y la dispersión de los datos generan una atenuación en la correlación.

La alta significación de la correlación detectada permite usar la ecuación de regresión obtenida para calcular la severidad del ictus con la escala 6S a partir de la escala de riesgo CHA_2DS_2-VASc. El valor clínico y diagnóstico de esta ecuación es un objetivo de gran interés para investigaciones futuras.

Limitaciones del estudio

El poder del estudio se ve limitado en parte por el tamaño de la muestra, por otro lado, no se logra una asociación anatomofuncional debido al limitado respaldo de neuro-imágenes, ya que el 55,2% de la población estudiada no contaba con tomografías. Sin embargo, esto no presentó una limitación importante en el objetivo fundamental del estudio, el cual era evaluar la capacidad clínica de una escala diseñada para predecir riesgo de ictus en la estimación de la severidad de ictus de etiología cardioembólica. Esta investigación es de naturaleza exploratoria, con la presunción de generar la base para una mayor confirmación, de una herramienta utilizada para la toma de decisión de anticoagulación, que pudiera ser a su vez útil para la evaluación rápida de pronóstico de severidad de ictus cardioembólico. No se utilizó la escala NIHSS, la cual es mucho más precisa y detallada para la determinación de la severidad del ictus isquémico, debido a su complejidad y al hecho de que en la emergencia de nuestro centro es poco utilizada, por lo que se optó por una escala más sencilla y fácil de usar como es la 6S y que por primera vez, esta última se compara con la escala CHA_2DS_2-VASc.

En conclusión, este estudio muestra un muy bajo uso de anticoagulación en pacientes con alto riesgo para ictus cardioembólico y

que la escala CHA_2DS_2-VASc puede ser una herramienta útil en la emergencia para predecir la severidad clínica del ictus en pacientes con fibrilación auricular, al compararla con la escala 6S en un análisis de correlación.

Financiamiento

No hubo ningún tipo de financiamiento.

Conflicto de interés

Los autores de este trabajo, declaramos no tener ningún conflicto de interés.

Números ORCID de los autores

- Miguel López-Hidalgo (MLH): 0000-0002-3242-2967
- José Luis Pinto (JLP): 0009-0007-2793-5649
- Antonio Eblen-Zajjur (AEZ): 0000-0002-0077-0318
- Euler Regis (ER): 0009-0008-6740-3388
- José Reina (JR): 0009-0005-7229-6773
- Ignacio Poggioli (IP): 0009-0000-5072-5075
- José I. Ramírez (JIR): 0009-0006-9792-514X

Contribución de los autores

MLP: Concepción, diseño, elaboración, obtención de datos, análisis estadístico, interpretación, revisión crítica, aprobación de MS. JLP: Concepción, diseño, interpretación, revisión crítica, aprobación de MS. AEZ: Concepción, diseño, elaboración, análisis estadístico, interpretación, revisión crítica, aprobación de MS. ER: Obtención de datos, análisis estadístico, interpretación, revisión crítica, aprobación de MS. JR: Obtención de datos, análisis estadístico, interpretación, revisión crítica, aprobación de MS. IP: Obtención de datos, interpretación, revisión crítica, aprobación de MS. JIR: Obtención de datos, interpretación, revisión crítica, aprobación de MS.

REFERENCIAS

1. **Braunwald E, Fauci S, Kasper DL, Hauser S, Longo D, Jameson**. Enfermedades Cerebrovasculares. Editor: Serrano H. Harrison Principios de Medicina Interna. 20° Edición, McGraw-Hill Interamericana, Ciudad de México; 2020. p. 2609-12.
2. **Steinberg JS, O'Conell H, Li S, Ziegler PD**. Thirty-second gold standard definition of atrial fibrilation and its relationship with susequent arrythmia patterns. Circulation: Arrythm Electrophys. 2018; 11: e006274
3. **Friberg L, Bergfedlt L**. Atrial fibrillation prevalence revisited. J Intern Med. 2013, 274: 461- 468.
4. **Katsanos AH, Kamel H, Healey JS, Hart RG**. Stroke prevention in atrial fibrilation. Circulation. 2020; 142:2371-2388.
5. **Gage B, Waterman A, Shannon W, Boechler M, Rich MW, Radford MJ.** Validation of clinical classification schemes for predicting stroke: results from the National Registry of Atrial Fibrillation. JAMA 2001; 285 (22): 2864-2870.
6. **Hayashi T.** Do the components of CHA_2DS_2-VAsc score affect stroke severity and outcome. Circ J 2016;80:74-75. https://www.jstage.jst.go.jp/article/circj/80/1/80_CJ-15-1201/_pdf
7. **Jover E, Roldán V, Gallego P, Hernández-Romero D, Valdés M, Vicente V**. Valor predictivo de la escala CHA_2DS_2-VASc en pacientes con fibrilación auricular de alto riesgo embólico en tratamiento anticoagulante. Rev Esp Cardiol 2012; 65, (6): 627-633 https://www.revespcardiol.org/es-valor-predictivo-escala-cha-2ds-articulo-S030089321200190X
8. **Vitturi BK, Gagliardi RJ**. Use of $CHADS_2$ and CHA_2DS_2-VASc scores to predict prognosis after stroke. Rev Neurol 2020;176:85-91 https://www.sciencedirect.com/science/article/pii/S0035378719304692

9. **Tanaka K, Yamada T, Torii T, Furuta K, Matsumoto S, Yoshimura T, Kei-ichiro T, Yoshifumi W, Naoki N, Jun-ichi K., Hiroyuki M.** Pre-admission CHADS2, CHA_2DS_2-VASc, and R2CHADS2 scores on severity and functional outcome in acute ischemic stroke with atrial fibrillation. J Stroke Cerebrovasc Dis 2015;24(7):1629–1635. *http://dx.doi.org/10.1016/j.jstrokecerebrovasdis.2015.03.036*
10. **Leyden P., Brott T, Tilley B, Welch KM, Mascha E.J, Levine S, Haley EC, Grotta J, Marler J.** Improves Reliability of the NIH stroke scale using video training. Stroke 1994; 25:2220-2226. *https://www.ahajournals.org/doi/epdf/10.1161/01.STR.25.11.2220*
11. **Racosta JM, Di Guglielmo F, Klein FR, Riccio PM, Giacomelli FM, González ME**. Stroke Severity Score based on Six Signs and Symptoms the 6S score: A simple tool for assessing stroke severity and in-hospital mortality. J Stroke 2014;16(3):178–183. Disponible en: https://pubmed.ncbi.nlm.nih.gov/25328876/
12. **Racosta J, Klein F, Riccio P, Pagani-Cassar F, Gonzalez-Toledo M, Muñoz-Giacomelli F, Jauregui A, Sposato L**. Simplified symptom-based score for the assessment of ischemic stroke severity. Neurology 2016;78 (1): Supp. 07.003. https://n.neurology.org/content/78/1_Supplement/P07.003
13. **María R, Hidalgo V, Campello AR, Santiago O, Vivanco DRM**. Monitorización cardiaca en la unidad de ictus: importancia del diagnóstico de fibrilación auricular en el ictus isquémico agudo. Rev. Esp Cardiol. 2009; 62(5):564-567. Disponible en: https://www.redheracles.net/media/upload/research/pdf/194060711321522522.pdf
14. **González Hernández A, Fabre Pi O, López Fernández JC, Díaz Nicolás S, Cabrera Hidalgo A.** Factores de riesgo, etiología y pronóstico en pacientes con ictus isquémico y diabetes mellitus. Rev Clin Esp 2008;208(11):546–550. Disponible en: https://www.sciencedirect.com/science/article/pii/S0014256508760314
15. **Abellán Alemán J, Ruilope Urioste LM, Leal Hernández M, Armario García P, Tiberio López G, Martell Claros N.** Control de los factores de riesgo cardiovascular en pacientes con ictus atendidos en Atención Primaria en España. Estudio ICTUSCARE. Med Clin. 2011;136(8):329–335. Disponible en: https://www.sciencedirect.com/science/article/pii/S0025775310009504
16. **Deguchi I, Hayashi T, Ohe Y, Kato Y, Nagoya H, Fukuoka T**. The CHA(2)DS(2)-VASc score reflects clinical outcomes in nonvalvular atrial fibrillation patients with an initial cardioembolic stroke. J Stroke Cerebrovasc Dis 2013;22(8):e34334-6. Disponible en: *http://dx.doi.org/10.1016/j.jstrokecerebrovasdis.2013.02.01817*
17. **Acciarresi M, Paciaroni M, Agnelli G, Falocci N, Caso V, Becattini C, Marcheselli S, Rueckert C, Pezzini A.** Prestroke CHA2DS2-VASc Score and Severity of Acute Stroke in patients with atrial fibrillation, findings from RAF study. J Stroke & Cerebrovas Dis 2017, 26 (6): 1363-1368**.** *https://doi.org/10.1016/j.jstrokecerebrovasdis.2017.02.011*
18. **Nasifov M, Ozmen E, Deniz C, Nadir A**. Association of CHA2DS2-VASc with successful recanalization in acute ischemic stroke patients undergoing endovascular thrombectomy. Adv Interv Cardiol 2022;18,3 (69):269-275.
19. **Wu HM, Chung CP, Lin YY**. Similar thrombolysis outcome in acute stroke patients with and without atrial fibrillation if prestroke CHA2DS2-VASc score is low. Medicine 2020; 99:2.

Invest Clin 65(4): 426 - 435, 2024 https://doi.org/10.54817/IC.v65n4a03

Correlations of serum 25-hydroxy-vitamin D, $CD4^+CD25^+CD127^-$ regulatory T cells and total immunoglobulin E in children with recurrent respiratory tract infections.

Yanfei Yang, Na Fan, Xingzhu Liu, Lin Wang, Zhihai Wang, Yao Hou, Ting Wang and Yuqin Wu

Ward of Special Needs, Kunming Children's Hospital. Yunnan Province, China.

Keywords: cluster of differentiation; correlation; 25-hydroxy-vitamin D; immunoglobulin; recurrent respiratory tract infection; regulatory T cell.

Abstract. Recurrent respiratory tract infections (RRTIs) have a complex pathogenic mechanism. There may be correlations between expression levels of serum 25-hydroxy-vitamin D (25-OH-D), regulatory T cells (Tregs), total immunoglobulin E (IgE) and RRTIs. We aimed to explore the correlations of serum 25-OH-D, cluster of differentiation 4 $(CD4)^+CD25^+CD127^-$ Tregs and total IgE in children with RRTIs. A total of 150 children with pneumonia were enrolled as the subjects and randomly assigned into a control group (97 children with non-RRTIs) and an observation group (53 children with RRTIs). The expression levels of serum 25-OH-D, $CD4^+CD25^+CD127^-$ Tregs and total IgE were compared in RRTI children with different genders, stages, sites of lesions and severities of illness. The correlation was tested by Pearson analysis. The expression level of serum 25-OH-D was significantly higher in children with RRTIs in the upper respiratory tract than that in the lower respiratory tract, whereas the expression level of total IgE was significantly lower in children with RRTIs in the upper respiratory tract ($p<0.05$). The expression level of 25-OH-D was negatively correlated with expression levels of $CD4^+CD25^+CD127^-$ Tregs and total IgE (r=-0.355, -0.314, $p<0.05$), while a positive correlation was found between expression levels of $CD4^+CD25^+CD127^-$ Treg and total IgE (r=0.237, $p<0.05$). The area under the curve of combination of 25-OH-D, $CD4^+CD25^+CD127^-$ Treg and total IgE expression levels for predicting RRTIs was 0.852. The combined detection of the three indicators is conducive to enhancing the detection rate of RRTIs.

Corresponding authors: Ting Wang & Yuqin Wu. Ward of Special Needs, Kunming Children's Hospital, Kunming 650103, Yunnan Province, China. Email: wangtingkch@ltyz-edu.cn; qudas0@163.com

Las correlaciones séricas de 25-hidroxivitamina D, $CD4^+CD25^+CD127^-$ linfocitos T reguladores e inmunoglobulina E total en niños con infecciones recurrentes del tracto respiratorio.

Invest Clin 2024; 65 (4): 426 – 435

Palabras clave: cluster of differentiation; correlacion; 25-hidroxi-vitamina D; inmunoglobulina; infeccion recurrente del tracto respiratorio, T cell reguladora.

Resumen. Las infecciones recurrentes del tracto respiratorio (ITRR) tienen un mecanismo patogénico complejo. Puede haber correlaciones entre los niveles de expresión de 25-hidroxivitamina D (25-OH-D) sérica, células T reguladoras (Treg), inmunoglobulina E total (IgE) y RRTI. Nuestro objetivo fue explorar las correlaciones de la 25-OH-D sérica, el grupo de diferenciación 4 $(CD4)^+CD25^+CD127^-$ Tregs y la IgE total en niños con IRRR. Se inscribió un total de 150 niños con neumonía como sujetos y se los asignó aleatoriamente a un grupo de control (97 niños sin RRTI) y un grupo de observación (53 niños con RRTI). Se compararon los niveles de expresión de 25-OH-D, $(CD4)^+CD25^+CD127^-$ Tregs en suero y de IgE total en niños con RRTI con diferentes géneros, estadios, sitios de lesiones y gravedad de la enfermedad. La correlación fue probada mediante análisis de Pearson. El nivel de expresión de 25-OH-D sérico fue significativamente mayor en niños con IRRI en el tracto respiratorio superior que en el tracto respiratorio inferior, mientras que el nivel de expresión de IgE total fue significativamente menor en niños con IRRI en el tracto respiratorio superior ($p<0,05$). El nivel de expresión de 25-OH-D se correlacionó negativamente con los niveles de expresión de $(CD4)^+CD25^+CD127^-$ Tregs y la IgE total ($r=-0,355$, $-0,314$, $p<0,05$), mientras que se encontró una correlación positiva entre los niveles de expresión de $(CD4)^+CD25^+CD127^-$ Treg e IgE total ($r=0,237$, $p<0,05$). El área bajo la curva de combinación de los niveles de expresión de 25-OH-D, $(CD4)^+CD25^+CD127^-$ Treg y de IgE total para predecir IRRI fue de 0,852. La detección combinada de los tres indicadores conduce a mejorar la tasa de detección de IRRI.

Received: 09-04-2024 Accepted: 25-08-2024

INTRODUCTION

Recurrent respiratory tract infections (RRTIs) possess a relatively complex pathogenic mechanism, which involves various pathogenic factors. Children are susceptible to RRTIs, with a major age of onset of 2-6 years old, and in terms of the prevalence rate, children with RRTIs account for approximately 20.00% of children with respiratory infections [1,2]. The incidence rate of RRTIs is about 16.80-18.70% in children in China, and 80.00% of children with RRTIs are aged below 5 years old [3]. 25-hydroxyvitamin D (25-OH-D) is mainly metabolized by vitamin D-25-hydroxylase. Studies have manifested that 25-OH-D is implicated in the development and progression of RRTIs,

exerting a profound impact on the body immunity of developing children [4,5]. Regulatory T cells (Tregs), a common subset of T cells, control the autoimmune response of the body. Animal experiments have revealed that the content of Tregs [cluster of differentiation 4 $(CD4)^+CD25^+$ Forkhead box P3 (Foxp3) Tregs] is higher in RRTI mice than that in normal mice, but it declines significantly after drug intervention [6,7]. Generally, immunoglobulin E (IgE) is mainly produced in plasma cells of the respiratory and digestive tracts, which has an extremely low expression level in blood of normal people (about 0.002% of total Ig in serum), and its abnormal expression is related to the development and progression of some diseases, including RRTIs.[8] Based on the above analysis, it can be concluded that there are certain correlations between expression levels of serum 25-OH-D, Tregs and total IgE and RRTIs.Kunming is situated in the Yunnan-Guizhou Plateau, China, where the incidence of RRTIs may be of specific characteristics. In addition, research on the relationship between RRTIs and expressions of 25-OH-D, $CD4^+CD25^+CD127^-$ Tregs and total IgE is lacking (or rare) at present, so it is necessary to carry out such research. In this study, therefore, the expression levels and relationships of 25-OH-D, $CD4^+CD25^+CD127^-$ Tregs and total IgE were explored with 150 children with pneumonia (including 53 children with RRTIs) as the subjects, aiming to provide a basis for clinical diagnosis and treatment of children with RRTIs in the plateau section.

PATIENTS AND METHODS

General data

According to the guidelines of the Declaration of Helsinki, the study was performed with approvals from the medical ethics committee of our hospital. One hundred and fifty children with pneumonia admitted to and treated in Kunming Children's Hospital, China from January 2020 to January 2023 were selected as the subjects. The children were assigned into a control group (97 children with non-RRTIs) and an observation group (53 children with RRTIs) using a random number table.

The inclusion criteria for the observation group were set as follows: 1) children aged 0-12 years old, without gender requirement, 2) those who were diagnosed with pneumonia and met the diagnostic criteria for RRTIs, 3) those who lived in the jurisdiction of Kunming, China and 4) those whose family members and caregivers had signed the informed consent and who were willing to participate in this study. The inclusion criteria for the control group were as follows: 1) children aged 0-12 years old, without gender requirement, 2) those who were diagnosed with pneumonia and did not meet the diagnostic criteria for RRTIs, 3) those who lived in the jurisdiction of Kunming, China, and 4) those whose family members and caregivers had signed the informed consent and who were willing to participate in this study.

The exclusion criteria involved: 1) children with all kinds of congenital diseases, cancers (liver, lung, brain, pancreas, thyroid, *etc.*) or severe deformities, 2) those with various hematological, immunological or motor disorders, 3) those with airway obstruction, external tracheal compression, asthma, bronchiectasis or foreign bodies in the bronchus, 4) those with abnormal diet (including those with various nutritional diseases), 5) those who had taken immunosuppressants within 3 months before enrollment, 6) those with hereditary or metabolic diseases, 7) those with anemia or obesity ($BMI>P_{95}$), or 8) those whose family members and caregivers were not informed or had not signed the informed consent or who had incomplete clinical data.

The control group was composed of 97 patients, including 61 (62.89%) boys and 36 (37.11%) girls, aged 0-12 (4.12 ± 1.25) years old. As to severity of illness, there were 51 mild cases, 24 moderate cases and 22 se-

vere cases. The observation group consisted of 53 patients, including 33 (62.26%) boys and 20 (37.74%) girls, with an age of 0-12 (4.23±1.27) years old. In terms of severity of illness, there were 27 mild cases, 16 moderate cases and 10 severe cases, respectively. As to the site of lesions, there were 34 and 19 cases of upper and lower respiratory tract infections, respectively. The general data such as age, gender and severity of illness were of no significant differences between the two groups ($p>0.05$), which were comparable.

Detection methods

After admission, the demographic data (age, gender, *etc.*) of patients were collected in both groups. The next morning, an appropriate amount (5 mL) of venous blood was collected from the elbow of each child in the company of their family members and caregivers. Then, the blood was centrifuged with a centrifuge (Beckman Coulter, USA, Optima MAX -TL) under the following conditions: centrifugal radius of 15 cm, centrifugal rate of 2000 rpm and centrifugal time of 5 min. Afterwards, the serum was harvested for measurement of 25-OH-D, $CD4^+CD25^+CD127^-$ Treg and total IgE expression levels. The expression level of 25-OH-D was detected by magnetic microparticle chemiluminescence assay, while the expression levels of $CD4^+CD25^+CD127^-$ Tregs and total IgE were measured by a flow cytometer and an automatic protein analyzer, respectively. The measurement was conducted strictly according to the specific standard operating procedures for detecting 25-OH-D, $CD4^+CD25^+CD127^-$ Tregs and total IgE [9].

The expressions of serum 25-OH-D, Tregs and total IgE in observation and control groups were measured and compared. Additionally, the expressions of serum 25-OH-D, $CD4^+CD25^+CD127^-$ Tregs and total IgE in the observation group at different stages (remission stage and attack stage), genders (boy and girl), sites of lesions (upper and lower respiratory tracts) and severities of illness (mild, moderate and severe) were measured and compared.

Statistical analysis

An Excel database was created, in which the baseline data and research data of all subjects were classified, numbered and counted. Next, such data were included in SPSS 23.0 software for processing. Count data were subjected to the χ^2 test and expressed as rate or percentage (%). Measurement data were expressed by mean ± standard deviation and subjected to the *t* test, and analysis of variance was employed for pairwise comparison of means of three samples. The correlation was tested by Pearson analysis. Receiver operating characteristic (ROC) curves were plotted, based on which the areas under ROC curves (AUCs) were calculated to analyze the predictive values of expression levels of 25-OH-D, $CD4^+CD25^+CD127^-$ Tregs and total IgE for the incidence of RRTIs. The value of AUC was between 0 and 1, where 1 represented a perfect classification and 0.5 represented random guessing. The best classification threshold was selected based on the ROC curve. At the selected optimal cutoff value, the corresponding sensitivity (true positive rate) and specificity (true negative rate) were calculated. At the selected cutoff value, the false positive rate (1-specificity) and false negative rate (1-sensitivity) were calculated. The significant level was set as $\alpha=0.05$ (bilateral), and $p<0.05$ denoted that the difference was statistically significant.

RESULTS

Expression levels of serum 25-OH-D, $CD4^+CD25^+CD127^-$ Tregs and total IgE in the two groups

The expression level of serum 25-OH-D in the observation group was significantly lower than that in the control group, whereas the expression levels of $CD4^+CD25^+CD127^-$ Tregs and total IgE were significantly higher than those in the control group ($p<0.05$) (Table 1).

Expression levels of 25-OH-D, $CD4^+CD25^+CD127^-$ Tregs and total IgE in children with RRTIs at different stages in the observation group

Children with RRTIs at remission stage in the observation group had a significantly lower expression level of serum 25-OH-D and significantly higher expression levels of $CD4^+CD25^+CD127^-$ Tregs and total IgE than those of the control group ($p<0.05$) (Table 2).

Expression levels of 25-OH-D, $CD4^+CD25^+CD127^-$ Tregs and total IgE in RRTI boys and girls in the observation group

In comparison with RRTI girls, RRTI boys exhibited comparable expression levels of serum 25-OH-D and $CD4^+CD25^+CD127^-$ Tregs ($p>0.05$), but a slightly elevated expression level of total IgE ($p<0.05$) (Table 3).

Expression levels of 25-OH-D, $CD4^+CD25^+CD127^-$ Tregs and total IgE in children with different severities of RRTIs in the observation group

A lower expression level of serum 25-OH-D and higher expression levels of $CD4^+CD25^+CD127^-$ Tregs and total IgE were detected in children with severe RRTIs compared to those in children with mild and moderate RRTIs ($p<0.05$) (Table 4).

Expression levels of 25-OH-D, $CD4^+CD25^+CD127^-$ Tregs and total IgE in children with RRTIs in the upper and lower respiratory tracts in the observation group

The expression level of serum 25-OH-D in children with RRTIs in the upper respiratory tract was significantly higher than that in the lower respiratory tract, and the ex-

Table 1
Expression levels of serum 25-OH-D, $CD4^+CD25^+CD127^-$ Tregs and total IgE in the two groups

Group	*n*	25-OH-D (ng/mL)	CD4+CD25+CD127-Treg (%)	Total IgE (U/mL)
Control	97	25.34±3.68	4.87±1.32	81.62±10.28
Observation	53	15.58±2.27	7.15±1.84	233.17±18.62
t		17.554	8.864	64.305
p		<0.05	<0.05	<0.05

Table 2
Expression levels of 25-OH-D, $CD4^+CD25^+CD127^-$ Tregs and total IgE in children with RRTIs at different stages in the observation group.

Stage	*n*	25-OH-D (ng/mL)	CD4+CD25+CD127-Treg (%)	Total IgE (U/mL)
Remission	53	22.31±2.25	4.48±1.34	98.67±12.33
Attack	53	15.64±2.17	6.81±1.55	233.61±19.55
t		15.534	8.279	42.502
p		<0.05	<0.05	<0.05

Table 3
Expression levels of 25-OH-D, $CD4^+CD25^+CD127^-$ Tregs and total IgE in RRTI boys and girls in the observation group.

Gender	*n*	25-OH-D (ng/mL)	CD4+CD25+CD127-Treg (%)	Total IgE (U/mL)
Girl	20	15.57±2.26	6.25±1.37	232.51±19.82
Boy	33	15.82±2.23	6.72±1.43	234.57±20.59
t		0.573	1.728	2.045
p		0.568	0.087	0.043

Table 4
Expression levels of 25-OH-D, $CD4^+CD25^+CD127^-$ Tregs and total IgE in children with different severities of RRTIs in the observation group.

Severity	*n*	25-OH-D (ng/mL)	CD4+CD25+CD127-Treg (%)	Total IgE (U/mL)
Mild	27	15.57±2.26	4.15±1.02	201.33±16.55
Moderate	16	15.82±2.23	5.84±1.23a**	239.75±20.58a**
Severe	10	13.08±1.85b**c*	6.89±1.52b**c	292.61±23.57b**c**
F		5.75	22.99	84.11
p		0.057	0.0000	0.0000

q test (Newman-Keuls method) for pairwise comparison of sample means (3), a: the first *vs.* the second, b: the first *vs.* the third, c: the second *vs.* the third. *p<0.05, **p<0.01.

Table 5
Expression levels of 25-OH-D, $CD4^+CD25^+CD127^-$ Tregs and total IgE in children with RRTIs in the upper and lower respiratory tracts in the observation group.

Site	*n*	25-OH-D (ng/mL)	$CD4^+CD25^+CD127^-$ Treg (%)	Total IgE (U/mL)
Upper respiratory tract	34	16.23±2.58	6.12±1.25	226.87±17.88
Lower respiratory tract	19	13.34±2.27	6.58±1.33	250.64±23.58
t		6.122	1.835	5.848
p		<0.05	0.069	<0.05

pression level of total IgE was significantly lower than that in the lower respiratory tract (p<0.05) (Table 5).

Results of correlation analysis

The results of Pearson correlation analysis revealed negative correlations of the expression level of serum 25-OH-D with the expression levels of $CD4^+CD25^+CD127^-$ Tregs and total IgE (r=-0.355, -0.314, p<0.05) and a positive correlation between expression levels of $CD4^+CD25^+CD127^-$ Tregs and total IgE (r=0.233, p<0.05) (Fig. 1).

Analysis results of predictive value

The AUC value of combination of 25-OH-D, $CD4^+CD25^+CD127^-$ Tregs and total IgE for predicting the incidence of RRTIs was 0.852, which was significantly larger than that of any of the three indicators alone (0.752, 0.654 and 0.643, respectively; p<0.05) (Fig. 2).

DISCUSSION

The expression level of 25-OH-D in children with RRTIs (0.5 months to 14 years old) is lower than that in healthy children (control group), and the insufficiency or deficiency of vitamin D is related to the occurrence of RRTIs [4]. The lack of serum 25-(OH)-D3 in children with RRTIs is an important reason for the decreased expression level of plasma LL-37 (one of the Cathelicidin antimicrobial peptides) [10]. This suggests that RRTI children have obvious vitamin D deficiency or deficit. In this study, the expression level of 25-OH-D in children with RRTIs was abnormal, which was significantly decreased compared with that in the control group (children with non-RRTIs). Such a decrease in the expression level of serum 25-OH-D may be ascribed to the following factors. Firstly, the immunomodulatory function of vitamin D is related to the expression of vitamin D

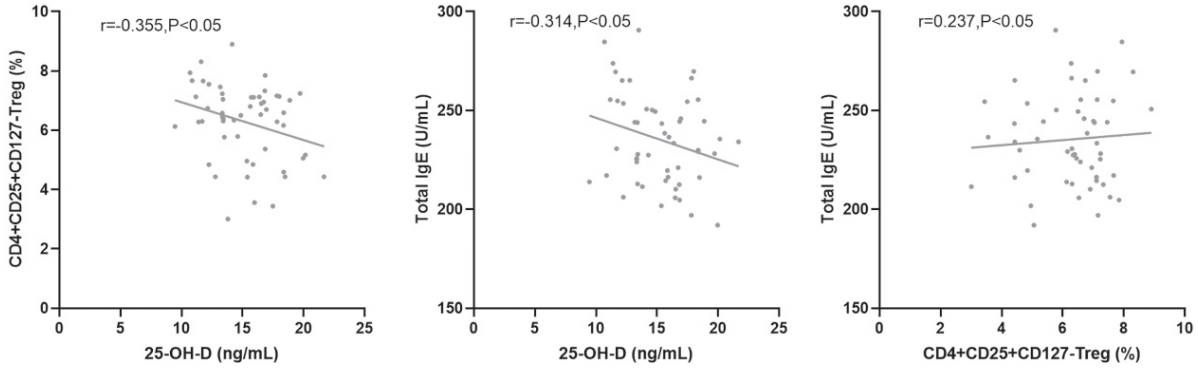

Fig. 1. Correlation analysis results of 25-OH-D, $CD4^+CD25^+CD127^-$ Tregs and total IgE levels.

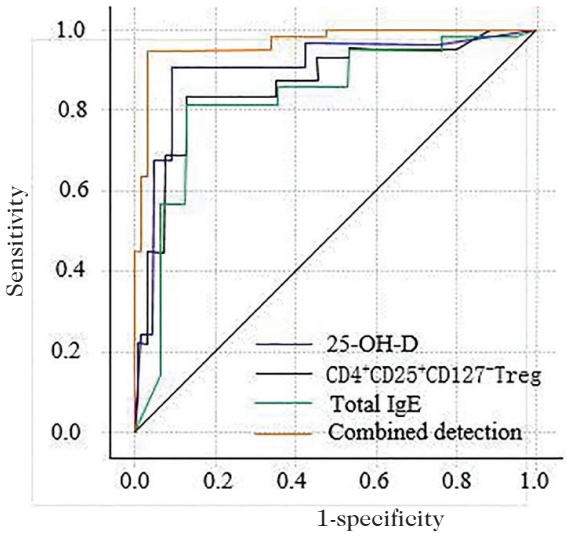

Fig. 2. ROC curves of predictive values of $CD4^+CD25^+CD127^-$ Tregs and total IgE for the incidence of RRTIs.

receptors (in vascular endothelium, myocardium, skeletal muscle, immune cells, *etc.*). Vitamin D receptors have been confirmed to have no expression in resting T lymphocytes. However, when the body is infected, T lymphocytes are activated and can participate in the mediation of 25-OH-D by expressing cytochrome P450 family member 27B1, and make it transform into $1,25(OH)_2D$. On this condition, the endogenous nature of vitamin D receptors is activated by stimuli, followed by combination (vitamin D and its receptors) and joint action to promote immune cells to produce corresponding cytokines, playing the role of immune regulation. As a result, body immunity is enhanced [11,12]. Secondly, 25-OH-D can interact with macrophages and monocytes, producing tubulins and defensins with antibacterial and antiviral activities in the induction period, thus affecting the phagocytic ability and chemotaxis of macrophages and monocytes, and enhancing the differentiation of monocytes to macrophages [13]. It follows that the decrease in the expression level of serum 25-OH-D in children with RRTIs is related to insufficient intake of vitamin D and repressed expression of vitamin D receptors.

Tregs impede the activation and proliferation of target cells inhibiting the expression of CD25 (interleukin-2 receptor subunit alpha, IL-2Ra) chain on the surface of target cells. Second, Tregs suppress the proliferation of effector cells and immunocompetence [14], i.e. Tregs secrete such inhibitory cytokines as IL-10 and transforming growth factor-β to participate in immune suppression of the body. In this study, the expression level of $CD4^+CD25^+CD127^-$ Tregs in children with RRTIs was subjected to a control study from the perspectives of disease stage, gender, site of lesions and severity of illness. It was found that the expression level of $CD4^+CD25^+CD127^-$ Tregs in children with RRTIs was abnormal, which was significantly higher than that in the control group (children with non-RRTIs), implying that the development and progression of RRTIs in children

are influenced by $CD4^+CD25^+CD127^-$ Tregs. Schenck *et al.* found that the expression level of lymphocytes (CD3, CD4) in RRTI children was lower than that in the control group (healthy children) [15]. Moreover, $CD4^+CD25^+CD127^-$ Tregs can effectively inhibit the immune response mediated by $CD4^+$ and $CD8^+$ effector cells[16,17]. This shows that $CD4^+CD25^+CD127^-$ Tregs exhibit abnormal proliferation and activation in RRTI children, giving rise to enhanced response advantage of Tregs, breaking the balance between T helper type 1 (Th1)/Th2/Th17 cell system and Treg cell system, and leading to the disorder of immune regulation. Eventually, RRTIs develop and progress.

In this study, the expression level of total IgE in children with RRTIs was compared from disease stage, gender, site of lesions and severity of illness. The results showed that the expression level of total IgE in children with RRTIs was abnormal and higher than that in the control group (children with non-RRTIs), signifying that the abnormal expression of total IgE is related to the development and progression of RRTIs. This is attributed to the fact that repeated respiratory infections affect the antigens, leading to the exhaustion of the immune system and increasing the expression level of total IgE in serum.

The results of Pearson correlation analysis uncovered that the expression level of serum 25-OH-D was negatively correlated with the expression levels of $CD4^+CD25^+CD127^-$ Tregs and total IgE (r=-0.355, -0.314), while the expression level of $CD4^+CD25^+CD127^-$ Tregs was positively correlated with that of total IgE (r=0.237). This demonstrates that the development and progression of RRTIs is a comprehensive pathological process, which may be caused by the interaction of serum 25-OH-D, $CD4^+CD25^+CD127^-$ Tregs and total IgE. It has previously been reported that the children with RRTIs (196 children aged 1 to 18 years old) had reduced serum 25-OH-D expression levels (61.00%), and vitamin D expression level was negatively correlated with age [18]. In this state, the expression levels of immunoglobulins (IgA, IgG) in children with RRTIs also decrease [19]. In this study, when the expression level of serum 25-OH-D in children with RRTIs dropped, that of total IgE rose, *i.e.*, there was a negative correlation between the two. It suggests that serum 25-OH-D may be involved in mediation of humoral immunity. Beale *et al*. proved that the severity of RRTIs was correlated with the level of vitamin D, and in RRTI children with a low immune level, the serum 25-OH-D level showed a positive relationship with the severity of RRTIs [20]. Hatam *et al*. confirmed that $CD4^+CD25^+CD127^-$ Tregs were abnormally expressed in children with RTTIs, which was an important pathogenesis of RRTIs.[21] It can be concluded that serum 25-OH-D, $CD4^+CD25^+CD127^-$ Tregs and total IgE may participate in the development and progression of RRTIs through interaction. Moreover, it was also found in this study that the AUC value of combination of 25-OH-D, $CD4^+CD25^+CD127^-$ Tregs and total IgE for predicting the incidence of RRTIs was 0.852, which was larger than that of any of the three indicators alone, with significant differences. Collectively, the combined detection of the three indicators is beneficial to improving the detection rate of RRTIs.

Nevertheless, this study is limited. The obtained predictive values are focused on the analysis of global RRTIs (upper and lower respiratory tract) compared to non-RRTIs. Further studies are ongoing in our group.

In summary, serum 25-OH-D, $CD4^+CD25^+CD127^-$ Tregs and total IgE are abnormally expressed in children with RRTIs, and their expressions are of great differences among children at different stages, sites of lesions and severities of illness. The expression of 25-OH-D has negative correlations with the expressions of $CD4^+CD25^+CD127^-$ Tregs and total IgE, and a positive correlation is observed between

the expressions of $CD4^+CD25^+CD127^-$ Tregs and total IgE. The combined detection of serum 25-OH-D, $CD4^+CD25^+CD127^-$ Tregs and total IgE is conducive to enhancing the detection rate of RRTIs.

ACKNOWLEDGMENTS

None.

Funding

This study was financially supported by the Health Science and Research Project of Kunming Municipal Health Commission (No. 2022-06-01-005).

Conflict of interest

The authors declare no conflict of interest.

ORCID's number authors

- Yanfei Yang (YY): 0009-0006-6324-5357
- Na Fan (NF): 0009-0000-9635-0360
- Xingzhu Liu (XL): 0009-0001-6107-5677
- Lin Wang (LW): 0009-0004-4028-0577
- Zhihai Wang (ZW): 0009-0007-0753-7782
- Yao Hou (YH): 0009-0003-6697-7391
- Ting Wang (TW): 0009-0007-9197-7499
- Yuqin Wu (YW): 0009-0008-1137-5250

Contribution of the authors

YY, TW and YW designed this study and significantly revised this paper; NF, XL, LW, ZW and YH performed this study and drafted this paper. All authors have approved the submission and publication of this paper.

REFERENCES

1. **Paśnik J.** Vaccines nonspecific - immunostimulation in patients with recurrent respiratory infections. Otolaryngol Pol 2016; 70(6): 31-39. *https://doi.org/10.5604/01.3001.0009.4819*
2. **Dong F, Yu H, Ma J, Wu L, Liu T, Lv G, Zhen J, Li X, Lewith G, Gu X.** Exploring association between gastrointestinal heat retention syndrome and recurrent respiratory tract infections in children: a prospective cohort study. BMC Complement Altern Med 2016; 16: 82. *https://doi.org/10.1186/s12906-016-1062-8*
3. **Wang X, Li X, Jin C, Bai X, Qi X, Wang J, Zhang L, Li N, Jin N, Song W, Gao H, Gao B, Zhang Y, Wang L.** Association between serum Vitamin A levels and recurrent respiratory tract infections in children. Front Pediatr 2021; 9: 756217. *https://doi.org/10.3389/fped.2021.756217*
4. **Zhang X, Ding F, Li H, Zhao W, Jing H, Yan Y, Chen Y.** Low serum levels of vitamins A, D, and E are associated with recurrent respiratory tract infections in children living in Northern China: A case control study. PLoS One 2016; 11(12): e0167689. *https://doi.org/10.1371/journal.pone.0167689*
5. **Magnus MC, Stene LC, Håberg SE, Nafstad P, Stigum H, London SJ, Nystad W.** Prospective study of maternal mid-pregnancy 25-hydroxyvitamin D level and early childhood respiratory disorders. Paediatr Perinat Epidemiol 2013; 27(6): 532-541. *https://doi.org/10.1111/ppe.12080*
6. **Chen X, Murakami T, Oppenheim JJ, Howard OMZ.** Differential response of murine CD4+CD25+ and CD4+CD25- T cells to dexamethasone-induced cell death. Eur J Immunol 2004; 34(3): 859-869. *https://doi.org/10.1002/eji.200324506*
7. **Chen M, Deng H, Zhao Y, Miao X, Gu H, Bi Y, Zhu Y, Guo Y, Shi S, Xu J, Zhao D, Liu F.** Toll-Like Receptor 2 modulates pulmonary inflammation and TNF-α release mediated by *Mycoplasma pneumoniae*. Front Cell Infect Microbiol 2022; 12: 824027. *https://doi.org/10.3389/fcimb.2022.824027*

8. **Ruskamp J, Smit H, Rovers M, Hoekstra M, Schilder A, Brunekreef B, Wijga A, Kerkhof M, de Jongste J, Sanders E.** Neonatal total IgE and respiratory tract infections in children with intrauterine smoke exposure. Arch Dis Child 2010; 95(6): 427-431. *https://doi.org/10.1136/adc.2009.162685*
9. **Fu Y, Lou H, Wang C, Lou W, Wang Y, Zheng T, Zhang L.** T cell subsets in cord blood are influenced by maternal allergy and associated with atopic dermatitis. Pediatr Allergy Immunol 2013; 24(2): 178-186. *https://doi.org/10.1111/pai.12050*
10. **Eroglu C, Demir F, Erge D, Uysal P, Kirdar S, Yilmaz M, Kurt Omurlu I.** The relation between serum vitamin D levels, viral infections and severity of attacks in children with recurrent wheezing. Allergol Immunopathol 2019; 47(6): 591-597. *https://doi.org/10.1016/j.aller.2019.05.002*
11. **Ginde AA, Mansbach JM, Camargo CA Jr.** Association between serum 25-hydroxyvitamin D level and upper respiratory tract infection in the Third National Health and Nutrition Examination Survey. Arch Intern Med 2009; 169(4): 384-390. *https://doi.org/10.1001/archinternmed.2008.560*
12. **Korf H, Decallonne B, Mathieu C.** Vitamin D for infections. Curr Opin Endocrinol Diabetes Obes 2014; 21(6): 431-436. *https://doi.org/10.1097/MED.0000000000000108*
13. **Watkins RR, Lemonovich TL, Salata RA.** An update on the association of vitamin D deficiency with common infectious diseases. Can J Physiol Pharmacol 2015; 93(5): 363-368. *https://doi.org/10.1139/cjpp-2014-0352*
14. **Qin S, Li L, Liu J, Zhang J, Xiao Q, Fan Y, Wei X.** CD4+CD25+Foxp3+ regulatory T cells regulate immune balance in unexplained recurrent spontaneous abortion via the Toll-like receptor 4/nuclear factor-κB pathway. J Int Med Res 2020; 48(12): 300060520980940. *https://doi.org/10.1177/0300060520980940*
15. **Schenck LP, Surette MG, Bowdish DM.** Composition and immunological significance of the upper respiratory tract microbiota. FEBS Lett 2016; 590(21): 3705-3720. *https://doi.org/10.1002/1873-3468.12455*
16. **Brusko TM, Hulme MA, Myhr CB, Haller MJ, Atkinson MA.** Assessing the in vitro suppressive capacity of regulatory T cells. Immunol Invest 2007; 36(5-6): 607-628. *https://doi.org/10.1080/08820130701790368*
17. **Tang Q, Bluestone JA.** The Foxp3+ regulatory T cell: a jack of all trades, master of regulation. Nat Immunol 2008; 9(3): 239-244. *https://doi.org/10.1038/ni1572*
18. **Ramasamy I.** Vitamin D metabolism and guidelines for Vitamin D supplementation. Clin Biochem Rev 2020;41(3):103-126. *https://doi.org/10.33176/AACB-20-00006*
19. **Dąbrowska-Leonik N, Bernatowska E, Pac M, Filipiuk W, Mulawka J, Pietrucha B, Heropolitańska-Pliszka E, Bernat-Sitarz K, Wolska-Kuśnierz B, Mikołuć B.** Vitamin D deficiency in children with recurrent respiratory infections, with or without immunoglobulin deficiency. Adv Med Sci 2018; 63(1): 173-178. *https://doi.org/10.1016/j.advms.2017.08.001*
20. **Beale DJ.** Analysis leads to unreliable results in study of Vitamin D and acute respiratory infection. J Am Geriatr Soc 2017; 65(5): 1103. *https://doi.org/10.1111/jgs.14797*
21. **Hatam LJ, Devoti JA, Rosenthal DW, Lam F, Abramson AL, Steinberg BM, Bonagura VR.** Immune suppression in premalignant respiratory papillomas: enriched functional CD4+Foxp3+ regulatory T cells and PD-1/PD-L1/L2 expression. Clin Cancer Res 2012; 18(7): 1925-1935. *https://doi.org/10.1158/1078-0432.CCR-11-2941*.

Invest Clin 65(4): 436 - 444, 2024 https://doi.org/10.54817/IC.v65n4a04

Karyotype analysis of fetus in pregnant women with different indications for amniocentesis.

Cen Ma, Lingyan Sun and Li Li

Department of Obstetrics and Gynecology Laboratory, The First Affiliated Hospital of Soochow University, Suzhou, China.

Keywords: prenatal diagnosis; amniocentesis; karyotype analysis; chromosomal abnormalities.

Abstract. To analyze the karyotype distribution in 1285 pregnant women and evaluate the association between karyotype and diagnostic indications of fetal chromosomal abnormalities, 1285 pregnant women with prenatal diagnostic indications and successful amniocentesis admitted to our hospital from July 2019 to June 2022 were selected as study subjects for fetal karyotype analysis. The distribution of prenatal diagnostic indications and abnormal karyotypes were recorded, and the association between abnormal karyotypes and different diagnostic indications was analyzed. Ninety-six abnormal chromosomal karyotypes in amniotic fluid cells were detected in the samples, with an abnormality rate of 7.47%. Chromosome numerical abnormalities accounted for 70.83% (68/96), and the detection rate was 5.29% (68/1285), the most common category of abnormal kariotypes, trisomy 21, was the most common among them, accounting for 44.79% (43/96). Advanced maternal age and high risk of serologic screening were the main indications for prenatal diagnosis. The highest detection rates were for abnormal non-invasive prenatal DNA testing and one parent carrying chromosome abnormality, 27.63% and 42.86%, respectively. Karyotype analysis of pregnant women with indications for amniocentesis is effective in screening for fetal chromosomal abnormalities and reducing congenital anomalies.

Corresponding author: Li Li, Department of Obstetrics and Gynecology Laboratory, The First Affiliated Hospital of Soochow University, Suzhou, China. E-mail: lili_edu.suda@hotmail.com

Análisis del cariotipo fetal de embarazadas con diferentes indicaciones de amniocentesis.

Invest Clin 2024; 65 (4): 436 – 444

Palabras clave: diagnóstico prenatal; amniocentesis; análisis del cariotipo; anomalías cromosómicas.

Resumen. El objetivo fue analizar la distribución del cariotipo de mujeres embarazadas y evaluar la asociación entre el cariotipo y las indicaciones diagnósticas de anomalías cromosómicas fetales. Un total de 1285 mujeres embarazadas, con indicaciones de diagnóstico prenatal y amniocentesis exitosa, admitidas en nuestro hospital desde julio de 2019 hasta junio de 2022 fueron seleccionadas como sujetos de estudio para el análisis del cariotipo fetal. Se registró la distribución de las indicaciones de diagnóstico prenatal y los cariotipos anormales, y se analizó la asociación entre los cariotipos anormales y las diferentes indicaciones de diagnóstico. En las muestras se detectó un total de 96 cariotipos cromosómicos anómalos en células de líquido amniótico, con una tasa de anormalidad del 7,47%. Las anomalías numéricas cromosómicas representaron el 70,83% (68/96) y la tasa de detección fue del 5,29% (68/1285), siendo la categoría más común de cariotipos anormales. Entre ellas, la trisomía 21 fue la más frecuente, con un 44,79% (43/96). La edad materna avanzada y el alto riesgo de cribado serológico fueron las principales indicaciones para el diagnóstico prenatal. Las tasas de detección más elevadas correspondieron a las pruebas prenatales no invasivas de ADN anómalo y a un progenitor portador de anomalía cromosómica, 27,63% y 42,86%, respectivamente. En conclusión, el cariotipo de las mujeres embarazadas con indicación de amniocentesis es un cribado eficaz para detectar anomalías cromosómicas fetales y reducir las anomalías congénitas.

Received: 06-05-2024 Accepted: 26-07-2024

INTRODUCTION

Chromosomal abnormalities are a common clinical genetic disorder that affects one in every 150 infants [1]. Infants with these disorders are often mentally disabled, with a variety of malformations and stunting [2]. At present, there is no effective treatment for this type of disease. The primary reliance is on prenatal screening and termination of pregnancy to avoid the birth of such fetuses. The standard prenatal diagnostic methods are divided into two categories: non-invasive prenatal testing and invasive prenatal testing[3]. Non-invasive prenatal DNA testing (NIPT), ultrasonography and maternal serum screening are commonly used non-invasive screening methods [2, 4, 5]. However, these methods cannot accurately detect genes in fetal cells, and there are cases of missed diagnosis and misdiagnosis [6]. Karyotyping after amniocentesis is still the gold standard for detecting fetal chromosomal abnormalities [7].

Amniocentesis is usually performed at 18-24 weeks of pregnancy to detect fetal chromosomal conditions by extracting and culturing amniotic fluid cells [8]. Karyotype analysis is highly specific and sensitive, and the diagnostic rate of fetal chromosomal ab-

normalities is almost 100% [9]. Prenatal diagnostic indications for amniocentesis usually include abnormal NIPT, high-risk maternal serum screening, advanced maternal age, abnormal ultrasonographic indications, paternal or maternal carrying chromosome abnormalities, and adverse pregnancy history [10, 11].

Despite the wealth of data available on the outcomes of amniocentesis, gaps remain in the literature, particularly concerning the comprehensive analysis of karyotype results by different indications for the procedure. Previous studies have often focused on single indications or a small subset of chromosomal abnormalities. The novelty of the present study lies in its comprehensive approach, analyzing a large, diverse cohort with a wide range of indications for amniocentesis. Therefore, this study aimed to assess the relationship between various prenatal diagnostic indications and fetal chromosomal abnormalities by performing a karyotype analysis of amniotic fluid cells in 1285 instances by amniocentesis in high-risk pregnant women.

PATIENTS AND METHODS

Sample collection

Our study design type is a present retrospective study. One thousand two hundred eighty-five pregnant women admitted to our hospital for amniotic fluid karyotyping from July 2019 to June 2022 were selected as the study population. The pregnant women aged 19 to 46 and 18 to 24 weeks of gestation. Detailed demographic and clinical data were gathered by completing questionnaires, conducting direct interviews with pregnant women, and assessing medical records. The study was approved by the First Affiliated Hospital ethics committee of Soochow University, and all participants were informed and signed the consent form.

Inclusion criteria: presence of prenatal diagnostic indications, including high risk of NIPT, advanced maternal age, high risk of serologic screening, abnormal ultrasonographic indications, history of adverse pregnancy and one parent carrying chromosomal abnormalities; amniocentesis for the first time.

Exclusion criteria: unsuccessful cultures of amniotic fluid cells twice; the presence of threatened abortion.

Amniocentesis

The pregnant women and their families were informed of the risks, and an amniocentesis was performed after signing the informed consent. Twenty mL of amniotic fluid was drawn from the pregnant women and centrifuged at 2000 r/min for 10 minutes. After centrifugation, the supernatant was discarded, and the cell suspension was inoculated in the amniocyte culture medium at 37°C and 5% CO_2 for 9 to 10 days. The amniotic fluid cells were collected when multiple clones with various metaphase cells were observed with an inverted microscope. After harvesting the cells, g-band staining was performed and canned by a Leica GLS120 Automated Nuclear Scanning System. Thirty karyotypes were routinely counted, and five karyotypes were analyzed following the International System for Human Cytogenetic Nomenclature (ISCN) standard [12].

Statistical analysis

Statistical analysis was performed using the IBM® SPSS 24.0® software. Count data were expressed using frequency and rate (%) and analyzed by chi-square test. $p<0.05$ was considered a statistically significant difference.

RESULTS

Distribution of different diagnostic indications

Among the 1285 pregnant women with diagnostic indications, most cases were prompted by high-risk maternal serum screening, accounting for 573 cases (44.59%), followed by advanced maternal age with 522 cases (40.62%). Less frequent indications included abnormal results from non-invasive prenatal testing (NIPT), which

led to 76 cases (5.91%), and abnormal ultrasonographic findings, which accounted for 67 cases (5.21%). The least common reasons for amniocentesis were a history of adverse pregnancy outcomes and parental chromosomal abnormalities, with 26 cases (2.02%) and 21 cases (1.63%) respectively (Table 1).

Table 1
Distribution of different diagnostic indications.

Clinical indicator	Cases	Proportion (%)
High-risk maternal serum screening	573	44.59
Advanced maternal age	522	40.62
Abnormal ultrasonographic indications	67	5.21
Abnormal NIPT	76	5.91
Paternal/maternal carrying chromosome abnormality	21	1.63
Adverse pregnancy history	26	2.02
Total	1285	100

Classification and detection rate of abnormal karyotypes

The study examined 1,285 cases of amniotic fluid samples from high-risk pregnant women. Of these, 96 (7.47%) cases showed chromosomal abnormalities. Numerical abnormalities were the most common, accounting for 68 (70.83%) abnormal karyotypes. The most frequent numerical abnormality was Trisomy 21, which was observed in 43 (44.79%) cases, followed by Trisomy 18 in 10 (10.42%) cases, Trisomy 13 in 2 (2.08%) cases, 47 XXX (trisomy X) in 2 (2.08%) cases, 47 XYY (Jacob's syndrome) in 1 (1.04%) case, and 47 XXY (Klinefelter syndrome) in 2 (2.08%) cases. Additionally, 1 (1.04%) case of 45 X (Turner Syndrome or TS) was detected. Structural abnormalities were observed in 28 (29.17%) cases, including 6 (6.25%) translocations, 13 (13.54%) inversions, and 9 (9.38%) chromosome polymorphisms (Table 2).

Table 2
Classification and detection rate of abnormal karyotypes.

Chromosomal karyotype	Number (n)	Occupancy% (n/96)	Detection rate% (n/1285)
Numerical abnormalities	68	70.83	5.29
Trisomy 21	43	44.79	3.35
Trisomy 18	10	10.42	0.78
Trisomy 13	2	2.08	0.16
47, XXX	2	2.08	0.16
47, XYY	1	1.04	0.08
47, XXY	2	2.08	0.16
45, X	1	1.04	0.08
Mosaicism	7	7.29	0.54
Structural abnormalities	28	29.17	2.18
Translocation	6	6.25	0.47
Inversion	13	13.54	1.01
Chromosome polymorphism	9	9.38	0.70
Total	96	100.00	7.47

Distribution of diagnostic indications in pregnant women with amniotic fluid karyotype abnormalities

The abnormal karyotype detection rate of one parent carrying a chromosome abnormality was 42.86% (9/21; calculation formula of detection rate (%): n/number of pregnant women per diagnostic indication in 1285 cases (Table 3)), which was the highest detection rate of all indications, followed by high-risk NIPT (27.63%) and abnormal ultrasonographic indications (14.93%). The more significant number of karyotype abnormalities was found in advanced maternal age, accounting for 30.21% (29/96), followed by high-risk maternal serum (26.04%) and abnormal NIPT (21.88%).

Distribution of abnormal karyotypes for different prenatal diagnostic indications

As shown in Table 4, trisomy 21 was most common in pregnant women with advanced maternal age. Trisomy 21 also has the highest proportion in other abnormal karyotypes of older pregnant women. Fetal chromosomal structural abnormalities are mainly distributed in abnormal serological screening, and one parent carries the abnormal chromosome. Fetal chromosomal numerical abnormalities are mainly distributed in advanced maternal age, abnormal NIPT, and high-risk maternal serum screening. However, in terms of the total number, fetal chromosomal abnormalities are mainly distributed between advanced maternal age and high-risk maternal serum screening.

DISCUSSION

This study aimed to assess the relationship between various prenatal diagnostic indications and fetal chromosomal abnormalities by performing a karyotype analysis of amniotic fluid cells in 1,285 high-risk pregnant women. The most common indications for amniocentesis were high-risk maternal serum screening (44.59%) and advanced maternal age (40.62%), followed by abnormal NIPT results (5.91%) and abnormal ultrasonographic findings (5.21%). Karyotype analysis detected chromosomal abnormalities in 96 cases, resulting in an abnormality rate of 7.47%. Numerical chromosomal abnormalities were more common, accounting for 70.83% of the abnormalities, with trisomy 21 being the most frequent (44.79%). Structural chromosomal abnormalities comprised 29.17% of the abnormalities, with inversions being the most common (13.54%).

The findings of this study are consistent with previous research on the distribution of prenatal diagnostic indications and the detection rates of chromosomal abnormalities. A study by Grgić *et al*. reported that the most common indication for amniocentesis was advanced maternal age [13]. Additionally, a study by Golshahi *et al.* reported that the most common indication for amniocentesis

Table 3

Distribution of diagnostic indications in pregnant women with amniotic fluid karyotype abnormalities.

Clinical indication	Abnormal karyotype(n)	Detection rate (%)	Proportion (%)
High-risk maternal serum screening	25	4.36	26.04
Advanced maternal age	29	5.56	30.21
Abnormal ultrasonographic indications	10	14.93	10.42
Abnormal NIPT	21	27.63	21.88
Paternal/maternal carrying chromosome abnormality	9	42.86	9.38
Adverse pregnancy history	2	7.69	2.08
Total	96	7.47	100.00

Table 4
Distribution of abnormal karyotypes for different prenatal diagnostic indications.

Diagnosis indicator	Chromosomal karyotype						
	a	b	c	d	e	f	Total
Trisomy 21	7	23	5	8			43
Trisomy 18	2	3	2	3			10
Trisomy 13	1			1			2
47, XXX	1		1				2
47, XYY				1			1
47, XXY	2						2
45, X		1					1
Mosaicism	3			4			7
Translocation	1		2	2	1		6
Inversion	3	2		2	6		13
Chromosome polymorphism	5				2	2	9
Total	25	29	10	21	9	2	96

a, High-risk maternal serum screening; b, Advanced maternal age; c, Abnormal ultrasonographic indications; d, Abnormal NIPT; e, Paternal/maternal carrying chromosome abnormality; f, Adverse pregnancy history.

was abnormal serum screening, similar to the results of the current study [14]. Also, this study's overall chromosomal abnormality detection rate of 7.47% is similar to other studies [15, 16]. However, the study of Sun *et al*. reported the detection rate of abnormal karyotypes to be 2.02%, which may be due to the sample size and methods used [17].

The high detection rate of numerical chromosomal abnormalities, particularly trisomy 21, is well-documented in the literature. A review by Liu *et a*l. found that trisomy 21 was the most common chromosomal abnormality detected prenatally, accounting for 46.77% of all abnormalities, which aligns with the 44.79% reported in the current study [18]. Additionally, the study of *Ocak et al*. confirms this finding with 46% of all abnormalities [19]. Regarding structural chromosomal abnormalities, the findings of this study are also consistent with previous research. A study by *Liu et al.* reported that deletion, duplication, inversion, and translocation were the most common structural abnormalities detected prenatally [18].

The distribution of chromosomal abnormalities among the different prenatal diagnostic indications also aligns with previous studies. Advanced maternal age and abnormal serum screening have been consistently associated with higher rates of chromosomal abnormalities, particularly numerical abnormalities like trisomy 21 [20]. The higher detection rate of structural abnormalities in cases with parental chromosomal abnormalities or abnormal NIPT results has also been reported in the literature [21, 22]. The abnormal NIPT group, a new kind of prenatal screening in which fetal DNA was extracted from maternal serum for testing, had the second-highest detection rate. It is commonly used in pregnancy screening because of its excellent safety and specificity [23]. NIPT mainly targets the detection of autosomal aneuploidy, and 12 cases of autosomal aneuploidy were detected in the NIPT high-risk group, including 8 cases of trisomy 21, 3 cases of trisomy 18 and 1 case of trisomy 13. However, according to the statistical results, the high risk of NIPT also implied the possibility of mosaicism, inversion, and translocation.

Prenatal ultrasonography cannot directly detect fetal chromosomal abnormalities, but it can detect some ultrasound soft markers associated with genetic abnormalities. These soft indicators include thickened nuchal fold, echogenic focus in the heart, choroid plexus cyst and others [24]. Positive ultrasound soft indicators showed an increased risk of aneuploidy in the fetus. In our study, abnormal karyotypes were detected in 10 pregnant women with abnormal ultrasound findings, with a detection rate of 14.93% (10/67), 8 of which were aneuploid. Ultrasonography in the middle of pregnancy is essential for prenatal screening of chromosomal abnormalities, especially in fetuses with chromosomal aneuploidy.

While traditional karyotyping via amniocentesis remains the gold standard for prenatal chromosomal analysis, new technologies are emerging that offer alternatives or supplements to this invasive procedure. Non-invasive prenatal testing (NIPT) using cell-free fetal DNA from the mother's blood has become an increasingly common screening tool, with an abnormal NIPT result prompting 5.91% of the amniocenteses in this study. NIPT has high detection rates for common aneuploidies like trisomies 21, 18, and 13, though it has limitations in identifying structural chromosomal abnormalities [25]. Additionally, chromosomal microarray analysis (CMA) and next-generation sequencing (NGS) are newer technologies offering higher resolution and the capability to detect submicroscopic chromosomal alterations that karyotyping might miss [26].

In conclusion, 96 karyotype abnormalities were detected in 1285 high-risk pregnant women, with an abnormality rate of 7.47%. NIPT, ultrasound, and serological screening help detect fetal chromosomal abnormalities. Nevertheless, karyotype analysis is still irreplaceable. Karyotype analysis of amniotic fluid cells is recommended for all pregnant women with indications of prenatal diagnosis. However, this study has limitations in that only the main indications were included in the statistics for pregnant women who met several indications. The sample size was small, and more research is required in future work.

Funding

None.

Conflict of competence

The authors declare no conflict of interest.

Authors' ORCID number

- Cen M (CM): 0009-0004-8751-3120
- Lingyan Sun (LS): 0000-0002-8818-3563
- Li Li (LL): 0009-0003-8984-8373

Contribution of authors

CM: Contributed to the conception of the work, data collection, conducting the study, and data analysis, and agreed to all aspects of the work. LS: Contributed to the conception of the work, conducted the study, revised the draft, approved the final version of the manuscript, and agreed to all aspects of the work. LL: Collection and entry of data, manuscript writing, translation and editing. All authors: Final approval of the manuscript.

REFERENCES

1. **Verma IC, Puri RD.** Global burden of genetic disease and the role of genetic screening. Semin Fetal Neonatal Med 2015; 20(5): 354-363. *https://doi.org/10.1016/j.siny.2015.07.002*.
2. **Carlson LM, Vora NL.** Prenatal Diagnosis: Screening and Diagnostic Tools. Obstet Gynecol Clin North Am 2017; 44(2): 245-256. *https://doi.org/10.1016/j.ogc.2017.02.004.*
3. **Xie D, Yang W, Fang J, Li H, Xiong L, Kong F, Wang A, Liu Z, Wang H.** Chromo-

somal abnormality: prevalence, prenatal diagnosis and associated anomalies based on a provincial-wide birth defects monitoring system. J Obstet Gynaecol Res 2021; 47(3): 865-872. *https://doi.org/10.1111/jog.14569.*

4. **Carbone L, Cariati F, Sarno L, Conforti A, Bagnulo F, Strina I, Pastore L, Maruotti GM, Alviggi C.** Non-invasive prenatal testing: current perspectives and future challenges. Genes 2020; 12(1): 15. *https://doi.org/10.3390/genes12010015.*
5. **Levy B, Wapner R.** Prenatal diagnosis by chromosomal microarray analysis. Fertil Steril 2018; 109(2): 201-212. *https://doi.org/10.1016/j.fertnstert.2018.01.005.*
6. **Wang J, Wang ZW, Zhou Q, Zhang B, Yin T, Yu B, Wang LL.** Lower detectability of non-invasive prenatal testing compared to prenatal diagnosis in high-risk pregnant women. Ann Transl Med 2019; 7(14): 319. *https://doi.org/10.21037/atm.2019.06.70.*
7. **Driscoll DA, Gross S.** Clinical practice. Prenatal screening for aneuploidy. New Eng J Med 2009; 360(24): 2556-2562. *https://doi.org/10.1056/nejmcp0900134.*
8. **Alfirevic Z, Navaratnam K, Mujezinovic F.** Amniocentesis and chorionic villus sampling for prenatal diagnosis. Cochrane Database Syst Rev 2017; 9(9): Cd003252. *https://doi.org/10.1002/14651858.cd003252.pub2.*
9. **Fang Y, Wang G, Gu L, Wang J, Suo F, Gu M, Gou L.** Application of karyotype analysis combined with BACs-on-Beads for prenatal diagnosis. Exp Ther Med 2018; 16(4): 2895-2900. *https://doi.org/10.3892/etm.2018.6574.*
10. **Dai R, Yu Y, Xi Q, Hu X, Zhu H, Liu R, Wang R.** Prenatal diagnosis of 4953 pregnant women with indications for genetic amniocentesis in Northeast China. Mol Cytogenet 2019; 12: 45. *https://doi.org/10.1186/s13039-019-0457-x.*
11. **Jindal A, Sharma M, Karena Z, Chaudhary C.** Amniocentesis. StatPearls. Treasure Island (FL). StatPearls Publishing; 2023.
12. **Stevens-Kroef M, Simons A, Rack K, Hastings RJ.** Cytogenetic Nomenclature and Reporting. Methods Mol Biol 2017; 1541: 303-309. *https://doi.org/10.1007/978-1-4939-6703-2_24.*
13. **Grgić G, Cerovac A, Hadžimehmedović A, Bogdanović G, Latifagić A.** Genetic amniocentesis: Indications, outcome and complications retrospective cohort study during 13 years. Clin Exp Obstet Gynecol(CEOG) 2021; 48(6): 1318-1323. *https://doi.org/10.31083/j.ceog4806209.*
14. **Golshahi F, khaleghinezhad k, Sahebdel B, Saedi N, Salari Z.** The Indications of amniocentesis for the diagnosis of aneuploidy among pregnant women. J Midwifery Reprod Health 2024; 12(2): 4264-4269. *https://doi.org/10.22038/jmrh.2022.66590.1943.*
15. **Younesi S, Taheri Amin MM, Hantoushzadeh S, Saadati P, Jamali S, Modarressi MH, Savad S, Delshad S, Amidi S, Geranorimi T, Navidpour F, Ghafouri-Fard S.** Karyotype analysis of amniotic fluid cells and report of chromosomal abnormalities in 15,401 cases of Iranian women. Sci Rep 2021; 11(1): 19402. *https://doi.org/10.1038/s41598-021-98928-3.*
16. **Li H, Li Y, Zhao R, Zhang Y.** Cytogenetic analysis of amniotic fluid cells in 4206 cases of high-risk pregnant women. Iran J Public Health 2019; 48(1): 126-131.
17. **Sun Y, Zhang P, Zhang N, Rong L, Yu X, Huang X, Li Y.** Cytogenetic analysis of 3387 umbilical cord blood in pregnant women at high risk for chromosomal abnormalities. Mol Cytogenet 2020; 13: 2. *https://doi.org/10.1186%2Fs13039-020-0469-6.*
18. **Liu Y, Sun XC, Lv GJ, Liu JH, Sun C, Mu K.** Amniotic fluid karyotype analysis and prenatal diagnosis strategy of 3117 pregnant women with amniocentesis indication. J Comp Eff Res 2023; 12(6): e220168. *https://doi.org/10.57264%2Fcer-2022-0168.*
19. **Ocak Z, Özlü T, Yazıcıoğlu HF, Özyurt O, Aygün M.** Clinical and cytogenetic results of a large series of amniocentesis cases from Turkey: report of 6124 cases. J Obs-

tet Gynaecol Res 2014; 40(1): 139-146. *https://doi.org/10.1111/jog.12144.*

20. Coppedè F. Risk factors for Down syndrome. Arch Toxicol 2016; 90(12): 2917-2929. *https://doi.org/10.1007/s00204-016-1843-3*.

21. Pylypjuk CL, Monarrez-Espino J. False-positive maternal serum Screens in the second srimester as sarkers of slacentally sediated somplications sater in pregnancy: a systematic review and meta-analysis. Dis Markers 2021; 2021(1): 5566234. *https://doi.org/10.1155/2021/5566234.*

22. Stavljenić-Rukavina A1. Prenatal diagnosis of chromosomal disorders - Molecular aspects. EJIFCC 2008; 19(1): 2-6.

23. Zhang H, Gao Y, Jiang F, Fu M, Yuan Y, Guo Y, Zhu Z, Lin M, Liu Q, Tian Z, Zhang H. Non-invasive prenatal testing for trisomies 21, 18 and 13: clinical experience from 146,958 pregnancies. Ultrasound Obstet Gynecol 2015; 45(5): 530-538. *https://doi.org/10.1002/uog.14792.*

24. Van den Hof MC, Wilson RD. Fetal soft markers in obstetric ultrasound. Int J Gynecol Obstet 2006; 95(1): 73-74. *https://doi.org/10.1016/j.ijgo.2006.02.002.*

25. Jayashankar SS, Nasaruddin ML, Hassan MF, Dasrilsyah RA, Shafiee MN, Ismail NA. Non-invasive prenatal testing (NIPT): reliability, challenges, and future directions. Diagnostics 2023; 13(15): 2570. *https://doi.org/10.3390/diagnostics13152570.*

26. Liu X, Liu S, Wang H, Hu T. Potentials and challenges of chromosomal microarray analysis in prenatal diagnosis. Front Genet 2022; 13: 938183. *https://doi.org/10.3389/fgene.2022.938183*.

Invest Clin 65(4): 445 - 453, 2024 https://doi.org/10.54817/IC.v65n4a05

Epidemiological and virological characterization of mpox cases in Venezuela during the multinational 2022-2023 outbreak.

Pierina D´Angelo[1], Carmen Loureiro[2]*, Rossana Jaspe[2], Yoneira Sulbarán[2], Lieska Rodríguez[1], Víctor Alarcón[1], Iraima Monsalve[1], José Manuel García[3], José Luis Zambrano[4], Héctor Rangel[2], and Flor H Pujol[2]*

[1]Dirección General de Diagnóstico, Instituto Nacional de Higiene "Rafael Rangel", Caracas, Miranda, Venezuela.
[2]Laboratorio de Virología Molecular, Centro de Microbiología y Biología Celular, Instituto Venezolano de Investigaciones Científicas, Caracas, Miranda, Venezuela.
[3]Dirección General de Epidemiología, Ministerio del Poder Popular para la Salud, Caracas, Miranda, Venezuela.
[4]Laboratorio de Virología Celular, Centro de Microbiología y Biología Celular, Instituto Venezolano de Investigaciones Científicas, Caracas, Miranda, Venezuela.
*Contributed equally.

Keywords: mpox; poxvirus; monkeypox; outbreak; Venezuela.

Abstract. Mpox (formerly known as monkeypox) is an infectious disease caused by MPXV, a member of the family *Poxviridae*. On July 23, 2022, the WHO declared the first Public Health Emergency of International Concern of Mpox due to an escalating global outbreak with low intensity. Two clades of MPXV and several lineages within each of these clades have been described. Clade I, also known as the Central African clade, causes a more severe and lethal disease than clade II, which circulates in West Africa. MPXV clade IIb caused the first international outbreak (2022), while clade Ib caused a more recent one (2023-2024). Venezuela reported 12 cases during the 2022-2023 outbreak. This study aims to describe the epidemiological and virological characteristics of these cases. The first three cases were from men infected outside Venezuela, while most of the subsequent ones were from men who acquired the disease in the country. All the cases were from men who have sex with men, and frequently also people living with HIV-1/AIDS. No critical outcome was observed in any of the patients. Sequence analysis showed that most of the MPXV belonged to clade IIb lineage B.1. The recurrent emergence of mpox epidemics warrants the further implementation of molecular epidemiology surveillance and vaccination programs.

Correspondence author: Flor H Pujol. Laboratorio de Virología Molecular, Centro de Microbiología y Biología Celular, Instituto Venezolano de Investigaciones Científicas, Caracas, Miranda, Venezuela. E-mail: fhpujol@gmail.com; Tel.+58.2125041623

Caracterización epidemiológica y virológica de los casos de mpox en Venezuela durante el brote multinacional 2022-2023.

Invest Clin 2024; 65 (4): 445 – 453

Palabras clave: mpox; poxvirus; viruela símica; brote; Venezuela.

Resumen. La mpox (antes conocida como viruela símica) es una enfermedad infecciosa causada por el virus MPXV, miembro de la familia *Poxviridae*. El 23 de julio de 2022, la OMS declaró la primera Emergencia de Salud Pública de Importancia Internacional de mpox, debido a un brote mundial en escalada, actualmente de baja intensidad. Se han descrito dos clados de MPXV y varios linajes dentro de cada uno de estos clados. El clado I, también conocido como clado centroafricano, causa una enfermedad más grave y letal que el clado II, el que circula en África occidental. El primer brote internacional (2022) fue causado por el clado IIb de MPXV, mientras que uno más reciente (2023-2024) es causado por el clado Ib. Venezuela notificó 12 casos durante el brote de 2022-2023. El objetivo de este estudio es describir las características epidemiológicas y virológicas de estos casos. Los primeros tres casos fueron de hombres que se infectaron fuera de Venezuela, mientras que la mayoría de los siguientes fueron de hombres que adquirieron la enfermedad en el país. Todos los casos fueron de hombres que tuvieron sexo con hombres y que viven con VIH-1/SIDA. No se observó ningún desenlace crítico en ninguno de los pacientes. El análisis de secuencias mostró que la mayoría de los MPXV pertenecían al linaje B.1 del clado IIb. La aparición recurrente de epidemias de mpox justifica una mayor implementación de programas de vacunación y vigilancia epidemiológica molecular.

Received: 17-10-2024 Accepted: 31-10-2024

INTRODUCTION

Mpox (formerly known as monkeypox) is an infectious disease caused by MPXV, a member of the *Poxviridae* family. MPXV belongs to the genus *Orthopoxvirus*. MPXV is an enveloped 200-250 nm virus with linear double-stranded DNA of approximately 200 kb. MPXV interacts with glycosaminoglycans at the surface of the susceptible cells to enter and replicate in the cytoplasm of the infected cell [1-3].

This infection causes a variety of clinical manifestations, particularly skin lesions and lymphadenopathy, but also can present with musculoskeletal pain, ocular manifestations, and malaise [4]. The infection spreads mainly through contact with infected humans or animals or contaminated materials. However, frequent cases and deaths have been observed in children, suggesting that routes of transmission other than sexual contact may also be effective in this new outbreak [5,6]. The likelihood of aerosol transmission seems to be low [7].

The disease has been known to infect humans since 1970. Several cases have been reported in Africa since then, with a few documented cases until 2022 in other countries outside the continent, primarily due to zoonotic transmission. On July 23, 2022, the WHO declared the first public health emergency of international concern of mpox due to an escalating global outbreak, which

is still ongoing at present, with low intensity [2,8]. By August 2024, nearly 100,000 cases have been reported in 122 countries, with a relatively low mortality rate (207 deaths) [9]. This outbreak has been characterized by human-to-human transmission, frequently among men who have sex with men (MSM). HIV co-infection is also frequent [1].

On August 14, 2024, the WHO declared a second public health emergency of international concern for mpox due to an ongoing global outbreak, this time developing in Africa, with the majority of cases in the Democratic Republic of Congo [4,10]. By the end of August 2024, the only cases described out of Africa were in Sweden and Thailand, with a history of travel from Africa. Both viral sequences were already available in the GISAID database on August 28, 2024 [11].

Two clades of MPXV and several lineages within each of these clades have been described. Clade I, also known as the Central African clade, is associated with higher severity and lethality (up to 10%) compared to clade II, which circulates in West Africa [12-14]. MPXV clade IIb caused the first international outbreak (2022), while the more recent one is caused by clade Ib.

The USA exhibited the highest number of mpox cases of the first outbreak worldwide: more than 33,000 by August 2024. In Latin America, Brazil, Colombia, Mexico, and Peru, there was also a high number of cases: more than 11,000 cases in Brazil, more than 4000 cases in Colombia and Mexico, and more than 3,500 cases in Peru until August 2024 [9].

Venezuela reported 12 cases during the 2022 outbreak [15,16]. This study aims to describe the epidemiological and virological characteristics of these cases.

MATERIALS AND METHODS

This is a descriptive study of the cases of mpox detected in Venezuela. The Instituto Nacional de Higiene Rafael Rangel (INHRR) is responsible for the molecular diagnosis of MPXV in Venezuela. It implemented an algorithm for the molecular detection of MPXV cases, previously discarding other confusing exanthema-inducing infections, Varicella-Zoster and Herpesvirus, by detecting IgM/IgG antibodies in the sera of suspected patients [16]. The presence of MPXV DNA was detected by qPCR, as previously described [16]. Based on the WHO/PAHO recommendations on strengthening surveillance, the country has decentralized molecular diagnosis since January 2023 into four states, and surveillance was intensified through the use of the Vesicular Eruptive Febrile Syndrome surveillance protocol.

Once qRT-PCR identified the cases, MPXV genomic DNA was amplified using ARTIC primers [17] for complete genome sequencing. Multiple libraries were prepared from the same sample to increase sequence coverage, using the DNA Prep library preparation kit with the Nextera DNA CD Indexes (Illumina, Inc. San Diego, CA, USA) for next-generation sequencing (NGS). The libraries were pooled and quantified (Qubit DNA HS, Thermo Scientific, Waltham, MA, USA). Their quality was checked (Bio-Fragment Analyzer, Qsep1-Lite, BiOptic, New Taipei City, Taiwan) before sequencing, and sequencing was carried out using an iSeq 100 platform and a 300-cycle V2 kit with paired-end sequencing.

The viral genome sequence assembly was performed using the Genome Detective Virus tool (https://www.genomedetective.com/). Nucleotide sequences of three partial complete genomes with more than 60% coverage have been deposited into the GISAID database with the accession IDs EPI_ISL_15014548 and EPI_ISL_19370098. The other two sequences (MPXV6 and MPXV10), with lower coverage and are not acceptable for GISAID, are available upon request.

FASTA file obtained from Genome Detective was analyzed using the Nextclade web tool Nextclade Web 1.14.1 (https://clades.nextstrain.org). MPXV genomes were aligned using MAFFT v.7 (https://mafft.cbrc.

jp/alignment/server/). Mega [18] was used for sequence identity determination.

RESULTS

Twelve cases of mpox were reported in Venezuela between June 2022 and March 2023 (Table 1). Five corresponded to imported cases, and seven were community-acquired. All patients were male, acquired through sexual contact (MSM), and 7/10 (70%) corresponded to people living with HIV-1/AIDS (PLWHA). The mean age was 30 years (range 24-37). Most of the cases corresponded to the capital region, 42% (5/12) of the Bolivarian State of Miranda, 25% (3/12) of the Capital District, and the remaining 8% one each from Barinas, Carabobo, Guarico and Zulia states (Table 1).

A complete genome sequence could be obtained for only one isolate (MPXV7, with 92.7% coverage), while partial sequences were obtained for three more isolates (Table 2). Even with the low coverage, it could be confirmed that all isolates were from MPXV clade IIb. A discrepancy was found for the isolate MPXV1 for lineage assignment between the different web algorithms available online (Table 2).

Most MPXV isolates detected in Venezuela belonged to the B.1 lineage. Ten thousand three hundred fifty-four total sequences were available in the GISAID database until August 29, 2024 [11]. From these, 8868 sequences belong to the B.1 lineage and its sublineages (3848 to the B.1 lineage and 5020 to the B.1.1 to the B.1.22 sublineages), being the B.1 lineage prevalent globally during the first international outbreak of mpox.

The MPXV1 isolate was classified as lineage B.1 by Nextclade, as were most isolates from this study, but B.1.6 by GISAID [11]. The B.1.6 assignment by GISAID is somehow unexpected since this lineage is strongly associated with mpox cases in Peru [19], and the country of infection for patient C1 was Spain.

Five hundred thirty-three B.1.6 MPXV sequences were available at GISAID on August 29, 2024 [11] (5.1% of the total sequences). Of the 439 B.1.6 sequences (82%) were from Peru (Fig. 1). Some B.1.6 isolates were also found in Colombia and Chile, while this isolate was utterly absent from Brazil (0/353 sequences), Bolivia (No MPXV sequence available), Argentina (0/11 sequences) and only 1/102 B.1.6 isolates in Ecuador. How-

Table 1
Demographic characteristics of patients infected with MPXV reported in Venezuela in 2022.

Patient ID	Sex and age	Date of diagnosis	Travel from	MSM	HIV-1	Outcome
C1	Male, 32	12/6/22	Spain	Yes	Negative	Good
C2	Male, 28	25/8/22	Brazil	Yes	Positive	Good
C3	Male, 31	23/8/22	Peru	Yes	Negative	Good
C4	Male, 24	10/9/22	None	Yes	Positive	Good
C5	Male, 30	6/9/22	None	Yes	Positive	Good
C6	Male, 36	19/9/22	None	Yes	Positive	Good
C7	Male, 31	20/9/22	None	Yes	Positive	Good
C8*	Male, 37	23/9/22	None	Yes	N/A**	Good
C9*	Male, 25	26/9/22	None	Yes	N/A	Good
C10	Male, 30	13/10/22	Colombia	Yes	N/A	Good
C11	Male, 26	9/12/22	None	Yes	Positive	Good
C12	Male, 33	3/3/23	Panamá	Yes	Positive	Good

*Reported contact with patient C7. **N/A: not available. Did not reported HIV status nor accepted an HIV test.

Table 2
Sequence analysis of MPXV Venezuelan isolates.

Isolate ID*	Patient ID	Accession ID	Genome coverage**	Clade	Lineage***
MPXV1	C1	EPI_ISL_15014548	64.2 %	IIb	B.1 or B.1.6
MPXV6	C6	NA****	37.3 %	IIb	B.1.19
MPXV7	C7	EPI_ISL_19370098	92.7 %	IIb	B.1
MPXV8	C8	NA****	56.8 %	IIb	B.1
MPXV10	C10	NA****	39.0 %	IIb	B.1

*For the other MPXV isolates, sequence information could not be obtained. **Percent nucleotides effectively sequenced along the whole genome. ***Lineage assignment according to the Nextclade algorithm. In the case of MPXV1, GISAID assigned this isolate to the B.1.6 lineage. ****NA: not available. Not submitted to GISAID because of low coverage.

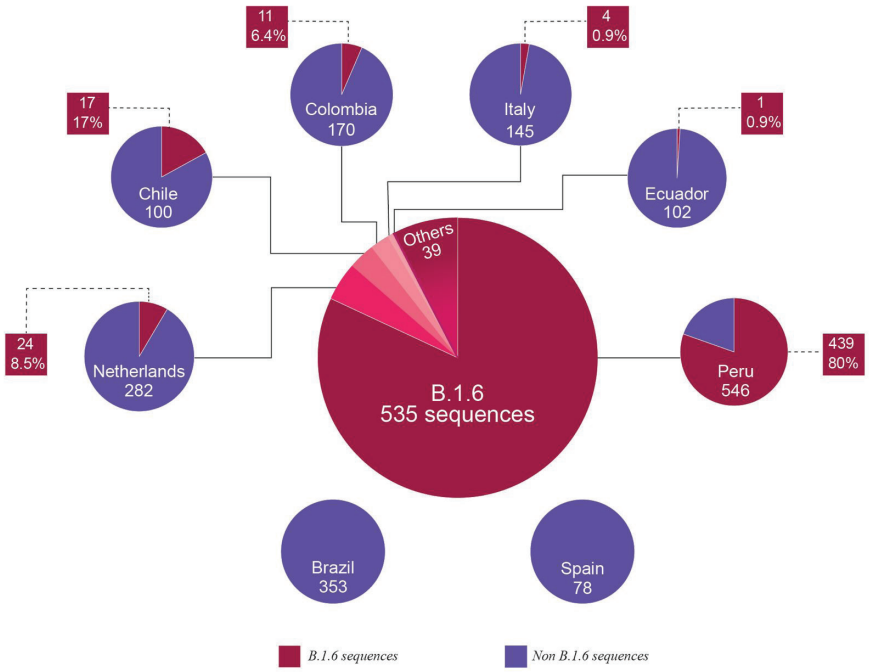

Fig. 1. Distribution of the MPXV lineage B.1.6 in the world. (GISAID, 2024).

ever, the earliest sequences for this lineage (earliest collection date June 5, 2022) were from the Netherlands, where 24/182 sequences (13%) were classified as B.1.6 by the GISAID database: the earliest collection date of B.1.6 isolates from Peru was June 25 of this year (from the first reported case in the country). Then, it cannot be discarded that the B.1.6 lineage was also circulating in Spain in June 2022 and not detected because of the relatively low number of sequences available from this country (n=78).

Another Venezuelan isolate was classified as B.1.19 by Nextclade (from patient C6). No information on lineage classification can be obtained from the GISAID database since this sequence could not be submitted due to low coverage (Table 2). A total of 58 sequences of the B.1.19 lineage were available on the GISAID database [11], making it a lineage with a low detection frequency. Most of the sequences are from Europe (n=39), 18 from North America, and none have been reported in South America. However, the

classification of this Venezuelan isolate as B.1.19 may be misleading because of the low coverage of this sequence.

The partial sequence of MPXV8 displayed more than 99.99% identity with the MPXV7 sequence, which agrees with the history of contact between patients C7 and C8 (Table 1).

DISCUSSION

Relatively few cases of mpox were reported in Venezuela. Comegna *et al.*, 2023 [20], suggested several factors to explain the low number of reported cases, including limited diagnostic capacity, particularly outside the capital city. However, as stated before, 4/12 cases were from states outside the capital region, and four diagnostic centers were performing molecular diagnosis of mpox in other states. The fact that many of the community-acquired cases in Venezuela were also PLWHA suggests that the fear of discrimination may have played a role in the low number of cases detected in the country. In addition, the lack of knowledge about this disease (both among patients and among health workers who are not trained to detect cases) may have hampered the identification of cases. Finally, as this outbreak often presented with a mild disease with low severity and cryptic manifestations, often in the genital area, many cases may have gone undetected [21]. Since PLWHA are more likely to seek medical care, with physicians aware of this disease, this increases the likelihood of detecting mpox cases. Most of the MPXV reported in Venezuela belonged to clade IIb lineage B.1.

The high number of mpox cases associated with the first international outbreak led to the evolution of this virus, with the subsequent emergence of lineages inside the clade IIb [2]. An example of this is the emergence of lineage B.1.6, which seems to have emerged in Peru [19]. The importance of genomic surveillance has been stressed with the COVID-19 pandemic. However, the contribution of MPXV genomic sequences to the GISAID database was not proportional to each country's mpox cases [2]. The genome length of this DNA virus (almost 200.000 base pairs) does not contribute to facilitating this task. Only one complete genome with satisfactory coverage could be obtained in our case. The analysis of these complete or partial genomic sequences allowed us to determine the circulation of the lineage B.1 of the clade IIb in the country.

As of the end of October 2024, only three cases of the second mpox outbreak (clade Ib) have been reported outside Africa (with a previous history of being in that continent) [9,10,22]. This second outbreak did not threaten public health in Latin America by the end of 2024. However, the recurrent outbreaks of this disease have shown the emergence of viral lineages with increased ability of human-to-human transmission [23]. This warrants the need for enhancing response interventions and surveillance systems, targeted vaccination, such as vaccination of high-risk individuals, persons in contact with mpox cases, ring vaccination in endemic areas [5,24,25], and educational campaigns on mpox [24,25].

ACKNOWLEDGEMENTS

To the Health Personnel who treated mpox cases effectively and accurately in the country.

Funding

This project was funded by the Ministerio del Poder Popular para Ciencia y Tecnología de Venezuela (MINCYT).

Conflict of competence

The authors declare that they have no conflict of competence.

ORCID numbers of authors

- Pierina D´Angelo (PA): 0000-0002-1658-6128
- Carmen L. Loureiro (CL): 0000-0003-3665-1107

- Rossana C Jaspe (RCJ): 0000-0002-4816-1378
- Yoneira Sulbaran (YS): 0000-0002-3170-353X
- Lieska Rodríguez (LR): 0009-0002-6721-855X
- Víctor Alarcón (VA): 0000-0002-4418-6690
- Iraima Monsalve (IM): 0009-0005-2620-7944
- José Manuel García (JMG): 0000-0002-2152-0887
- José Luis Zambrano (JLZ): 0000-0001-9884-2940
- Héctor R Rangel (HRR): 0000-0001-5937-9690
- Flor H. Pujol (FHJ): 0000-0001-6086-6883

Contributions of authors

Substantial contribution to the conception and design of the study; Critical review of the article; Approval of the final version to be published (all authors). PA: Data collection and molecular diagnosis of cases. CL: Amplification of the viral genome for sequencing. RCJ y YS: Next-generation sequencing. LR,VA,IM, JMG: Data collection and epidemiological analysis of cases. JLZ: Critical review of the manuscript and design of the figure. HRR: Critical review of the study and manuscript. FHJ: Supervision of the study; Writing the first version of the manuscript.

REFERENCES

1. **Liu BM, Rakhmanina NY, Yang Z, Bukrinsky MI.** Mpox (Monkeypox) Virus and its co-infection with HIV, sexually transmitted infections, or bacterial superinfections: double whammy or a new prime culprit? Viruses 2024; 16: 784. *doi: 10.3390/v16050784.*
2. **Moros ZC, Loureiro CL, Jaspe RC, Sulbarán Y, Delgado M, Aristimuño OC, Franco C, Garzaro DJ, Rodríguez M, Rangel HR, Liprandi F, Pujol FH, Zambrano JL.** Web-tools for the genomic analysis of the 2022 Monkeypox virus global outbreak. Inv Clin. 2023; 64: 68-80. *https://doi.org/10.54817/IC.v64n1a06.*
3. **Zinnah MA, Uddin MB, Hasan T, Das S, Khatun F, Hasan MH, Udonsom R, Rahman MM, Ashour HM.** The re-emergence of Mpox: old illness, modern challenges. Biomedicines 2024; 12: 1457. *doi: 10.3390/biomedicines12071457.*
4. **Sah R, Apostolopoulos V, Mehta R, Rohilla R, Sah S, Mohanty A, Mehta V, Feehan J, Luna C, de Novales FJM, Al-Tawfiq JA, Cascio A, Samayoa-Bran AJ, Bonilla-Aldana DK, Rodriguez-Morales AJ.** Mpox strikes once more in 2024: declared again as a Public Health Emergency of International Concern. Travel Med Infect Dis 2024: 102753. *doi: 10.1016/j.tmaid.2024.102753.*
5. **Gostin LO, Jha AK, Finch A.** The Mpox Global Health Emergency — A time for solidarity and equity. N Engl J Med 2024; 391: 1265-1267. *doi: 10.1056/NEJMp241039.*
6. **Vakaniaki EH, Kacita C, Kinganda-Lusamaki E, O'Toole Á, Wawina-Bokalanga T, Mukadi-Bamuleka D, Amuri-Aziza A, Malyamungu-Bubala N, Mweshi-Kumbana F, Mutimbwa-Mambo L, Belesi-Siangoli F, Mujula Y, Parker E, Muswamba-Kayembe PC, Nundu SS, Lushima RS, Makangara-Cigolo JC, Mulopo-Mukanya N, Pukuta-Simbu E, Akil-Bandali P, Kavunga H, Abdramane O, Brosius I, Bangwen E, Vercauteren K, Sam-Agudu NA, Mills EJ, Tshiani-Mbaya O, Hoff NA, Rimoin AW, Hensley LE, Kindrachuk J, Baxter C, de Oliveira T, Ayouba A, Peeters M, Delaporte E, Ahuka-Mundeke S, Mohr EL, Sullivan NJ, Muyembe-Tamfum JJ, Nachega JB, Rambaut A, Liesenborghs L, Mbala-Kingebeni P.** Sustained human outbreak of a new MPXV clade I lineage in eastern Democratic Republic of the Congo. Nat Med 2024; 13. *doi: 10.1038/s41591-024-03130-3.*

7. **Beeson A, Styczynski A, Hutson CL, Whitehill F, Angelo KM, Minhaj FS, Morgan C, Ciampaglio K, Reynolds MG, McCollum AM, Guagliardo SAJ.** Mpox respiratory transmission: the state of the evidence. Lancet Microbe 2023; 4: e277-e283. *doi: 10.1016/S2666-5247(23)00034-4.*
8. **WHO**. 2022. https://www.who.int/europe/news/item/23-07-2022-who-director-general-declares-the-ongoing-monkeypox-outbreak-a-public-health-event-of-international-concern. Accessed on September 30, 2024.
9. **CDC.** 2022-2023 Mpox Outbreak Global Map. 2024. https://www.cdc.gov/poxvirus/mpox/response/2022/world-map.html. Accessed on August 28, 2024.
10. **WHO**. 2024. https://www.who.int/news/item/14-08-2024-who-director-general-declares-mpox-outbreak-a-public-health-emergency-of-international-concern. Accessed on September 30, 2024.
11. **GISAID.** 2024. https://www.epicov.org/epi3/frontend#1e17b0. Accessed on August 28, 2024.
12. **Berthet N, Descorps-Declère S, Besombes C, Curaudeau M, Nkili Meyong AA, Selekon B, Labouba I, Gonofio EC, Ouilibona RS, Simo Tchetgna HD, Feher M, Fontanet A, Kazanji M, Manuguerra JC, Hassanin A, Gessain A, Nakoune E.** Genomic history of human monkey pox infections in the Central African Republic between 2001 and 2018. Sci Rep 2021; 11: 13085. *doi: 10.1038/s41598-021-92315-8.*
13. **Bunge EM, Hoet B, Chen L, Lienert F, Weidenthaler H, Baer LR, Steffen R.** The changing epidemiology of human monkeypox-A potential threat? A systematic review. PLoS Negl Trop Dis 2022; 16: e0010141. *doi: 10.1371/journal.pntd.0010141.*
14. **Likos AM, Sammons SA, Olson VA, Frace AM, Li Y, Olsen-Rasmussen M, Davidson W, Galloway R, Khristova ML, Reynolds MG, Zhao H, Carroll DS, Curns A, Formenty P, Esposito JJ, Regnery RL, Damon IK.** A tale of two clades: monkeypox viruses. J Gen Virol 2005; 86: 2661-2672. *doi: 10.1099/vir.0.81215-0.*
15. **PAHO.** 2024. https://shiny.paho-phe.org/mpox/. accessed on September 30, 2024.
16. **D'Angelo P, Loureiro CL, Jaspe RC, Sulbaran YF, Rodríguez L, Alarcón V, García JM, Zambrano JL, Liprandi F, Rangel HR, Pujol FH.** First case of Monkeypox in Venezuela: partial complete genome sequence allowed its grouping into the West African Clade II. Trop Med Infect Dis 2022; 8: 2. *doi: 10.3390/tropicalmed8010002.*
17. **Welkers M, Jonges M and van den Ouden A.** Monkeypox virus whole genome sequencing using combination of NextGenPCR and Oxford Nanopore V.1 https://www.protocols.io/view/monkeypox-virus-whole-genome-sequencing-using-comb-n2bvj6155lk5/v1?step=1.1. Accessed on August 29, 2024.
18. **Tamura K, Stecher G, Kumar S.** MEGA11: Molecular Revolutionary Genetics Analysis version 11. Mol Biol Evol 2021; 38: 3022-3027. *doi: 10.1093/molbev/msab120.*
19. **Molina IS, Jimenez-Vasquez V, Lizarraga W, Sevilla N, Hurtado V, Padilla-Rojas C.** Sub-lineage B.1.6 of hMPXV in a global context: Phylogeny and epidemiology. J Med Virol 2023; 95: e29056. *doi: 10.1002/jmv.29056.*
20. **Comegna M, Flora-Noda DM, Carrión-Nessi FS, Adamidis I, Moreno J, Landaeta ME, Forero-Peña DA.** The arrival of Mpox in Venezuela: Why so few cases? Travel Med Infect 2023; 54: 102599. *doi: 10.1016/j.tmaid.2023.102599.*
21. **Acharya A, Kumar N, Singh K, Byrareddy SN.** Mpox in MSM: tackling stigma, minimizing risk factors, exploring pathogenesis, and treatment approaches. Biomed J 2024: 100746. *doi: 10.1016/j.bj.2024.100746.*
22. **ECDC.** 2024. Confirmed mpox clade Ib case in Germany, risk remains low for EU/EEA. https://www.ecdc.europa.eu/en/news-events/confirmed-mpox-clade-ib-case-germany-risk-remains-low-eueea. Accessed on October 27, 2024.
23. **Delamonica B, Davalos L, Larijani M, Anthony SJ, Liu J, MacCarthy T.** Evolutionary potential of the monkeypox geno-

me arising from interactions with human APOBEC3 enzymes. Virus Evol 2023; 9: vead047. *doi: 10.1093/ve/vead047.*

24. Adamu AA, Okeibunor J, Doshi RH, Wiysonge CS. Enhancing mpox response in Africa with implementation science. Lancet 2024; 30: S0140-6736(24)01807-5. *doi: 10.1016/S0140-6736(24)01807-5.*

25. Sah R, Abdelaal A, Asija A, Basnyat S, Sedhai YR, Ghimire S, Sah S, Bonilla-Aldana DK, Rodriguez-Morales AJ. Monkeypox virus containment: the application of ring vaccination and possible challenges. J Travel Med 2022; 29(6): taac085. *doi: 10.1093/jtm/taac085.*

Invest Clin 65(4): 454 - 461, 2024 https://doi.org/10.54817/IC.v65n4a06

Hallazgo de flebolitos en la región bucal: Reporte de dos casos.

Oscar Arturo Benítez-Cárdenas, Elhi Manuel Torres Hernández, Esteban Raúl Mar Uribe y Jairo Mariel Cárdenas

Departamento de Cirugía Bucal y Maxilofacial, Facultad de Estomatología de la Universidad Autónoma de San Luis Potosí, San Luis Potosí, México.

Palabras clave: flebolitos; patología vascular; trombo; calcificación.

Resumen. Los trombos formados en vasos sanguíneos, aunque suelen tener un flujo sanguíneo normal, pueden experimentar la deposición de minerales, dando como resultado la formación de flebolitos y, cuando afectan la región bucal, pueden provocar asimetría facial debido a un aumento de volumen, confiriendo a la mucosa un aspecto azulado. A pesar de que el diagnóstico de flebolitos suele ser incidental, se hace necesario diferenciarlos de otras calcificaciones. En este artículo, se presentan dos casos clínicos relevantes. El primero está asociado con un evento traumático y se diagnosticó clínicamente como un probable sialolito. El segundo caso, inicialmente diagnosticado como flebolito, no mostraba asociación con patología vascular. Estos casos subrayan la importancia de considerar la posible presencia de flebolitos en el diagnóstico diferencial de lesiones vasculares y otras calcificaciones en la región bucal. Además, se destaca la necesidad de un enfoque cuidadoso y una evaluación detallada para determinar el origen y la naturaleza de las calcificaciones en la mucosa oral para garantizar un tratamiento apropiado y evitar complicaciones potenciales.

Autor de Correspondencia: Jairo Mariel Cárdenas. Dirección: Av. Manuel Nava 2, San Luis Potosí, S.L.P. México. Tel: 00524448262300 ext. 5131; Fax: 00524448139743. E-mail: llairo@yahoo.com.mx

Finding phleboliths in the oral region: Report of two cases.

Invest Clin 2024; 65 (4): 454 – 461

Keywords: phleboliths; vascular pathology; thrombus; calcification.

Abstract. Thrombi formed in blood vessels, although typically experiencing normal blood flow, may undergo mineral deposition, resulting in the formation of phleboliths. When affecting the oral region, they can lead to facial asymmetry due to volume increase, imparting a bluish appearance to the mucosa. Despite phlebolith diagnosis often being incidental, distinguishing them from other calcifications becomes imperative. This article presents two pertinent clinical cases: the first associated with a traumatic event clinically diagnosed as a probable sialolith, and the second case, initially identified as a phlebolith, showed no association with vascular pathology. These cases underscore the importance of considering the presence of phleboliths in the differential diagnosis of vascular lesions and other calcifications in the oral region. Furthermore, it highlights the necessity for a meticulous approach and detailed assessment to determine the origin and nature of calcifications in the oral mucosa to ensure appropriate treatment and mitigate potential complications.

Recibido: 24-11-2023 Aceptado: 29-06-2024

INTRODUCCIÓN

Los trombos formados en vasos sanguíneos con interrupción normal del flujo sanguíneo pueden sufrir la deposición de minerales, formando los flebolitos. Los cuales están principalmente asociados a lesiones diagnosticadas como malformaciones vasculares (MV) o hemangiomas (considerados como tumores vasculares benignos) [1–4]. Chin y col. [5], menciona n que los primeros hallazgos, desde un punto de vista anatómico, sobre los flebolitos, se realizaron tras observar nódulos calcificados intravenosos en disecciones de pelvis humana. Según Garry y col. [2], los flebolitos son trombos organizados calcificados, que no surgen libremente en la luz de las venas, sino que se fijan desde el principio como trombos en la pared de un vaso. Una vez pasado un tiempo, el trombo empieza a tener más organización; se pueden distinguir 2 secciones, una central (en la cual aún se reconocen muchos glóbulos rojos) y otra secundaria, en forma de medialuna, donde se observa una gran cantidad de fibrina y una capa de tejido conectivo en el interior. En un estadio más organizado, la sección secundaria muestra fibras irregularmente dispuestas en sentido concéntrico densamente empaquetadas, característico de los flebolitos. Cuando ya se encuentra organizado, comienza la calcificación desde el interior hacia el exterior del trombo y el centro forma un campo redondeado y homogéneo; una vez fusionada la fibrina con los glóbulos rojos, absorben sales de fosfato de calcio y carbonato de calcio. Su periferia la recubre una capa densamente fibrosa[2]. La clasificación de las MV de la Sociedad Internacional para el Estudio de Anomalías Vasculares (ISSVA por sus siglas en inglés) de 2018, las divide en 4 tipos: simples (capilares, linfáticas, venosas y arteriovenosas) y combinadas, de vasos principales y asociadas a otras anomalías [6]. Además de las MV, también se asocian a hemangiomas intramusculares

(HIM; entidad actualmente no clasificada por la ISSVA) [7,8], siendo el músculo masetero el más afectado de la región de cabeza y cuello [9]. Las malformaciones vasculares son anomalías que se forman por alteraciones durante el desarrollo y morfogénesis de los vasos. Se pueden observar en el momento del nacimiento o pueden aparecer en la primera infancia, suelen aumentar su tamaño de manera proporcional al crecimiento del niño, aunque también la infección, cambios hormonales (pubertad o embarazo) o traumatismos pueden desencadenar su expansión repentina [10-12]. El diagnóstico de flebolitos suele ser incidental por hallazgo, durante estudios de imagen de rutina o estudios de lesiones vasculares. Sin embargo, requieren diferenciarse de otras calcificaciones, tales como sialolitos, tonsilolitos, ganglios linfáticos calcificados, placas ateroescleróticas en la arteria carótida, cisticercosis y/u osteomas cutáneos miliares[13,14]. Los flebolitos que afectan la región bucal clínicamente pueden causar asimetría facial como consecuencia del aumento de volumen y - a su vez- brinda un aspecto azulado a la mucosa [8,14]. A la palpación se pueden percibir nódulos indurados. Puede o no presentar sintomatología, siendo estos en ocasiones dolorosa.

La literatura científica contemporánea proporciona una diversidad de casos clínicos que arrojan luz sobre la presencia y manifestaciones de flebolitos en la región bucal. En un estudio reciente, Sato y col. [15], presentaron un caso de múltiples flebolitos mediales a la rama mandibular derecha, identificados como un hallazgo incidental durante una exploración oral, previa a una intervención quirúrgica general. Este caso resalta la importancia de la detección temprana de lesiones bucales sin presentar signos visibles a la exploración médica. Castro-Abrantes y col. [16], documentaron un caso de malformación vascular con múltiples flebolitos en un paciente que experimentaba cuerpos duros a la palpación que se extendían desde la región de la apófisis coronoides hasta la base de la mandíbula. Este hallazgo enfatiza la necesidad de considerar los flebolitos en el diagnóstico diferencial de las lesiones mandibulares, especialmente en pacientes con manifestaciones clínicas sugerentes de patologías vasculares y óseas. Por otro lado, un informe de Freitas y col. [17], describen un caso de flebolitos en la región posterior de la mucosa bucal izquierda que no estaban relacionados con parestesia o disfasia, pero presentaban dolor. El análisis histopatológico y por tomografía reveló depósitos concéntricos de laminillas calcificadas con focos de material anfofilo amorfo calcificado y una zona periférica revestida por tejido de musculo liso compatible con las paredes vasculares. El diagnostico final fue de múltiples flebolitos hamartosos calcificados. Sivrikaya y col. [18], refieren un paciente que presentó hinchazón dolorosa en la región bucal izquierda con evidente lesión mucosa azulada; al análisis por radiografía y tomografía se observaron múltiples flebolitos. Tal información es de gran importancia por los hallazgos clínicos, las posibles localizaciones inespecíficas, así como el probable tratamiento. Este último puede ser invasivo o no, dependiendo de la ubicación, accesibilidad, profundidad de la invasión, edad, estética y riesgos de posibles hemorragias en el tratamiento quirúrgico. Finalmente, Costa y col. [19], presentaron el caso de una consulta por nódulo benigno, levemente doloroso en la región cigomática derecha. A través de biopsia se diagnosticó como flebolito asociado a hemangioma evolucionado, lo cual demostró la importancia del reconocimiento adecuado de los flebolitos para un manejo clínico apropiado.

Estos casos recientes subrayan la diversidad de presentaciones clínicas de los flebolitos en la región bucal y destacan la necesidad de una evaluación clínica exhaustiva para su detección y diagnóstico adecuados.

En el presente artículo, se presentan dos casos clínicos, el primero, asociado con un evento traumático, clínicamente diagnosticado como probable sialolito versus flebolito y el segundo caso, con diagnóstico inicial de flebolito no asociado a patología vascular.

CASOS CLÍNICOS

Caso 1

Se presenta paciente femenina de 29 años de edad, sin antecedentes crónicos degenerativos, con motivo de consulta por asimetría facial posterior a un trauma contuso, de dieciocho meses de evolución, considerándose de lento y progresivo crecimiento. A la exploración clínica se evidencia la asimetría facial debido al aumento de volumen en la región bucal del lado izquierdo (Fig. 1A). No se observaron cambios de color ni de temperatura; se identifica de superficie blanda con múltiples nódulos indoloros, perceptibles a la palpación, no se observan cambios de coloración ni de temperatura; se identifica de superficie blanda, múltiples nódulos perceptibles a la palpación de forma indolora. A la exploración intraoral no presenta limitación a la apertura, mucosas hidratadas, conductos de glándulas salivales mayores permeables con adecuada producción salival y mucosa yugal del lado izquierdo con ligera tonalidad azulada. De acuerdo con los datos clínicos previamente mencionados, se decide realizar una tomografía computarizada para valorar estado y posición de las lesiones palpables. En la reconstrucción 3D de la tomografía, se observaron 3 nódulos isodensos en el hueso de la región bucal del lado izquierdo; uno de mayor tamaño y dos menores a éste (Fig. 1B).

Debido a las características imagenológicas de los nódulos y a la exploración clínica, se da la impresión diagnóstica de flebolitos, por lo que se decide su escisión quirúrgica bajo anestesia local. El procedimiento quirúrgico consistió en realizar la técnica de asepsia y antisepsia, se infiltró lidocaína 2% con epinefrina en la mucosa y submucosa yugal del lado izquierdo y se realizó una incisión 1cm por debajo al plano paralelo al conducto de Stenon, se hizo disección roma con una pinza moquito hasta acceder a los nódulos que estaban inmersos a la bola adiposa de Bichat.

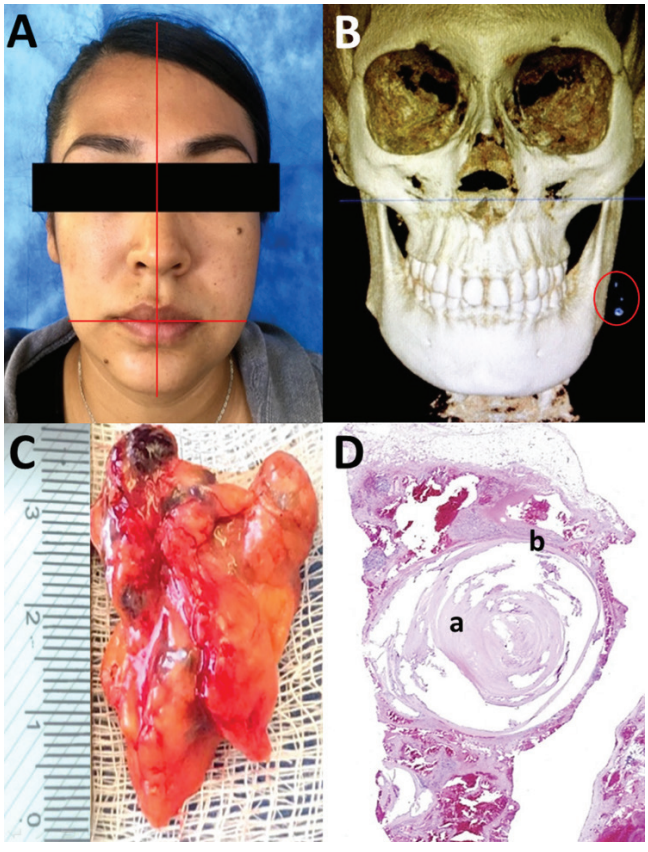

Fig. 1. Caso 1. A. Fotografía frontal de la paciente con asimetría facial por aumento de volumen en región bucal izquierda, sin cambios de coloración. B. Reconstrucción 3D de tomografía facial muestra masas isodensas en el hueso en región bucal izquierda. C. Pieza quirúrgica de 35mm x 30mm con tonalidades amarillas, rojizas y violáceas. D. Imagen histológica muestra tejido adiposo residual, malformaciones vasculares y flebolito en la luz vascular: a. flebolito, b. endotelio.

Se pinzó y traccionó el tejido adiposo con pinzas mosco, para después extraerla. Durante el procedimiento hubo sangrado mínimo, al finalizar, se colocaron puntos de sutura simples con vicryl 4-0. Se obtuvo una pieza quirúrgica de aproximadamente 37x30 mm, de aspecto adiposo con zonas de hematoma (Fig. 1C). A la palpación superficial de consistencia blanda y a la palpación profunda se percibían múltiples nódulos indurados. Al analizar la biopsia se identificó un hallazgo histopatológico en el cual se identifica el depósito de calcio formando estructuras redondas y pétreas circunscritas de endotelio vascular (Fig. 1D).

Caso 2

Paciente femenino de 15 años de edad, sin antecedentes crónico degenerativo ni alérgico. Inicia su padecimiento actual 6 meses previos a su consulta, refiriendo que la madre nota ligera asimetría facial debido a un aumento de volumen en la hemicara izquierda, por lo que decide ir con un cirujano oral y maxilofacial particular para recibir una valoración especializada. A la exploración clínica se observa un aumento de volumen en la región bucal lado izquierdo (Fig. 2A), se identifica de consistencia blanda con múltiples nódulos palpables e indoloros, sin cambios térmicos ni cromáticos. A la exploración intraoral, se evidencia un ligero aumento de volumen en mucosa yugal del mismo lado, sin cambios cromáticos, conductos de glándulas salivales permeables, con buena calidad y cantidad de producción salival. En base a la exploración clínica se tiene la impresión diagnóstica de flebolitos, por lo que se solicita examen imagenológicos a través de tomografía. A su valoración, se observan múltiples nódulos isodensos a hueso en región bucal y maseterina de lado izquierdo (Fig. 2B). Por lo que se decide realizar una biopsia excisional de los nódulos de la región bucal para el diagnóstico definitivo. Para el procedimiento, se realizó la técnica de asepsia y antisepsia pertinente, se infiltró lidocaína al 2% con epinefrina en la mucosa y submucosa yugal del lado izquierdo, y realizar una incisión de 1 cm por debajo al plano paralelo al trayecto del conducto de Stenon, se hizo disección roma con una pinza mosquito hasta acceder a los nódulos que estaban inmersos a la bola adiposa de Bichat. Se pinzó y traccionó el tejido adiposo con pinzas mosco, para después extraerla.

Se continuó con la disección roma con pinzas mosquito hasta localizar los nódulos calcificados, una vez que se localizaron, se

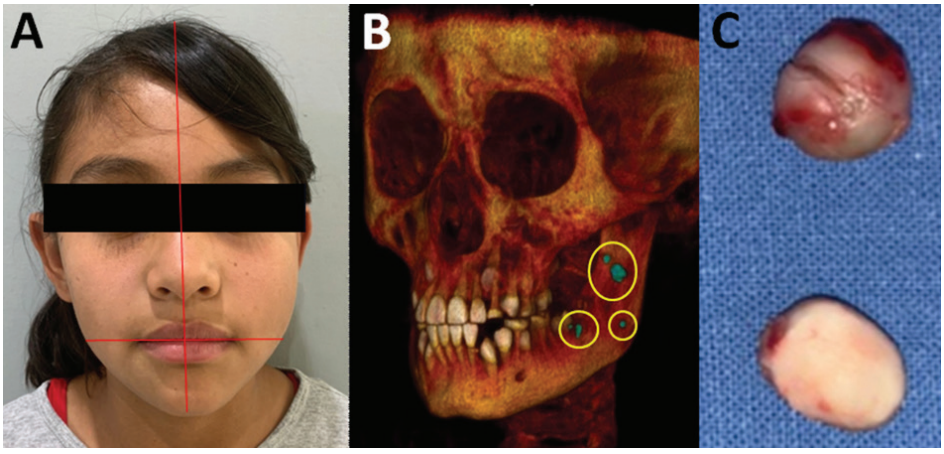

Fig. 2. Caso 2. A. Fotografía frontal de la paciente con ligera asimetría facial por aumento de volumen en región bucal izquierda. B. Reconstrucción 3D de tomografía muestra múltiples masas isodensas en el hueso en región bucal y maseterina izquierda. C. Piezas quirúrgicas: 2 fragmentos ovoides, uno de 10 x 9mm y otro de 10 x 7mm.

pinzaron y traccionaron con pinzas mosco, y se removieron, obteniendo 2 piezas quirúrgicas (Fig. 2C). El sangrado durante la cirugía fue mínimo; se realizó el cierre de la incisión quirúrgica con puntos simples con vicryl 4-0.

DISCUSIÓN

Los flebolitos son trombos calcificados comúnmente asociados a hemangiomas intramusculares y malformaciones vasculares, aunque se han reportado casos raros como calcificaciones solitarias y no asociadas a estas lesiones [14]. También se han relacionado a eventos traumáticos, siendo la causa que los origina [3], tal como el primer caso que se describe. Clínicamente, el signo más común de las MV es una masa de tonalidad púrpura-azulada de crecimiento lento que, a la palpación, suele ser fluctuante, dicha masa puede presentarse en la primera infancia. Los flebolitos pueden encontrarse en glándulas salivales principalmente la parótida, en músculos y tejidos blandos como labios o mejilla. Las malformaciones vasculares son resultado de un error congénito en la morfogénesis vascular, lo cual sucede entre la cuarta y la décima semana de vida intrauterina. El tratamiento de las anomalías vasculares depende de muchos factores, tales como el estadio de desarrollo de la lesión, la edad del paciente, la localización y la intensidad de la lesión. En la mayoría de los casos los hemangiomas sufren una involución total o casi completa, y no suelen requerir tratamiento, aunque sí control y seguimiento clínico, caso contrario a las malformaciones vasculares [20]. Las indicaciones de tratamiento están vinculadas a la asociación con dolor, daño articular, desfiguración o eventos hemorrágicos [21].

Cuando es necesario el tratamiento, a menudo se requiere un procedimiento quirúrgico único, u otras terapias como el láser Nd:YAG, terapia combinada con esteroides[20], escleroterapia (como el etanol deshidratado, tetradecilsulfato de sodio, polidocanol y la bleomicina) con o sin resección quirúrgica subsiguiente [11], embolización, relleno de cera ósea, infiltración de pegamento de fibrina, terapia electroquímica, entre otras [22,23]. En ambos casos mencionados se realizó la escisión quirúrgica sin previo tratamiento; en el segundo caso, asociado a una MV, hubiera sido valiosa la valoración previa para descartar alguna anomalía vascular y evitar un sangrado considerable durante el procedimiento quirúrgico. Ante la sospecha de una anomalía vascular, el US Doppler es el primer estudio de imagen a solicitar, ya que es un estudio económico y no invasivo; además, permite diferenciar entre una lesión de alto y bajo flujo, y se podría identificar la presencia de flebolitos. Una vez identificada la presencia de una anomalía vascular, la resonancia magnética permitirá identificar y definir la extensión de la lesión así como su relación con otras estructuras [22]. Los flebolitos suelen ser laminados, con un núcleo radiopaco, aunque en ocasiones éste puede ser radiolúcido; los flebolitos de menor tamaño son uniformemente radiopacos [24]. En los estudios de imagen de los casos presentados, las lesiones se mostraron como múltiples masas de núcleo y halo radiopaco de aspecto laminado, reforzando la impresión diagnóstica de flebolitos.

Los flebolitos no deben confundirse con los sialolitos; los HIM masetéricos se encuentran en estrecha relación anatómica con la glándula parótida; sin embargo, la sialolitiasis causará obstrucción del conducto de Stenon y sialoadenitis, hallazgos que no se observan en los dos casos presentados; además, la ovalidad del flebolito en comparación con la forma típicamente elíptica del sialolito, puede servir como criterio para distinguirlos [25].

En conclusión, la presencia de flebolitos en la región bucal es un hallazgo clínico relevante que puede estar asociado a diversas condiciones, como malformaciones vasculares, hemangiomas intramusculares, y eventos traumáticos. Los flebolitos pueden provocar asimetría facial y tener manifestaciones clínicas variables, lo que resalta la im-

portancia de considerarlos en el diagnóstico diferencial de lesiones bucales. Los estudios de imagen, como la tomografía computarizada, son fundamentales para confirmar el diagnóstico y planificar el tratamiento adecuado. En los casos presentados, la escisión quirúrgica fue el tratamiento elegido; sin embargo, la evaluación previa para descartar anomalías vasculares habría sido beneficiosa, especialmente para evitar complicaciones durante el procedimiento quirúrgico. Es crucial destacar la importancia del diagnóstico diferencial entre flebolitos y otras calcificaciones bucales como los sialolitos, para garantizar un manejo clínico adecuado y evitar tratamientos innecesarios. Además, se subraya la necesidad de una evaluación multidisciplinaria y un seguimiento adecuado para garantizar el éxito del tratamiento y prevenir recurrencias.

Financiamiento

No se recibió financiamiento.

Conflicto de interés

Los autores declaran que no existe ningún conflicto de intereses económicos, personales o profesionales que puede obstaculizar este trabajo.

Números ORCID de los autores

- Oscar A. Benítez Cárdenas (OABC): 0009-0006-5780-2890
- Elhi M. Torres Hernández (EMTH): 0009-0008-3824-3039
- Esteban Raúl Mar Uribe (ERMU): 0009-0002-1421-1071
- Jairo Mariel Cárdenas (JMC): 0000-0002-4733-7271

Contribución de los autores

OABC, EMTH, ERMU y JMC participaron en la propuesta, concepto y diseño del trabajo, EMTH y ERMU realizaron la preparación de materiales, la recopilación de datos y el análisis de los casos. OABC Y JMC escribieron el primer borrador del manuscrito, diseño de las figuras y discusión en el manuscrito. Todos los autores analizaron los artículos, así como participaron activamente en cada de una de las revisiones enviando sus comentarios, sugerencias y aprobación el manuscrito final.

REFERENCIAS

1. **Becerra-Heredia JL, Fiori-Chíncaro GA, Agudelo-Botero AM.** Flebolitos en la región maxilofacial: un desafío para el diagnóstico por imágenes. Rev Cient Odontol (Lima). 2021 Dec 9;9(4):e086.
2. **Garry S, Wauchope J, Moran T, Kieran SM.** Phleboliths in a vascular malformation within the parotid gland. J Pediatr Surg Case Rep 2022: 83: 102327.
3. **Gouvêa Lima G de M, Moraes RM, Cavalcante ASR, Carvalho YR, Anbinder AL.** An isolated phlebolith on the lip: an unusual case and review of the literature. Case Rep Pathol 2015;2015:507840.
4. **Mallya SM, Lam EWN, Board A, Radiology M, Chapman K, Science C.** White and Pharoah ' s Oral Radiology Principles and Interpretation. 8Th Edition. 2019. ELSEVIER.
5. **Chin On Luk A, Cleaveland P, Olson L, Neilson D, Siringam SJ.** Pelvic phlebolith: a trivial pursuit for the urologist? J Endourol 2017: 31(4): 342-347.
6. **ISSVA classification for vascular anomalies.** Available from: https://www.issva.org/
7. **Kanaya H, Saito Y, Gama N, Konno W, Hirabayashi H, Haruna S.** Intramuscular hemangioma of masseter muscle with prominent formation of phleboliths: A case report. Auris Nasus Larynx 2008; Dec;35(4):587-591.
8. **Sano K, Ogawa A, Inokuchi T, Takahashi H, Hisatsune K.** Buccal hemangioma with phleboliths. Report of two cases. Or Surg Or Med Or Pa. 1988;65(2):151–156.
9. **Park JW, Kim CH, Moon CW.** Intramuscular hemangioma in buccal cheek: A case

report. J Korean Assoc Oral Maxillofac Surg 2017;43(4):262–266.
10. **Scolozzi P, Laurent F, Lombardi T, Richter M.** Intraoral venous malformation presenting with multiple phleboliths. Oral Surg Oral Med. Oral Pathol Oral Radiol Endod 2003;96(2):197–200.
11. **Sousa Costa JR, Torriani MA, Hosni ES, D'Avila OP, de Figueiredo PJ.** Sclerotherapy for vascular malformations in the oral and maxillofacial region: Treatment and follow-up of 66 lesions. J Oral Maxillofac Surg 2011;69(6):e88–92.
12. **Eivazi B, Ardelean M, Bäumler W, Berlien HP, Cremer H, Elluru R, Koltai P, Olofsson J, Richter G, Schick B, Werner JA**. Update on hemangiomas and vascular malformations of the head and neck. Eur Arch Otorrinolaringol 2009;266(2):187–197.
13. **March S, Noffke CEE, Raubenheimer EJ, Chabikuli NJ.** Radiopacities in soft tissue on dental radiographs: Diagnostic considerations. SADJ 2015;70(2):53–57.
14. **Mandel L, Perrino MA.** Phleboliths and the vascular maxillofacial lesion. J Oral Maxillofac Surg 2010;68(8):1973–1976.
15. **Sato S, Takahashi M, Takahashi T.** A case of multiple phleboliths on the medial side of the right mandible. Case Rep Dent 2020; 27;2020:6694402.
16. **Castro-Abrantes T, Barra SG, Silva LVO, Abrahão AC, Mesquita RA, Abreu LG.** Phleboliths of the head and neck Region - A case report. Ann Maxillofac Surg 2022; 12(2):231-233.
17. **Freitas AO, Mota MRL, Sousa FB, Nogueira RLM, Lima-Verde MEQ, Azevedo NO, Alves APN.** Multiple calcified hamartomatous phleboliths in buccal mucosa. Oral Surg Oral Med. Oral Pathol Oral Radiol Endod 2023;136 (1): e69.
18. **Sivrikaya EC, Cezairli B, Ayranci F, Omezli MM, Erzurumlu ZU.** Buccal vascular malformation with multiple giant phleboliths: a rare case presentation and review of the literature. Oral Maxillofac Surg 2019;23(3):375-380.
19. **Costa-Cavalcante SCR, Costa-Alves K, Breda-Junior MA, Lima SBJA, Bessa-Nogueira RV.** Solitary phlebolith in the zygomatic region: a case report. Oral Surg Oral Med. Oral Pathol Oral Radiol Endod 2020; 130(3): e188.
20. **Buckmiller LM, Richter GT, Suen JY.** Diagnosis and management of hemangiomas and vascular malformations of the head and neck. Oral Dis 2010;16(5):405–418.
21. **Wójcicki P, Wójcicka K.** Epidemiology, diagnostics and treatment of vascular tumours and malformations. Adv Clin Exp Med 2014;23(3):475–484.
22. **Dubois J, Alison M.** Vascular anomalies: what a radiologist needs to know. Pediatr Radiol 2010;40(6):895–905.
23. **Ramakrishnan K, Palanivel I, Narayanan V, Chandran S, Gurram P.** Management of vascular malformations in the oral and maxillofacial region: A systematic review. J Stomatol Oral Maxillofac Surg 2021;122(6):588–599.
24. **O'Riordan B.** Phleboliths and salivary calculi. Br J Oral Surg 1974;12(2):119–131.
25. **Mandel L, Surattanont F.** Clinical and imaging diagnoses of intramuscular hemangiomas: The wattle sign and case reports. J Oral Maxillofac Surg 2004;62(6):754–758.

Invest Clin 65(4): 462 - 469, 2024 https://doi.org/10.54817/IC.v65n4a07

Giant ovarian tumors: uncommon ovarian tumors. Report of four cases.

Rosa Ríos[1], Bayron Castro[2], Oscar Hurtado[3], Carlos Briceño-Pérez[4] and the GOT Study Group

[1] Servicio de Ginecología y Obstetricia. Maternidad "Dr. Armando Castillo Plaza". Servicio Autónomo Hospital Universitario de Maracaibo, Venezuela.
[2] Servicio de Cirugía Oncológica. Servicio Autónomo Hospital Universitario de Maracaibo, Venezuela.
[3] Hospital Regional General del Instituto Venezolano de los Seguros Sociales, Uyapar, Estado Bolívar, Venezuela.
[4] Departamento de Obstetricia y Ginecología. Facultad de Medicina, Universidad del Zulia, Maracaibo, Venezuela.

Keywords: giant ovarian tumors; ovary; tumors; cysts; cystadenoms.

Abstract. Over time, the large size of some tumors has been described with fascination. The term "giant" is frequently used to refer to these large gynecologic tumors. Also, to call them "giants", their measurements >10 cm, >15 cm, >20 cm are usually used, and sometimes the limits for their definition are not mentioned. Others define "large" as those >5 cm, those measuring 10-20 cm or those reaching above the umbilicus. In the English-speaking literature, there has been an agreement for more than 53 years on defining uterine or ovarian tumors weighing more than 25 lb as "giants", because, in 1971, Beacham *et al*, reviewed the uterine or ovarian tumors reported between 1946-1970, weighing 25 lb. or more. The present study aimed to report the clinical characteristics and management of four uncommon cases of giant tumors, with good surgical management, that evolved successfully and without complications. We defined as "giants", gynecologic tumors weighing 25 lb or more and the used parameter was weight, not measurements. Four tumors were benign, cystadenoma-type, and three serous. Two patients were nulliparous, and two were of indigenous race. All four patients were of extreme ages. The tumors weighed 46.738, 65.256, 26.675 and 27.116 lb (21.200, 29.600, 12.100 and 12.300 kg).

Correspondence author: Carlos Briceño-Pérez. Facultad de Medicina, Universidad del Zulia. ObGyn Department. Maracaibo, Venezuela. Phone: +584146731325. Email: cabripe@hotmail.com

Tumores gigantes de ovario: una rara serie de 4 casos.

Invest Clin 2024; 65 (4): 462 – 469

Palabras clave: tumor gigante de ovario; ovario; tumores; quistes; cistadenomas.

Resumen. El gran tamaño de algunos tumores se ha descrito con fascinación, a lo largo del tiempo. El término "gigante" se utiliza con frecuencia para referirse a estos tumores ginecológicos de gran tamaño. También, para llamarlos "gigantes", se suelen utilizar sus medidas >10 cm, >15 cm, >20 cm; y en ocasiones no se mencionan los límites para su definición. Otros definen los "grandes" como aquellos >5 cm, los que miden 10-20 cm o los que llegan por encima del ombligo. En la literatura anglosajona, ha habido acuerdo durante más de 53 años en definir los tumores uterinos u ováricos que pesan más de 25 libras, como "gigantes", ya que, en 1971, Beacham y col., revisaron los tumores uterinos u ováricos reportados entre 1946-1970, que pesaban 25 libras o más. El presente estudio tuvo como objetivo relatar las características clínicas y el manejo de 4 raros casos que, a pesar de ser tumores "gigantes", con buen manejo quirúrgico, todos evolucionaron sin complicaciones y con éxito. Definimos como "gigantes" los tumores ginecológicos que pesaban 25 libras o más y el parámetro utilizado fue el peso, no las medidas. Los 4 tumores eran benignos, de tipo cistadenoma, serosos (3). Dos pacientes eran nulíparas, 2 eran de raza indígena. Las 4 pacientes eran de edades extremas. Los tumore pesaron 46.738, 65.256, 26.675 y 27.116 lb (21.200, 29.600, 12.100 y 12.300 kg).

Received: 18-03-2024 Accepted: 28-06-2024

INTRODUCTION

The large size of some tumors has been described with fascination over time. These include gynecological ones, of which cases of enormous growth are described, especially before the advent of ultrasound (US)[1]. The terminology of these large tumors contains very varied and confusing qualifiers, including "immense", "extensive", "voluminous", "massive", "large", "very large", "giant", "gigantic", *etc.* [1,2]. The term "giant" is often used to refer to these large gynecological tumors. Also, to call them "giants", their measurements >10 cm [3], >15 cm [4], >20 cm[5], are usually used; and sometimes the limits for their definition are not mentioned[1,3,4-8]. Others define "large" ovarian cysts as those >5 cm [4], those measuring 10-20 cm[5] or those reaching above the umbilicus[9]. In the English-speaking literature, there has been an agreement for more than 55 years on defining uterine or ovarian tumors weighing more than 25 lb., as "giants"[1,2,10]. This is because, in 1971, Beacham *et al.* [11] reviewed the uterine or ovarian tumors reported between 1946-1970, weighing 25 lb. or more. These authors noted the following: 1. they defined as "giants" only gynecologic tumors weighing 25 lb. or more; and 2. the parameter used for their definition was weight, not measurements. In clinical practice, it is difficult to gather a series of four cases of this size, for which the present work set out the aim of reporting the clinical features and the management of four cases of giant ovarian tumors (GOT) that weighed 46.738, 65.256, 26.675 and 27.116 lb (21.200, 29.600, 12.100 and 12.300 kg) (Fig. 1).

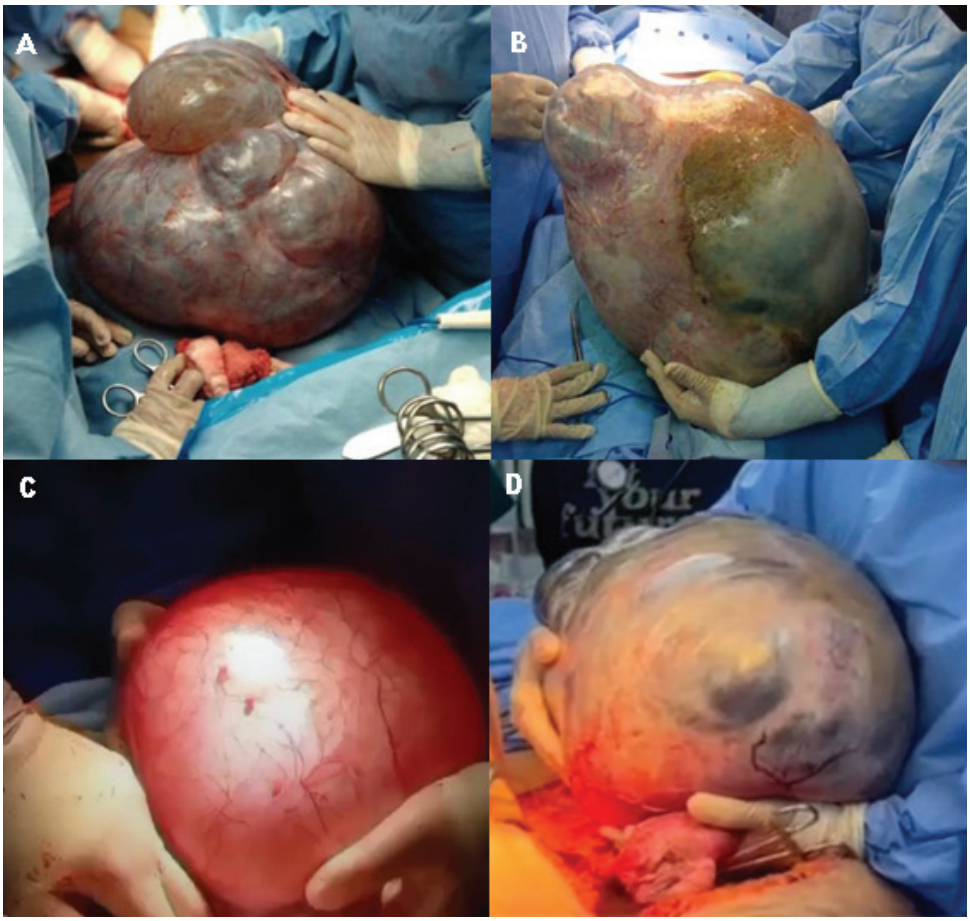

Fig. 1. Four cases of Giant Ovarian Tumor. A: Case 1, 46.738 lb or 21.200 Kg, B: Case 2, 65.256 lb or 29.600 Kg, C: Case 3, 26.675 lb or 12.100 Kg, D: Case 4, 27.116 lb or 12.300 Kg.

CASES REPORT

Case 1

MM, 57 years, consulted the Autonomous Service University Hospital of Maracaibo (OGS-ASUHM) or Maternity Dr. Armando Castillo Plaza, Venezuela, on October 29-20, due to dyspnea at medium exertion and increased volume in the abdomen, from eight months before. Genital bleeding of the meno-metrorrhagia type of moderate quantity, bright red, without clots, not fetid. Abdomen: AC: 125 cm, palpable tumor of approximately 90 x 80 cm, non-mobile, non-painful, ascites is evident; preoperative laboratory tests: normal. Abdominal-pelvic US: evidenced from the xiphoid region to the hypogastrium, a large lesion occupying liquid content, multilocated with echoes of medium echogenicity, rounded, poorly defined irregular contours, without vascularization, measurement by quadrants with an approximate diameter of 41.7 x 35.0 x 35.7 mm (Fig. 2A). Conclusion: Injury occupying the abdominal-pelvic space. Admission diagnoses (October 29-20): Giant tumor of the left ovary. 2. Chronic arterial hypertension. On November, 13-20 an exploratory laparotomy was performed with the following operative findings: 1. Giant tumor of the left ovary with cystic content, approximately 100 x 100 cm, with an estimated weight of approximately 15 kg. upon inspection. 2. Left oophorectomy was performed, and the frozen biopsy reported papillary mucinous cystadenoma, which was negative for malignancy. 3. Right ovary without alterations. 4. Abdominal

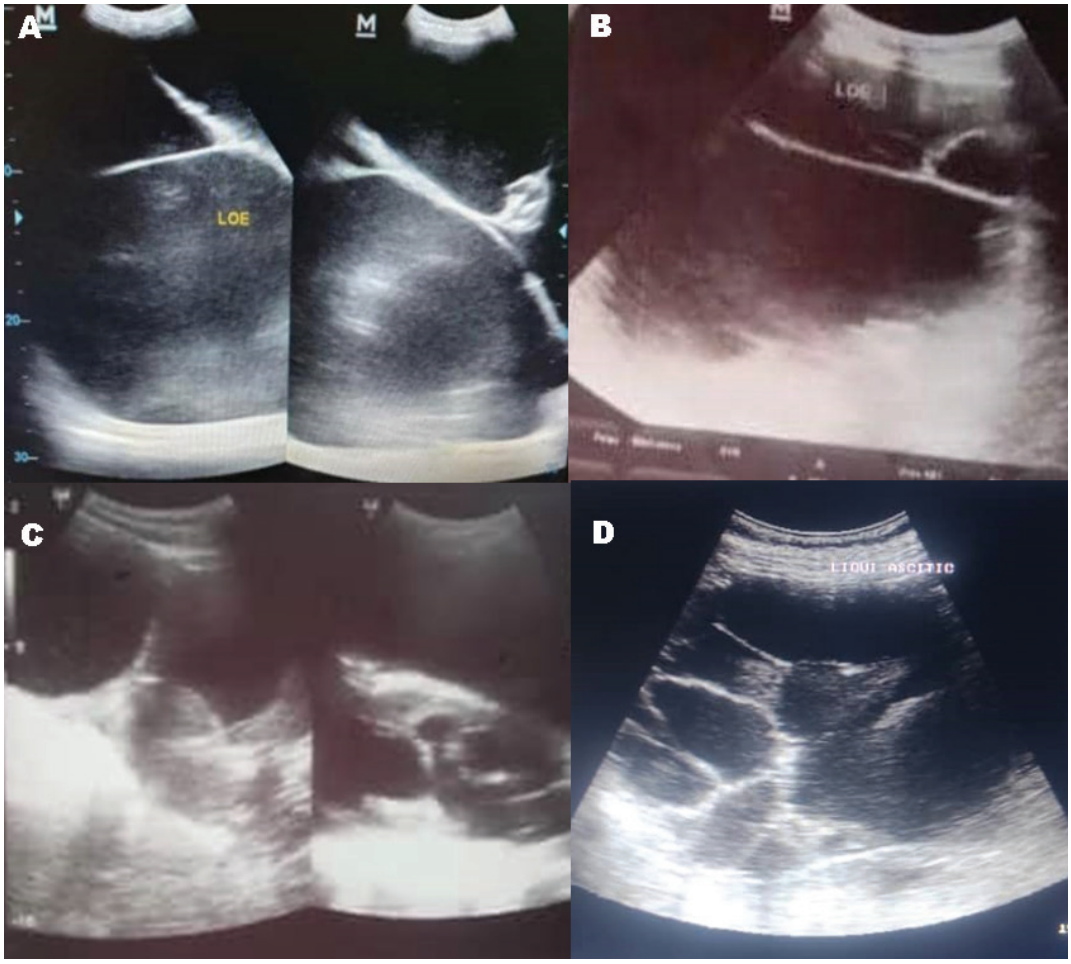

Fig. 2. Ultrasound images of four cases of Giant Ovarian Tumor. A: Case 1, B: Case 2, C: Case 3, D: Case 4.

cavity lavage was performed. 5. The abdominal cavity was closed. Postoperative evolution was expected, and was discharged on the 13th postoperative day (November, 26-20). The anatomopathological study (December, 04-20) reported a left ovarian tumor that measured 30 x 25 cm, and weighed 46.738 lb (21.200 kg), with a diagnosis of mucinous cystadenoma of the left ovary (Fig.1A). The immediate, mediate, and late (June 2021 and November 2022) postoperative controls were normal.

Case 2

SMPP, 43 years old, was admitted to OGS-ASUHM on April 08-22 for presenting dyspnea at medium exertion and increased volume in the abdomen 3 years earlier. The abdomen was globular, distended, and had an ascites wave. Abdominal-pelvic US (11, 29-19): large lesion occupying abdominal-pelvic space, of probable ovarian etiology (Fig. 2B), simple cyst of the left ovary, uterine fibroids. MRI (February, 04-20): Abdominal-pelvic space occupation lesion. Giant ovarian cyst. Tumor markers (January 24-20): β-chorionic gonadotropin, alpha-fetoprotein and CA-125 normal. Admission diagnoses (April 08-20): Giant ovarian tumor. Plan: 1. Laboratory tests 2. Admission for surgery. On April, 18-22 an exploratory laparotomy was performed with operative findings: 1. Giant right ovary tumor, with a cystic appearance, estimated weight of

approximately 30 kg. 2. Endometrial polyp of 2 x 1 cm., without macroscopic evidence of malignancy. A right oophorectomy was performed, and the frozen biopsy reported serous cystadenoma, negative for malignancy. Total abdominal hysterectomy, left oophorectomy, and appendectomy were performed. Abdominal cavity lavage was performed. Normal postoperative evolution. Discharged on the 18th postoperative day (May 06-22). Weight at discharge: 95.019 lb. Anatomopathological report (May, 20-22): tumor that measured 30 x 25 cm, weighed 65.256 lb. (29.600 kg), right ovary serous cystadenoma (Fig. 1B). Immediate and mediate postoperative medical controls were normal.

Case 3

BBIG, a 16-year-old adolescent, was admitted to OGS-ASUHM on 04, 20-22 due to increased abdominal volume. Abdomen, palpable supra-umbilical mobile tumor, not painful. β-HCG: 4.33 U/ml, CA-125: 48.70 U/ml, CA-19.99: 6.85U/ml., Alpha-fetoprotein: 4.16 ng/ml, CEA: 1ng/mL. Abdominal-pelvic US: space-occupying lesion of probable ovarian nature, rule out the retroperitoneal origin, correlate with abdominopelvic CT (Figure 2C). Abdominal-pelvic computed tomography: image of probable ovarian nature, hypodense, with regular contours, density similar to liquids, thin walls, measuring approximately 36.2 x 25 x 16.2 cm. and covering the entire abdominal and pelvic region. On 04, 21-22 an exploratory laparotomy was performed, showing a giant cystic tumor of the right ovary, which measured approximately 40 x 50 cm. and weighed 26.675 lb. (12.100 kg) (Fig. 1C). The transoperative frozen biopsy reported papillary serous cystadenoma, without evidence of malignancy. Postoperative evolution was satisfactory, and she was discharged in good general condition on 04 25, 2022, 5th postoperative day.

Case 4

L.O.A., 64 years old, consulted on March 2023 for an increased volume in the left abdominal iliac fossa region of progressive growth 6 months ago, without extenuating circumstances. Concomitantly refers to pain in that area. She was evaluated, and an abdominal-pelvic tomography imaging study was indicated, which reported a cystic tumor in the pelvic cavity. Elective surgery was planned. Ca 19-19: 15 (0-47), CA-125: 41 (0-35), verified value. Abdominal-pelvic computed tomography (CT): (March 03-23): tumor of cystic appearance, large size, occupying the pelvic cavity extending to the upper abdomen of 27x 20cm., in diameter with a displacement of neighbouring structures and highly suggestive of ovarian tumor. Liquid collection, incipient ascites at the level of the pelvic cavity. Abdominal US (march 14-23): suggestive signs of giant mucinous type cystic tumor. Minimal ascites (Figure 2D). Chest X-ray PA (July,14-23): Slight elevation of left hemidiaphragm. Cytology and ascitic fluid cell block (March, 13-23): chronic inflammatory smear with reactive mesothelial changes. Evaluation by oncologic surgery (March, 22-23): GOT, scant ascites. Dx Admission: GOT. Surgical intervention (August, 05-23): exploratory laparotomy: ovarian protocol. Findings: 50 mL inflammatory fluid, tumor of left ovary, 70 x 50 cm, firmly adherent to the left uterine horn, cystic, of mixed consistency. Uterus, right ovary, right uterine tube: normal. Procedure: Peritoneal fluid sampling, tumor exteriorization, total abdominal hysterectomy with tumor inclusion, right salpingo-oophorectomy, vaginal vault closure, right and left parietocolic slide, right and left diaphragm and prevesical fascia and Douglas pouch sampling, omentectomy, appendectomy, plane synthesis, placement of drains in subcutaneous cellular tissue, asepsis and final cure. Tumor histological type (biopsy): serous cystadenoma, benign, weight: 27.116 lb (12.300 kg) (Fig. 1D). Hospitalization for 48 hours with satisfactory clinical evolution.

DISCUSSION

GOT are uncommon in the present day due to early diagnosis and treatment [4,5,8,9,10,12]. GOT have previously been reported prior to 1929 with nine tumors weighing between 200 and 300 pounds, 87 weighing greater than 100 and 203 weighing between 50 and 100. The most remarkable descriptions of GOT are those of Spohn, in 1962, who reported 148.6 kg (328 lb) [10].

Tumors in the ovary generally are epithelial tumors. Serous hysto-type is the more common [5,9]. They are characteristically unilateral, only 5-10% presenting bilaterally [9,13], and can develop at any age; however, they are more common during the reproductive years[3,12,13]. GOT are uncommon among postmenopausal and are extremely uncommon in the pediatric and adolescent populations [6]. In this series, all four tumors were unilateral and not at reproductive ages but at extreme ages (3 over 40 years and one adolescent). Two of the four patients were nulliparous, and 2 of the 4 were large multiparas. Two of the four were of indigenous race. The four reported GOT weighed 46.738, 65.256, 26.675 and 27.116 lb (21.200, 29.600, 12.100 and 12.300 kg) (Fig. 1).

There is an extensive list of differential diagnoses: peritoneal cyst, para-ovarian cyst, appendiceal mucocele, cystic adenomyosis, liver, pancreatic or choledochal cyst, lymphocele, cystic lymphangioma, duplication intestinal cyst, bladder diverticulum; to name just a few [14].

The most common clinical signs are rapidly expanding abdominal distension and a palpable mass; they may be accompanied by nonspecific abdominal pain, vomiting, constipation, ovary torsion, and rupture [3.] Our four patients with GOT, reported increased abdominal volume.

Tumor markers play a vital role, with carcinoembryonic antigen (CEA), CA-125, and CA19-9 more likely elevated. CA-125 was performed in 3/4 patients and CA-19-9 in 2/4; were normal [5].

Needle aspiration for cytology provides inaccurate results, and owing to its associated complications, it is not recommended [13]. We did not do needle aspiration for cytology.

The primary imaging modality for evaluating ovarian and adnexal masses is US, which allows accurate identification in approximately 90% of cases [3,15]. Unfortunately, imaging studies such as US, CT and magnetic resonance (MRI) do not always determine the cyst's origin, thus limiting its diagnostic usefulness [15]. In our four patients, US and other image studies described the lesions but were inconclusive.

The choice's treatment is surgery. Removing the cyst intact for histology is the gold standard [15]. It can be accomplished by *en bloc* removal of the tumor with or without controlled drainage of tumor fluid. The lateral decubitus is the preferred position in which to operate. Resection of mass intact through a transverse elliptical incision with intense intraoperative and postoperative monitoring will provide the safest and optimal setting [4,15]. These four tumors, were removed intact *en bloc*, without fluid drainage or aspiration, and the resection of four masses was through longitudinal incisions.

Some epidemiological factors to consider before surgery include the patient's age, desire to have children, nutritional status, access to medical facilities and the surgeon's experience. Careful planning will be necessary to obtain favorable results, with a multidisciplinary approach to management, pre-and postoperatively, by the gynecologists, onco-surgeons, anesthesiologists, intensivists and dieticians [16].

Surgical management must consider various factors, especially in adolescents, where the operative strategy is to cure and maintain fertility [3,6]. During surgery, it is advisable to perform a cystectomy rather than an oophorectomy [12]. Cryopreservation

of ovarian tissue from the unaffected ovary might be an option to preserve fertility.

Many potential problems have been associated: respiratory failure, intraoperative fluids shifts, adequate exposure, orthostatic hypotension and adynamic intestine [3,12]. Despite our four cases being GOT, they all evolved without complications and were successfully managed.

Samples of peritoneal fluid for cytology must be collected. Some advocate progressive preoperative drainage [6,12]. Decompression of the cystic component before mass excision is often necessary to avoid lesions to the adjacent structures.

Laparoscopy can be used as an option for diagnostic purposes in the differential diagnosis. The tumor can be inspected, and when there are signs of malignancy, the surgeon may change the procedure to an open laparotomy. Laparoscopically in GOT, especially those that reach the umbilicus, there is a risk of perforation when the trocar is inserted [3]. Although many studies have advocated and claimed successful removal of giant ovarian cysts laparoscopically, hardly any study has claimed laparoscopic removal [9]. In these four cases, during laparotomy, we collected samples of peritoneal fluid for cytology, did not decompress the cyst before excision of the mass and did not use laparoscopy.

In summary, giant ovarian tumors are only weighing 25 lb. or more. Giants ovarian tumors are uncommon. The used parameter for their definition is weight, not measurements. With good surgical management, as in these four cases, they can evolve successfully without complications.

ACKNOWLEDGMENTS

To Ana Carvajal, Betty Iguarán, the OGS-ASUHM and the OGS-RGH-IVSS staffs.

To collaborators: Rosa Rubio, Paula Morán, Paula Toledo, Neysaré Monegro, Germana González, Leonela Rivero, Jesús Roo, Dreilis García, Parrasqueby Loukidis, Liliana Sánchez, María Díaz, Daniel Solano.

Funding

The authors declare no funds.

Conflicts of interest

The authors declare no conflict of interest.

Informed consent

An explanation and collection of informed consent to the surgical procedure were achieved by the patients, as well as the consent for publication in scientific journals.

ORCID number of authors

- Rosa Ríos (RR): 0009-0001-2056-3519
- Bayron Castro (BC): 0009-0008-0806-9383
- Oscar Hurtado (OH): 0009-0004-5813-069X
- Carlos Briceño-Pérez (CB-P): 0000 0002 3270 8236

Author´s contributions

CB-P had the idea to make the study. CBP, RR, and BC made the study design. CBP, RR, BC and OH made the data collection, data analysis and interpretation, critical review of the intellectual content and final approval of the manuscript.

REFERENCES

1. **Briceño-Pérez C, Alaña F, Atencio de Ávila D, Betancourt de Benítez C, Schloeter L, Portillo B, Briceño-Sanabria L.** Grandes miomas uterinos. Rev Obstet Ginecol Venez 2001;61:35-42. Available in: https://www.sogvzla.org/wp-content/uploads/2023/03/2001_vol61_num1_9.pdf
2. **Briceño-Pérez C.** Tumores uterinos y ováricos: ¿Gigantes? o Grandes. Rev Obstet Ginecol Venez 2007;67(1):3-4.

3. **Pramana C, Almarjan L, Mahaputera P, Wicaksono SA, Respati G, Wahyudi F, Hadi C.** A Giant ovarian cystadenoma in a 20 year old nulliparous woman: a case report. Front Surg 2022; 9:895025. *doi: 10.3389/fsurg.2022.895025*
4. **Ye LY, Wang JJ, Liu DR, Ding GP, Cao LP.** Management of giant ovarian teratoma: a case series and review of the literature. Oncol Lett 2012;4: 672-676. *doi: 10.3892/ol.2012.793.*
5. **Shrestha BM, Shrestha S, Kharel S, Aryal S, Rauniyar R, S Kuikel, Tiwari SB, Chaurasia H, Chapagain S, Shrestha P**. Giant ovarian mucinous cystadenocarcinoma: a case report. Clin Case Rep 2022;10:e06067. *doi: 10.1002/ccr3.6067.*
6. **Persano G, Severi E, Cantone N, Incerti F, Ciardini E, Noccioli B.** Surgical approach to giant ovarian masses in adolescents: technical considerations. Pediat Rep 2018; 10(3)7752. *doi: 10.4081/pr.2018.7752.*
7. **Leite C, Barbosa B, Santos N, Oliveira A, Casimiro C.** Giant abdominal cyst in a young female patient: A case report. Int J Surg Case Rep 2020;72:549-555. *doi: 10.1016/j.ijscr.2020.06.085.*
8. **Corias F, Pedeeriva F, Cozzi G, Ammar L, Lembo MA, Barbi E.** A giant ovarian cyst in an adolescent. J Pediatr 2018;199:279. *doi: 10.1016/j.jpeds.2018.03.015.*
9. **Bhasin SK, Kumar V, Kumar R.** Giant ovarian cyst: A case report. JK Science 2014;16(3):131-133.
10. **O'Hanlan KA.** Resection of a 303.2 pound tumor. Gynecol Oncol 1994;54:365-371. *doi: 10.1006/gyno.1994.1225.*
11. **Beacham W, Webster H, Lawson E, Roth L.** Uterine and/or ovarian tumors weighing 25 pounds or more. Am J Obstet Gynecol 1971;109:1153-1161. *doi: 10.1016/0002-9378(71)90657-0.*
12. **Fobe D, Vandervurst T, Vanhoutte L.** Giant ovarian cystadenoma weighing 59 kg. Gynecol Surg 2011;8:177-179. *https://doi.org/10.1007/s10397-010-0593-0.*
13. **Madhu YC, Harish K, Gotam P**. Complete resection of a giant ovarian tumour. Gynecol Oncol Rep 2013; 6:4-6. *doi: 10.1016/j.gynor.2013.05.001.*
14. **Shrestha BM, Shrestha S, Kharel S, Aryal S, Rauniyar R, S Kuikel, Tiwari SB, Chaurasia H, Chapagain S, Shrestha P.** Giant ovarian mucinous cystadenocarcinoma: a case report. Clin Case Rep 2022;10:e06067. *doi: 10.1002/ccr3.6067.*
15. **Leite C, Barbosa B, Santos N, Oliveira A, Casimiro C.** Giant abdominal cyst in a young female patient: A case report. Int J Surg Case Rep 2020;72:549-55. *doi: 10.1016/j.ijscr.2020.06.085.*
16. **González-Machado JD, Fonseca-Sosa FK.** Cistoadema mucinoso gigante de ovario. Rev Obstet Ginecol Venez 2024; 84(1):78-83. *https://doi.org/10.51288/00840112.*

Invest Clin 65(4): 470 - 475, 2024 https://doi.org/10.54817/IC.v65n4a08

Severe necrotic colitis in an adolescent with polypharmacy and high clozapine doses according to his ancestry.

Trino Baptista[1,2,3], José de Leon[4,5], Antonio Guizar[2,6] and Laura Evia[2]

[1]Departamento de Fisiología, Facultad de Medicina, Universidad de Los Andes, Mérida, Venezuela.
[2]Clínica NeuroORIGEN, Queretaro, México.
[3]Facultad de Medicina, Universidad Anahuac Queretaro, Queretaro, México.
[4]Mental Health Research Center at Eastern State Hospital, Lexington, KY, USA.
[5]Biomedical Research Centre in Mental Health Net (CIBERSAM), Santiago Apostol Hospital, University of the Basque Country, Vitoria, Spain.
[6]Universidad Americana de Europa (UNADE), Spain.

Keywords: clozapine; constipation; colitis; ethnicity; polypharmacy.

Abstract. The antipsychotic drug Clozapine (CLZ) is approved for treatment-resistant schizophrenia and reduction in the risk of recurrent suicidal behavior in schizophrenia or schizoaffective disorder. However, it is increasingly used in psychiatry and neurology worldwide in numerous off-label conditions. Clozapine is associated with diverse side effects which require careful monitoring in its use for prevention and treatment. The quality of CLZ use and pharmacovigilance varies considerably among Latin American countries. CLZ-induced gastrointestinal hypomotility (CIGH) is a relevant clinical problem, ranging from innocuous constipation to lethal necrotic colitis. Thus, optimal prevention, early detection, and treatment of CIGH deserves considerable attention. We describe here the case of a 15-year-old Mexican boy diagnosed with Oppositional Defiant- and Attention-Deficit/Hyperactivity Disorder who developed severe necrotic colitis after nine months of CLZ treatment, leading to permanent ileostomy. We ascribed this unfortunate outcome to careless polypharmacy that did not consider drug-related antimuscarinic activity, deficient clinical monitoring, and lack of attention to ethnicity concerning drug dosing. This case is of educational value for the mental health team in order to promote the proper use of CLZ, which may be life-saving in patients with severe mental disorders.

Corresponding author: Trino Baptista. Departamento de Fisiología, Facultad de Medicina, Universidad de Los Andes, Mérida, Venezuela. E-mail: trinobaptista@gmail.com

Severa colitis necrotizante en un adolescente con polifarmacia y dosis elevada de clozapina con relación a su origen étnico.

Invest Clin 2024; 65 (4): 470 – 475

Palabras clave: clozapina; colitis; constipación; etnicidad; polifarmacia.

Resumen. El antipsicótico Clozapina (CLZ) está aprobado en el tratamiento de la esquizofrenia resistente y para reducir el riesgo suicida en esta condición y en el trastorno esquizoafectivo. Sin embargo, su uso no aprobado en psiquiatría y neurología ha aumentado recientemente en todo el mundo. La CLZ se asocia a diversos efectos indeseables, los cuales ameritan monitorización cuidadosa para su prevención y tratamiento. La hipomotilidad gastrointestinal (HMGI) asociada al uso de Clozapina (CLZ), es un problema clínico relevante que se manifiesta desde un nivel de constipación inocua hasta colitis necrotizante letal. En consecuencia, la prevención óptima, detección temprana y el tratamiento de la HMGI amerita atención considerable. Presentamos el caso de un adolescente mexicano de 15 años con los diagnósticos de Trastornos Oposicionista-Desafiante y Déficit de Atención con Hiperactividad, que desarrolló colitis necrotizante severa que condujo a ileostomía permanente luego de 9 meses de tratamiento con CLZ. Atribuimos este cuadro clínico al uso inadecuado de polifarmacia en donde no se valoró adecuadamente al efecto antimuscarínico de los medicamentos, y al desconocimiento del impacto de grupo étnico en la dosificación de la CLZ. Este caso clínico es de valor educativo para el equipo de salud mental, con el fin de promover el uso adecuado de la CLZ, que puede ser una medida vital en pacientes con enfermedades mentales severas.

Received: 02-09-2024 Accepted: 07-11-2024

INTRODUCTION

The atypical antipsychotic drug Clozapine (CLZ) was synthesized in 1958. However, it was not until the years 1990-92 that the Food and Drug Administration (FDA) approved its use in the United States (US) for treatment-resistant schizophrenia (TRS) and the extension of the label for the reduction in the risk of recurrent suicidal behavior in schizophrenia or schizoaffective disorder. These are the only label indications for CLZ use in the whole field of psychiatry [1].

However, CLZ use in psychiatry and neurology has significantly increased in the last twenty years for off-label indications such as dementia-related behavioral disorders, bipolar disorders, anxiety, autism spectrum, suicidality, drug use in psychosis, borderline personality, and neurological patients with movement disorders and/or psychosis [1]. While there are now available treatments more specific for these neurological disorders, they are not readily accessible in Latin American countries, and numerous neurologists still use off-label CLZ at low doses as adjunctive therapy, in general benefiting from CLZ-alleviating effects on anxiety and insomnia.

This trend is also due to the increasing understanding of CLZ pharmacokinetics, drug interactions, the role of ethnicity, genes, and adverse drug reactions (ADRs) [2,3].

CLZ has numerous ADRs, such as pneumonia, agranulocytosis, metabolic syndrome,

orthostatic hypotension, bradycardia, syncope, seizures, myocarditis, cardiomyopathy, mitral valve incompetence, hepatotoxicity, pancreatitis, sialorrhea, cancer, and gastrointestinal hypomotility (CIGH) [1]. The proper use of CLZ, thus, request for an *ad hoc* mental health team training, ideally including drug-serum monitoring, since many of those ADRs correlate with the drug blood levels. Latin American countries considerably differ in CLZ-ADR monitoring, pharmacovigilance, and related research quality. In Venezuela, there was even a recent CLZ shortage, and it is now provided without any mandatory regular blood monitoring, as suggested by experts [4,5].

The CIGH disorders range from mild constipation to severe and often lethal gut obstruction and necrosis, such as we describe in the following case.

CASE PRESENTATION

The mother's patient signed an informed consent for publishing this case. On Day 1, T.B., examined a 15-year-old Mexican non-smoking boy with severe restlessness, insomnia, and verbal and physical violence towards his mother and pets. He was of Indigenous American ethnicity with limited economic resources. At 12 years of age, he was diagnosed with severe Oppositional Defiant Disorder and Attention-Deficit/Hyperactivity Disorder and required a one-month hospitalization in a public institution. He was prescribed lithium carbonate (900 mg/day), methylphenidate (18 mg/day) and risperidone (up to 8 mg/day), this last agent being the only antipsychotic drug recommended for those disorders [6]. His irregular outcome led to poor school adaptation.

In the first interview, he exhibited an intelligence in the lower limit of normality, irritability, extreme restlessness (running in and out of the office) and a quarrelsome attitude toward his mother, who had Type II Bipolar Disorder with good insight.

Clozapine, 6.25 mg at bedtime, was started off-label (day 1). Therapeutic drug monitoring was unavailable. The slow titration was based on standard clinical tolerance and weekly serum C-reactive protein (CRP). The dose was slowly increased to 100 mg in three weeks, resulting in only a minimal improvement in sleep.

After no significant improvement, the family placed the patient in a short-term psychiatric inpatient unit for three weeks, with no participation of the previous treating psychiatrists (days 31 to days 52). He was prescribed six psychiatric drugs: CLZ 300 mg/day (100 mg three times a day), olanzapine 20 mg/day (10 mg twice a day), quetiapine 200 mg/day (100 mg twice a day), sodium valproate 1500 mg/day (500 mg three times a day), lamotrigine 50 mg/day (25 mg twice a day), and diazepam 20 mg/day (10 mg twice a day). Propranolol was added for suspected akathisia 40 mg/day (20 mg twice a day). The white blood cell (WBC) count remained normal, but no other laboratory tests were completed. Worried by the combination of three antipsychotics with antimuscarinic activity, TB constantly insisted, by phone, on monitoring for constipation but was told that disrupting behavior interfered with that. He prescribed preventive daily lactulose at bedtime.

After three weeks of minimal improvement (day 53), the patient was transferred to an outpatient facility without continuous medical or nursing monitoring. Approximately six months on CLZ (day 180), the patient started to complain of abdominal discomfort, and after two weeks, he was transferred to a hospital (day 194), where he was diagnosed with sepsis, renal failure, and severe gastrointestinal obstruction. The emergency surgery revealed massive dry fecal content and necrotic colon and led to a colon removal except for a small sigmoid portion with permanent ileostomy. After surgery, zuclopentixol, 20 mg every 3 weeks, levetiracetam 1000 mg/day (500 mg twice

a day), and oral clonazepam 2 mg/day at bedtime were prescribed. On the phone, the family informed TB they wanted to restart CLZ administration, but contact was lost afterwards.

DISCUSSION

The term CLZ-associated CIGH has been used to describe an extensive set of possible complications in the digestive system[7,8]. The World Health Organization (WHO) pharmacovigilance database receives reports on adverse drug reactions (ADRs). On July 19, 2019, CIGH was the fifth cause of fatal outcomes in CLZ patients, with 326 fatal outcomes associated with 2814 cases of constipation, toxic megacolon, and/or paralytic ileus [2,3]. CIGH develops [7,8] gradually during CLZ treatment, but up to 50% of patients may be unaware while gastrointestinal motility is objectively decreased [9,10].

Preventive laxatives and careful use of agents with antimuscarinic properties are recommended at the start of CLZ treatment [7,8].

This is a case of severe, almost lethal colonic necrosis in a young man. CLZ and its metabolite norclozapine have high antimuscarinic activity, which reduces gastrointestinal motility [11].

During the first month of treatment under T.B. control, a carefully slow CLZ titration, including CRP monitoring, was conducted since he had Indigenous American ethnicity following a recent guideline [2]. Later, the complications probably happened by a combination of at least three significant factors:

1. Lack of proper bowel monitoring. First, at home, it happened due to the constant hostility between the patient and his relatives. In the unsupervised outpatient facility, medical assessment happened only after two weeks of severe constipation and abdominal pain.

2. High doses of CLZ and polypharmacy. After one month on CLZ with poor response, another consultant psychiatrist tried to manage the challenging behavior in the hospital by increasing CLZ to 300 mg/day, and adding valproate (1.500 mg/day), quetiapine (200 mg/day) and olanzapine (20 mg/day). In retrospect, this was an unwise decision due to a lack of drug serum levels and clinical monitoring. The CLZ dose (300 mg/day) was higher than the 225 mg/day recommended for male non-smokers among patients of Indigenous American ancestry [2].

In this regard, our research group has defined six personalized schedules for inpatients: 1) ancestry from Asia or the original people from the Americas with lower metabolism (obesity or valproate) needing minimum therapeutic dosages of 75–150 mg/day, 2) ancestry from Asia or the original people from the Americas with average metabolism needing 175–300 mg/day, 3) European/Western Asian ancestry with lower metabolism (obesity or valproate) needing 100–200 mg/day, 4) European/Western Asian ancestry with average metabolism needing 250–400 mg/day, 5) in the U.S. with ancestries other than from Asia or the original people from the Americas with lower clozapine metabolism (obesity or valproate) needing 150–300 mg/day, and 6) in the U.S. with ancestries other than from Asia or the original people from the Americas with average clozapine metabolism needing 300–600 mg/day.2.

Moreover, olanzapine is also mainly metabolized by the cytochrome P450 1A2 (CYP1A2) like CLZ [2,3], and due to the patient's ancestry, he was expected also to have higher plasma olanzapine concentration. As CIGH is a dose-dependent adverse reaction, which is more appropriately defined as concentration-dependent, the patient probably dis-

played very high serum antimuscarinic activity by high plasma concentrations of CLZ and norclozapine and from the additions from the plasma concentrations of olanzapine and quetiapine [11]. Valproate can inhibit CLZ and olanzapine, particularly in early treatment [2]. CIGH complications such as ileum and necrosis result from a complex set of antimuscarinic-induced hypomotility and inflammation. The associated inflammation probably inhibited CYP1A2 and caused significant increases in CLZ and olanzapine concentrations and possibly milder quetiapine concentrations [3].

These pharmacokinetic issues request for blood level CLZ and norclozapine monitoring. Unfortunately, Chile is the only Latin American country where public mental health facilities provide such monitoring in sections of Psychiatric Institutions designed as 'CLZ clinics' [4].

3. Whereas the indication of CLZ in children and adolescents with schizophrenia is well established [12], that is not the case for CLZ off-label indications, such as the present case. Among other potential factors, CLZ might display a heterogeneous and unexpected side effect profile, which are not necessarily explained by ancestry or its pharmacological properties [13].

CONCLUSIONS

The use of CLZ in psychiatry and neurology is rapidly increasing, mostly as off-label indications. Thus, the proper monitoring and treatment of diverse, potentially lethal CLZ-related ADRs, besides neutropenia, is mandatory. This case shows how CIGH may lead to almost lethal consequences, and it could have been prevented by taking into account the complex pharmacokinetic and pharmacodynamic properties of CLZ and the other drugs used in this case, ethnicity, monitoring constipation's severity and proper use of laxatives [2,7,8,10].

Psychiatric educators play a crucial role in training all mental health members on these issues in a CLZ-treated patient. This is particularly important in Venezuela, where there are no current mandatory guidelines for CLZ use in psychiatry and neurology. Hence, we recommend improving the knowledge about CLZ pharmacokinetics and drug interactions and using it as monotherapy when possible.

ACKNOWLEDGEMENTS

The authors thank the patient's family for authorizing this publication.

Funding

None

Conflict of interest

None

Authors' ORCID number

- Trino Baptista (TB): 0000-0001-6839-4614
- Jose de Leon (JDL): 0000-0002-7756-2314
- Antonio Guizar (AG): 0009-0005-0661-0576
- Laura Evia (LE): 0000-0009-2527-698X

Author contribution

TB and JDL wrote the manuscript. TB was the former treating physician. AG and LE assisted TB in treating the patient and revised the manuscript.

REFERENCES

1. **Leung JG, de Leon J, Frye MA, Singh B, Cotes RO, McElroy SL.** The modernization of clozapine: a recapitulation of the past in the United States and the view forward. J. Clin. Psychopharmacol

2022; 42: 565–580. *doi.org/10.1097/ JCP. 0000000000001606.*

2. **de Leon J, Baptista T, Motuca M, Ruan CJ, Schoretsanitis G, De Las Cuevas C.** Promoting safer clozapine dosing in the Americas. Braz J Psychiatry 2022. 22; 363-365. *doi: 10.47626/1516-4446-2021-0041.*
3. **de Leon J.** Reflections on the complex history of the concept of clozapine-induced inflammation during titration. Psychiatr Danub 2022. 34: 411-421. *doi.org/ 10.24869/psyd.2022c.411.*
4. **Baptista T, Motuca M, Serrano A, Perez Lo Presti A, Fernandez-Arana A, Olmos I, Pabon A, Yepez JGA, Alejo Galarza GJ, Rivera Ramirez NM, Elkis H, Sanz EJ, De Las Cuevas C, de Leon J.** An expert review of clozapine in Latin American countries: Use, monitoring, and pharmacovigilance. Schizophr Res. 2024. 268. 60-65. *doi: 10. 1016/j.schres.2023.10.025.*
5. **Baptista T, Serrano A, Presti APL, Fernandez-Arana A, Elkis H, Motuca M, Olmos I, Schoretsanitis G.** Clozapine safety monitoring and related research in psychiatry and neurology in South America: A scoping review. Schizophr Res. 2024; 268: 29-33. *doi: 10.1016/j.schres.2023.07.029.*
6. **Pringsheim T, Hirsch L, Gardner D, Gorman DA**. The pharmacological management of oppositional behavior, conduct problems, and aggression in children and adolescents with attention-deficit hyperactivity disorder, oppositional defiant disorder, and conduct disorder: a systematic review and meta-analysis. Part 2: antipsychotics and traditional mood stabilizers. Can J Psychiatry 2015;60: 52-61. *doi: 10.1177/070674371506000203.*
7. **Every-Palmer S, McLean RM, Ellis PM, Harrison-Woolrych M.** Life-threatening clozapine-induced gastrointestinal hypomotility: an analysis of 102 cases. J Clin Psychiatry 2008. 69:759-768. *doi: 10.4088/jcp.v69n0509.*
8. **Every-Palmer S, Newton-Howes G, Clarke MJ.** Pharmacological treatment for antipsychotic-related constipation. Cochrane Database Syst Rev. 2017. 24:1(1):CDO11128. *doi: 10.1002/14651858.CD011128.*
9. **Baptista T, Carrizo E, Fernandez E, Connell L, Servigna M, Parra, A, Quintero J, Pabón A, Sandia I, Uzcáteguid E, Serrano A, Pirela N, Villarreal L.** Colonic transit diagnostic test shows significant gastrointestinal hypomotility in clozapine-treated patients in comparison with subjects treated with other antipsychotics. Schizophr Res. 2015. 166: 207-211. *doi: 10.1016/j. schres.2015.05.025*.
10. **Baptista T.** A fatal case of ischemic colitis during clozapine administration Rev Bras Psiquiatr. 2014;36:358. *doi. org/10.1590/1516-4446-2014-1402.*
11. **de Leon J, Odom-White A, Josiassen RC, Diaz FJ, Cooper TB, Simpson GM.** Serum antimuscarinic activity during clozapine treatment. J Clin Psychopharmacol 2003; 23:336-341. *doi:10.1097/01. jcp.0000085405.08426.73.*
12. **Correll CU, Arango C, Fagerlund B, Galderisi S, Kas MJ, Leucht S**. Identification and treatment of individuals with childhood-onset and early-onset schizophrenia. Eur Neuropsychopharmacol 2024; 82:57-71. *doi: 10.1016/j.euroneuro.2024.02.005.*
13. **Pringsheim T, Hirsch L, Gardner D, Gorman DA.** The pharmacological management of oppositional behaviour, conduct problems, and aggression in children and adolescents with attention-deficit hyperactivity disorder, oppositional defiant disorder, and conduct disorder: a systematic review and meta-analysis. Part 2: antipsychotics and traditional mood stabilizers. Can J Psychiatry 2015 60: 52-61. *doi: 10.1177/070674371506000203.*

Invest Clin 65(4): 476 - 494, 2024 https://doi.org/10.54817/IC.v65n4a09

High throughput sequencing technology and its clinical application in circulating tumor DNA detection in patients with tumors.

Chonghe Xu[1], Dangui Zhou[2*] and Mei Zhu[2]*

[1]School of Basic Medical Sciences, Capital Medical University, Beijing, People's Republic of China.
[2]Department of Clinical Laboratory, the Affiliated Chaohu Hospital of Anhui Medical University, Chaohu, Anhui, People's Republic of China.
[*]These authors contributed equally to this work.

Keywords: high throughput sequencing; tumor; circulating tumor DNA; tumor diagnosis; tumor treatment; tumor prognosis.

Abstract. The high-throughput sequencing (HTS) is now a highly favoured technology in the field of genome research. A distinctive feature of this sequencing method is its data-yielding capability, which is capable of generating more than 100 times than the first-generation Sanger sequencing platform. HTS technology has been widely adopted for its advantages, including high throughput, sensitivity, automaticity, information density and cost-effectiveness. Not only does it help in the treatment and diagnosis of multiple diseases, but it also provides new insights into the research in molecular biology of tumors. Moreover, circulating tumor DNA (ctDNA) tests based on HTS technology are increasingly extensively implemented for clinical purposes. In this review, we will focus on the significant achievements and performances of the HTS, and first-hand data from extensive experience will be summarized and analyzed to discuss the advantages and specifics associated with each sequencing system and further summarize the characteristics of their clinical applications.

Correspondence author. Mei Zhu, Department of Clinical Laboratory, the Affiliated Chaohu Hospital of Anhui Medical University, No. 64 Chaohu North Road, Chaohu, Anhui, PR China. E-mail: zhumei@ahmu.edu.cn

Tecnología de secuenciación de alto rendimiento y su aplicación clínica en la detección de ADN tumoral circulante en pacientes oncológicos.

Invest Clin 2024; 65 (4): 476 – 494

Palabras clave: secuenciación de alto rendimiento; tumores; ADN tumoral circulante, diagnóstico de tumores; tratamiento de tumores; pronóstico de tumores.

Resumen. La secuenciación de alto rendimiento (HTS) es una tecnología popular en el campo de la investigación genómica. Una característica distintiva de este método de secuenciación es su capacidad de generación de datos, que puede generar 100 veces más datos que la Plataforma de secuenciación Sanger de primera generación. La tecnología superconductora de alta temperatura es ampliamente utilizada debido a sus ventajas de alto rendimiento, alta sensibilidad, automatización, densidad de información y rentabilidad. No solo ayuda a tratar y diagnosticar múltiples enfermedades, sino que también proporciona nuevas ideas para la investigación de biología molecular tumoral. Además, la detección de ADN tumoral circulante (ctDNA) basada en la tecnología HTS se utiliza cada vez más ampliamente con fines clínicos. En esta revisión, nos centraremos en los principales logros y rendimiento de HTS, y resumiremos y analizaremos datos de primera mano de una amplia experiencia, discutiremos las ventajas y detalles específicos de cada sistema de secuenciación y resumiremos aún más las características de su aplicación clínica.

Received: 15-08-2024 Accepted: 17-10-2024

INTRODUCTION

The past decade has witnessed the introduction and broad application of HTS technologies. Not only can it perform chromosome mapping, but it can also conduct deep sequencing and whole genome sequencing analysis on blood, body fluids and excreta such as urine, feces, sputum, cerebrospinal fluid, sperm, saliva, vaginal secretions, milk and effusions [1-7]. This revolutionary technology facilitates diagnosis at the genetic level and is especially suitable for complex diseases that are highly heterogeneous and involve both genes and mutations, such as tumors[8]. ctDNA is an important biomarker, a circulating cell-free DNA (cfDNA) generated by the apoptosis, necrosis and secretion process of tumor cells, and it contains relatively complete genetic information about tumour cells [9]. Additionally, it contains the same mutations as the DNA in tumor cells, including insertions, deletions, rearrangements, copy number variations and methylations. Therefore, using HTS technology to test for ctDNA can provide crucial information on the diagnosis, treatment and prognosis of tumors [10].

In this review, we introduced the main features of the HTS, such as first-generation Sanger sequencing, second-generation HTS platforms (454 Life Sciences pyrosequencing, Illumina/Solexa technology and SOLiD ligase-mediated sequencing) and third-generation high throughput - next generation sequencing (HT-NGS) platforms (Ion Torrent technology, Single-molecule real-time (SMRT) sequencing and Nanopore sequencing technology). In addition, this article also

describes the application of ctDNA in the diagnosis, treatment and prognosis of tumors.

Overview of high-throughput sequencing platform

First-generation Sanger sequencing

In the mid-1970s, DNA sequencing saw a major technological innovation, the Sanger dideoxy synthesis method, proposed by Sanger. The advent of this method provided scientists with a new means of determining four different nucleotide bases in single-stranded DNA using radio-labelling [11,12]. Sanger sequencing technology, as a landmark development in the field of DNA sequencing, has dramatically advanced the process of genomics research. However, this technology has certain limitations in practical application, i.e., the amount of DNA that can be processed in each experiment is limited. Although this limitation made Sanger sequencing unable to meet the demand for high throughput in some cases, it laid the foundation for developing subsequent sequencing technologies. In pursuing higher throughput and more efficient sequencing technologies, scientists have made continuous efforts and eventually succeeded in developing the second, third and even higher throughput sequencing platforms [13-15]. Their high throughput and accuracy enable researchers to access genetic information more quickly and accurately, providing powerful support in areas such as disease diagnosis, personalized medicine and biotechnology.

Second-generation HTS platforms

The second-generation HTS uses a different analysis principle than the first-generation Sanger sequencing. The key technologies of the second-generation HTS platform include bridge sequencing and synthetic sequencing. These technologies have enabled the platform to have a wide range of applications in areas such as genomics research, variant detection and gene expression analysis. However, despite the significant advances in sequencing length and accuracy of the second-generation platforms, they still have some limitations, such as shorter read lengths and higher error rates.

454 Life Sciences pyrosequencing

A unique sequencing method has attracted much attention in exploring the early development of NGS technologies. In 2000, Jonathan Rothberg successfully developed the first commercially available NGS platform, which was innovative in that it used a unique mechanism to read the signals of individual nucleotides added to a DNA template. It utilizes the properties of luciferase, which generates light signals when new nucleotides are added to a DNA strand, and these signals are subsequently captured and converted into readable data[16]. This method combines pyrosequencing technology with single-molecule emulsion PCR; sequencing is done through a synthetic process in which four nucleotide bases are added one by one to a DNA template. Each time a new nucleotide is added, it triggers the production of a different coloured light, which is caused by the release of pyrophosphate from the microwells [12,17]. In general, pyrosequencing is centred on the concept of "sequencing by synthesis", which is in sharp contrast to the traditional Sanger sequencing method, which is done by detecting the release of pyrophosphate to determine whether a specific nucleotide has been added to the DNA strand. Pyrophosphate is released when a nucleotide is added to a growing DNA strand. These pyrophosphate releases are detected, and a signal is generated. By monitoring these signals, we can determine the bases on the DNA template strand at each position. The essential advantage of this method is that it does not require ddNTPs, which means that no terminating strand synthesis is required during sequencing, thus increasing the accuracy and efficiency of sequencing[14,18]. During the nucleotide doping, more than one nucleotide may be doped into the same position. This situation leads to the

formation of a homopolymer because the nucleotide used lacks molecules capable of preventing further doping. This fully doped homopolymer will form in one cycle [19].

With the rapid development of NGS technologies, various sequencing platforms are emerging. Roche discontinued support of the platform in 2016, which resulted in the platform being phased out, and other more efficient and accurate sequencing platforms are gradually replacing it as technology advances. This change reflects the rapidly evolving field of sequencing technology and the importance of continually updated platforms and technologies.

Illumina/Solexa technology

In 2006, Solexa introduced an innovative sequencing technology that employs a reversible terminator strategy to enhance adapter-linked DNA fragments through bridge amplification. This method allows the bases on the template strand to be read employing a nucleotide-by-nucleotide process that involves successive nucleotide doping, a cleaning step, imaging, and a subsequent cleavage step [14,15,20,21]. The extraction and segmentation of DNA is the primary step aimed at breaking down complex DNA molecules into smaller, manageable fragments. This process usually involves using specific enzymes to cut the DNA, resulting in fragments of a certain length. Next, these DNA fragments need to be ligated to specific adapter sequences to facilitate subsequent sequencing steps. Adapter sequences are short pieces of DNA or RNA sequences that bind to the ends of the DNA fragments and provide an interface for connection to the sequencing machine. Once the adapter sequences have been successfully ligated to the DNA fragments, these conjugates are transferred to a flow cell. The flow cell is a unique device that precisely positions the DNA fragments on the cell surface. The DNA fragments are copied in large numbers through clonal amplification, forming clonal "clusters". These clusters consist of many identical single-stranded DNA fragments that are physically tightly packed to facilitate high-throughput sequencing by sequencing machines [17,19,22].

During each sequencing cycle, four fluorescently labelled nucleotides compete for the opportunity to bind to the template strand. This is a competitive process in which only nucleotides complementary to the corresponding nucleotide on the template strand can be successfully doped. Once a nucleotide has been doped, the laser detects a signal due to fluorescent labelling, identifying which nucleotide has been doped into the template strand. After identification, the next step is to remove the blocking group and fluorescent marker from the doped nucleotide. This step is in preparation for the next sequencing cycle, making the template strand available again for new nucleotides to be doped. During this process, the nucleotide sequence on the template strand is gradually built up, with each sequencing cycle adding a point of information for the final determination of the entire DNA sequence. The efficiency of this sequencing strategy lies in its ability to quickly and accurately determine the DNA sequence by detecting fluorescent signals and complementary nucleotide incorporation. As the sequencing cycle is repeated, sequence information of the entire genome is gradually revealed [21-23].

Illumina sequencing has become an indispensable tool in modern genomics research. This technology supports a wide range of sequencing protocols, covering areas ranging from comprehensive sequencing at the genome level to more specific exon sequencing, targeted sequencing, and macrogenomics for studying microbial communities. It is also widely used for methods such as RNA sequencing, chromatin immunoprecipitation sequencing (CHIP-seq) and methylome analysis [17].

However, despite the Illumina sequencing platform's market-leading position due to its high output capacity and broad applicability, this short-read technology still has limitations in certain areas. In particular, in

many applications in genomics, short read lengths limit resolution and accuracy. This means that when high precision is required to resolve genome structure or identify low-frequency variants, short-read technologies may not provide sufficient information [13]. Therefore, for these specific research needs, it may be necessary to use a combination of other sequencing technologies, such as long reads or single molecule sequencing, to obtain higher-resolution sequence data. Despite these limitations, Illumina sequencing technology continues to be essential in advancing genomics and biomedical research.

SOLiD ligase-mediated sequencing

In 2007, Applied Biosystems introduced a new sequencing platform, Supported Oligonucleotide Ligation Detection (SOLiD). This platform is similar to other sequencing technologies in that it detects the fluorescence intensity of dye-labelled molecules to determine the sequence of DNA fragments. However, the SOLiD platform employs a unique sequencing technique known as DNA ligase-based sequencing [12,24]. A distinguishing feature of this technique is that it generates relatively short read lengths, typically 35 base pairs [25,26]. Nonetheless, the SOLiD platform was a significant breakthrough at the time, providing new tools for genomics research.

The technology involves cutting the template DNA into small fragments and ligating them to a known junction sequence. This process ensures that the DNA fragments can be efficiently captured and sequenced. Next, these junction-connected DNA fragments are transferred to a particular type of beads, which are subsequently immobilized on a glass surface. These fragments can be clonally amplified on the beads using emulsion PCR, resulting in many identical DNA fragments. During the sequencing stage, the sequence of each DNA fragment is determined by a two-base colour coding method. This method relies on different dye pairs to identify and record each nucleotide in the DNA sequence. The SOLiD sequencing platform is particularly adept at detecting single nucleotide polymorphisms (SNPs), which can be detected with an astonishing 99.85% accuracy. This high level of accuracy makes SOLiD a powerful tool for genomics research, especially for SNPs detection. With this kind of precise sequencing, researchers can better understand genetic variations and their relationship with diseases, providing a scientific basis for personalized medicine and disease diagnosis [12,27,28].

Like other NGS systems, SOLiD's computational infrastructure is more costly and less convenient to operate. Nonetheless, SOLiD technology has been widely used in several fields, including but not limited to whole genome resequencing, transcriptomics research, targeted resequencing, and epigenomics analysis. Currently, these three leading second-generation high-throughput sequencing platforms are available on the market, as shown in Fig. 1. The commercialization of these platforms provides powerful tools for researchers and promotes research progress in related fields. Meanwhile, with the continuous development of science and technology, more sequencing platforms are under development and are expected to join this competitive market in the future. This will help further promote the development of genomics research and provide more possibilities for biomedical research.

Third-generation HTS platforms

Third-generation sequencing technology is gradually changing our understanding of genomics. Compared with the previous two generations of platforms, the advantage of third-generation sequencing is that it provides longer read lengths and higher accuracy. The third generation of HTS platforms uses single-molecule sequencing technology, capable of simultaneously sequencing millions to billions of DNA molecules. The core of this technology is represented by the Ion Torrent technology, Single Molecule Real-Time Sequencing and Nanopore sequencing technology, as shown in Fig. 2.

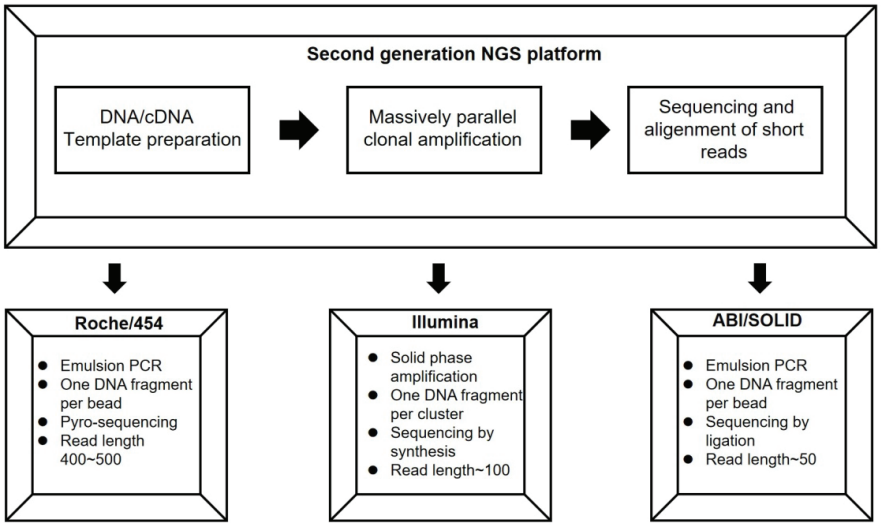

Fig. 1. Characteristics of the three leading second-generation HTS platforms.

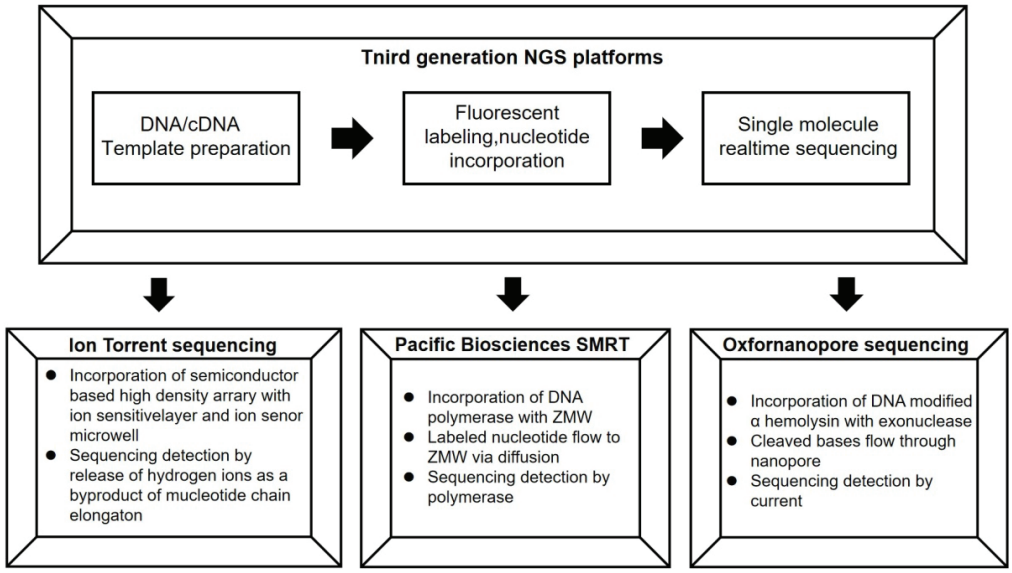

Fig. 2. Characteristics of the three leading third-generation HTS platforms.

Ion Torrent technology

Ion Torrent technology is a nucleotide synthesis-based sequencing (SBS) method, which has many similarities in principle with the 454 pyrophosphate sequencing platform, but the technical means used in detecting the correct insertion of nucleotides differs between the two methods. In Ion Torrent technology, molecules are first fragmented, and then these fragmented molecules are bound to the surface of specific beads. Next, the target molecules on these beads are clonally amplified by emulsion PCR, resulting in a large number of identical target molecules on each beads. This step is a core component of the Ion Torrent technology, ensuring effective capture of target molecules and providing efficient sequencing. After this process, each bead can be regarded as an independent sequencing reaction unit, which lays the foundation for the subsequent sequencing steps [12,17,20,22].

Treated beads are dispensed into tiny holes on the chip during sequencing. These microholes form a microarray, with each hole corresponding to a specific sequencing reaction. When beads are placed in these microholes, a synthetic-based sequencing reaction is performed on each bead [22,29]. During DNA replication, each newly added nucleotide causes a slight change in the pH of the solution. This change is captured by the sensor and converted into a voltage signal, enabling the monitoring of nucleotide addition. Specifically, when a nucleotide pairs successfully with a complementary base on the DNA strand, it releases a hydrogen ion, causing the pH to drop. This pH change is detected by the sensor and converted into a voltage signal. No voltage spike occurs if no nucleotides are added in this round. Two hydrogen ions are released when two neighbouring nucleotide sites are filled with the same nucleotide simultaneously, causing the voltage signal to double. This doubled voltage change provides a direct signal to distinguish between neighbouring nucleotides. By continuously monitoring the addition of nucleotides and the corresponding voltage changes during each sequencing cycle, we can accurately determine the sequence of bases on a DNA strand [17,22].

Ion Torrent technology is favoured in the sequencing field for its highly efficient detection system, which does not rely on expensive cameras, light sources or scanners, resulting in a significant increase in detection speed compared to traditional 454 pyrophosphate sequencing [17]. This advantage has made the Ion Torrent method the preferred choice for various applications. However, the technology is not without its limitations. Studies have shown that while there is a correlation between the number of base integrations and voltage changes, it is not a perfect relationship. As a result, the problem of homopolymer template elongation remains, which is caused by cumulative light intensity changes [30]. Despite this challenge, the Ion Torrent technology remains essential in modern gene sequencing due to its speed and accuracy.

Single-molecule real-time (SMRT) sequencing

In 2011, Single Molecule Real-Time Sequencing (SMRT) technology was introduced by Pacific Biosystems, marking a new advancement in the field of gene sequencing on long-read platforms. This technology is unique because it can sequence up to 30-50 kb or longer DNA fragments, far beyond what conventional sequencing technologies can handle [17,31]. SMRT sequencing centres on the tight binding of a specially formulated DNA polymerase to the target DNA, a process that occurs in SMRT cells [17]. The design of these SMRT cells is unique in that they contain tens of thousands of tiny chambers, each equipped with a DNA polymerase and a zero-mode waveguide (ZMW) well[23]. This innovative design allows the sequencing process to be performed at the level of individual molecules, resulting in efficient and accurate sequencing of DNA sequences. ZMW plays a crucial role, which is a tiny structure that precisely directs light energy to a specific, relatively small-sized region. This property makes the ZMW a critical factor in enabling single-molecule sequencing[17]. In preparation for sequencing, the SMRT technology takes an innovative approach, unlike traditional methods of fixing DNA strands. Specifically, high-fidelity DNA polymerase and single-stranded DNA templates are added to the SMRT cell chamber to serve as templates for DNA replication at the bottom of the ZMW [23,27]. This design allows the DNA replication process to occur at the level of individual molecules, resulting in efficient and accurate sequencing of DNA sequences. An essential step in this process involves the addition of different phosphorylated fluorescein markers to these tiny chambers. These markers are present to enable precise monitoring of DNA polymerase activity. When DNA replication occurs, DNA polymerase must recognize and integrate nucleotides

complementary to the template DNA. Phosphorylated fluorescein markers added to the ZMW minicells play a crucial role in this process. They can interact specifically with DNA polymerase activity, thus enabling researchers to distinguish and detect different events during DNA replication [23].

In ZMW technology, integrating nucleotides is a crucial step that triggers the release of fluorescein. Once the fluorescein is released from the bottom of the ZMW, it is no longer in the detection state and emits a specific fluorescent signal. The uniqueness of this fluorescent signal means that each nucleotide produces a different fluorescence pattern. In practice, the fluorescence signals from the tiny chamber of the ZMW are captured by a high-definition video system and converted into digital signals. These digital signals are then analyzed to determine the nucleotide sequence on the DNA template. Since each nucleotide has unique fluorescence properties, the sequence of the DNA can be determined by identifying and interpreting these fluorescence signals [15,17,23]. In SMRT cells, up to one million ZMWs are integrated on a single chip. These tiny chambers are the core units in the sequencing process, performing both nucleotide integration and imaging. Each ZMW independently captures and records real-time images of nucleotide integration. This ability to process in parallel dramatically increases the speed and throughput of sequencing [15,17].

Nanopore sequencing technology

As an innovative single-molecule sequencing method emerging in recent years, Nanopore sequencing technology has made significant progress in genomics research. Unlike traditional sequencing techniques based on nucleotide integration, nanopore sequencing technology offers an entirely new strategy. This technology utilizes nanopores as sensors to directly detect biological macromolecules, such as DNA and RNA, at the single-molecule level, thus enabling real-time monitoring at the single-molecule level [15,32].

Nanopore sequencing technology eliminates the cumbersome PCR amplification and chemical labelling steps during operation. This means that researchers do not need to perform complex pre-processing of samples when performing sequencing, greatly simplifying the experimental process. More importantly, this technology allows direct use of cell lysates for sequencing without the need for additional sample preparation, which not only saves experimental time but also reduces experimental costs. These advantages make nanopore sequencing technology more efficient and more widely applicable in single-molecule sequencing [27].

Nanopore sequencing technology is an innovative DNA sequencing method that utilizes protein nanopores embedded in a polymer membrane. In this process, when a DNA molecule passes through a nanopore known as a molecular motor protein, it causes a disorder in the nanopore protein, which generates electrical signals. The conversion of these electrical signals is the core principle of nanopore sequencing technology, which enables researchers to determine the DNA sequence by analyzing these signals[14,27,33,34]. Based on nanopore sequencing technology, researchers can determine the sequence of a DNA molecule by detecting changes in the electrical currents it generates as it passes through the nanopore. The key to this technique is that each nucleotide causes unique current changes that can be detected and recorded precisely. By analyzing these current changes, we can tell the sequence of nucleotides in a DNA molecule [23].

The nanopore technology could offer a wide range of applications in fields such as personalized medicine, agriculture and scientific research. In addition, the portability of nanopore sequencing technology allows sequencers to be taken into the field for direct sequencing, greatly expanding the range of sequencing applications and increasing the efficiency of field studies [14,32-37]. This technology provides a direct and efficient means to study the properties of DNA and is essential

for research in genomics, molecular biology and other related fields.

Application of HTS technology in tumor diagnosis and treatment

Tumors have claimed numerous lives as malignant cells continuously mutate and evolve as they divide. Most patients died from fatal metastasis and cancer recurrence. However, with mature HTS technology, researchers have obtained significant genetic information on tumor pathogenesis, drug resistance and metastasis, which will help in the early screening and identification of tumors, selection of therapies and monitoring of prognosis.

Diagnosis of tumors

Early diagnosis and prompt treatment are critical to controlling the growth of tumors. Genetic testing is characterized by the ease of sampling, which allows researchers to minimize the harm to their subjects. In order to alleviate the pain associated with traditional invasive pathological biopsies, researchers have turned to body-fluid-based sequencing to assist in the diagnosis of cancer. Circulating tumor DNA (ctDNA) is derived from single- or double-stranded DNA and DNA-protein complexes shed by tumor tissue. The presence of mutated DNA fragments is observed at relatively high concentrations in the circulation of most patients with metastatic cancer and low but detectable concentrations in a significant proportion of patients with localized cancer. This characteristic ensures that ctDNA exhibits particular specificity and can serve as a biomarker for clinical purposes [38].

Lung cancer is one of the most common cancers, and its early diagnosis plays a crucial role in improving patients' quality of life. However, low-dose computed tomography (LDCT), a widely used method for early detection of lung cancer, cannot accurately distinguish between malignant and benign lung nodules. Many studies have shown that HTS technology can detect specific mutations strongly associated with lung cancer in ctDNA extracted from body fluid samples[39-41]. Sumitra et al. identified tumor-related alterations in 94% of patients with limited-stage small cell lung cancer (LS-SCLC) and 100% of patients with extensive-stage small cell lung cancer (ES-SCLC) by performing targeted ctDNA sequencing and whole genome sequencing on their body fluid samples. This study demonstrates that targeted ctDNA sequencing can identify potential treatment targets in more than half of the patients and shows advantages over traditional invasive biopsy [42].

Additionally, Peng *et al.* have developed a method to determine whether a lung tumor can be surgically removed by performing ultra-deep sequencing on the targeted mutations in ctDNA. Moreover, the accuracy of ctDNA testing is 63%, 83%, 94%, and 100% for stages I, II, III, and IV lung cancer, respectively. The overall sensitivity comes to 80%, considering age and serum biomarker tests, and the specificity rises to 99% [43]. This body-fluid-based screening can reduce the risk of unwanted damage and metastasis and assess the tumor progression by analyzing tumor mutation load.

Based on previously mentioned evidence, it can be concluded that HTS technology is also widely used to diagnose other types of tumors. Himisha et al. have discovered that the genome characterization of castration-resistant neuroendocrine prostate cancer (CRPC-NE) can be identified by analyzing ctDNA in patients' plasma samples. This reduces the trauma associated with traditional invasive pathological biopsies and provides timely guidance for clinical adjustment of medication [44]. Cai et al. developed a genetic diagnosis model based on whole-genome analysis of 5-hydroxymethylcytosine (5hmC) obtained from cfDNA samples of 2,554 individuals. The model demonstrated superior diagnostic performance to AFP and could distinguish between early-stage hepatocellular carcinoma (HCC) and non-HCC with an AUC of 0.884 in the

validation set [45]. In addition, Yurika et al. found that the methylated SEPT9 gene in serum ctDNA was highly significant in the early diagnosis of HCC with both high sensitivity and specificity[46]. However, it should be noted that although HTS-based body fluid biopsy technology provides a new direction for tumor diagnosis, most of the test results still need to be combined with other imaging or serological indicators and cannot be used independently as a diagnostic gold standard.

Furthermore, it is necessary to validate the test in a larger population. In addition, the lack of research on related gene test chips has severely limited its application scope. However, this problem can likely be solved with the development of technology and the related industrial chain.

Treatment for tumors

It is important to note that low-frequency mutations can occur during the division of tumor cells. Therefore, tumor cells can carry different genetic mutations even if they appear histologically similar, while different tumor cells can carry the same mutations. By comparing the gene sequences of primary and metastatic neoplasms, physicians can assess the effectiveness of their treatment and develop personalized therapies. They also gain insight into the potential mechanisms behind tumor drug resistance, laying a solid foundation for accurate diagnosis and treatment of tumors.

Targeted therapy

Today, several signalling pathways and associated mutations associated with tumor formation have become effective drug targets. As a result, targeted therapies based on tumor genes have become mainstream. As the most common BRAF mutation, the V600E mutation is strongly associated with the particular invasiveness of rectal cancer cells in metastatic colorectal cancer cases. Resistance to chemotherapy has been observed in cases with V600E mutations, and resistance to EGFR inhibitors is gradually increasing. Scott et al. demonstrated that using NGS technology, the concomitant use of EGFR and BRAF inhibitors in combination with irinotecan was effective in patients with the V600E mutation. The discovery informed the development of new targeted therapeutic regimens and laid a solid foundation for new targeted therapies [47].

Dasatinib is a small-molecule tyrosine kinase inhibitor that can be used as a first- and second-line treatment for gastrointestinal mesenchymal tumors (GIST). Zhou et al. found that dasatinib can be employed as a preferred treatment option for patients with wild-type GIST or GIST with the D842V mutation who are unable to take regorafenib, as they identified genetic variations related to the tumor signalling pathway by NGS technology [48]. Christian et al. investigated the clinical efficacy of the combination of ibrutinib, rituximab and high-dose methotrexate (HDMTX) in central nervous system lymphoma (CNSL). The results proved that the combination is safe and effective. In addition, the analysis of ctDNA in cerebrospinal fluid samples enables researchers to monitor disease progression in patients with CNSL and to adjust targeted therapy [49] promptly. In recent years, site-specific therapies (including HTS-guided targeted therapies) emerged as a promising option for patients with metastatic cancer of unknown primary site (CUP). A phase 2 clinical trial conducted at 19 institutions in Japan by Hidetoshi et al. demonstrated that CUP site-specific therapy based on NGS technology had favorable survival outcomes.

Moreover, targeted therapy based on the tumor-associated mutations showed excellent therapeutic responses, even in patients with CUP [50]. In conclusion, NGS technology can provide a reference for clinical drug selection and efficacy evaluation by detecting target genes and other tumor-related genes, which has great potential in pursuing individualized treatment today. Nevertheless, it is essential to acknowledge the current limitations of the evidence base, primarily de-

rived from small, single-ethnic clinical trials. When the mutation type is considered rare, the subjective decision to administer chemotherapy over targeted therapies in the clinic may also affect the study results.

Chemotherapy

Chemotherapy has consistently been the focus of research. as one of the leading traditional means of treating tumors. In addition, gene sequencing technologies, represented by HTS technology, have undoubtedly facilitated the chemotherapy of tumors. Most patients diagnosed with triple-negative breast cancer (TNBC) receive neoadjuvant chemotherapy. Approximately one-third of them can achieve complete pathological remission with neoadjuvant chemotherapy, but two-thirds will have residual disease and a high risk of recurrence. Milan et al. conducted ctDNA sequencing using HTS technology in 196 early-stage TNBC patients with residual disease after neoadjuvant chemotherapy and circulated tumor cell (CTC) analysis in 123 patients. The results showed that the presence of ctDNA and CTC in early-stage TNBC patients after neoadjuvant chemotherapy was associated with distant tumor metastasis. The detection of ctDNA and CTC in early-stage TNBC patients after neoadjuvant chemotherapy was found to be independently associated with disease recurrence and serve as an important indicator for assessing patient status after future neoadjuvant chemotherapy [51]. Colorectal cancer is one of the most common tumors worldwide, with surgical resection, chemotherapy, radiotherapy, and targeted therapy representing the principal treatment modalities. Resistance to chemotherapy drugs in some tumor patients has also posed a significant challenge for clinicians. Li et al. from Peking University combined the i-CR platform with HTS technology to construct a new in vitro tumor model, enabling personalized drug testing and personalized treatment for patients within 2-3 weeks and providing an entirely new treatment option for colorectal cancer [52].

Osteosarcoma is one of the malignant tumors for which early and effective preoperative chemotherapy is crucial to the survival of patients. However, the previous combination of methotrexate (MTX), doxorubicin (DOX), and cisplatin (DDP) has been found to have significant differences in therapeutic efficacy among patients, with a higher incidence of adverse effects. Thus, there is an urgent need to develop new drug combinations. Zhang et al. from Central South University revealed the heterogeneity of potential therapeutic target genes. They elucidated the synergistic mechanism of DOX and HDACs inhibitors for treating osteosarcoma through RNA sequencing and second-generation sequencing (HTS) of osteosarcoma samples. This provides a foundation for developing entirely new chemotherapeutic drug combinations and will undoubtedly inspire the subsequent researchers [53]. Researchers can also develop effective chemotherapy sensitizers by studying drug-resistance genes and resistance mechanisms. A team of researchers has already demonstrated that SMOi inhibitors can release the drug resistance of breast cancer tumor cells and improve their chemosensitivity to doxorubicin by studying the resistance mechanism in breast cancer dependent on the Hh signalling pathway [54]. Based on sequencing relevant tissue or body fluid samples from patients using HTS technology, physicians can comprehensively assess the expected therapeutic effects before chemotherapy to appropriately risk-stratify patients in a clinical setting. However, it is important to consider whether the relevant experimental results exclude potential interactions with other types of treatment given after chemotherapy, and another vital influence is the duration of follow-up, as a short follow-up period may lead to biased experimental data. In conclusion, further clinical studies of NGS results are required before they can be relied upon as a risk assessment tool.

Radiotherapy

Radiotherapy is an effective and cost-efficient treatment. In recent years, with the continuous improvement of radiotherapy equipment and technology, the cure rate of radiotherapy has increased, with the side effects gradually decreasing. While genetic therapies are gradually replacing chemotherapy and targeted therapy, radiotherapy remains an important treatment option. However, based on the patient's sensitivity to radiotherapy, HTS technology can still guide the use of radiotherapy. In a recent study, Raffaello et al. statistically employed HTS technology to investigate the relationship between ctDNA and tumor regression grade (TRG) of surgical specimens in 25 consecutive patients with locally advanced colorectal cancer (LARC) who had undergone long-term neoadjuvant chemo-radiotherapy (Na-ChRT). The results showed that the side effects of Na-ChRT were significantly associated with positive liquid biopsies on the day of surgery. This suggests that ctDNA assessment using HTS technology may identify LARC patients with a poor response to NA-ChRT to avoid potentially ineffective treatment [55].

Radiotherapy is one of the critical tools in treating lymphoma, which can improve the therapeutic effect and alleviate the symptoms. However, some patients still experience relapse or a poor prognosis due to resistance to radiotherapy. Luo *et al.* employed CRISPR to construct an activated cell line library, screened for radiotherapy-resistant cells and performed HTS and bioinformatics analyses to identify genes associated with radiotherapy resistance. Sixteen of the screened genes were identified as potential genes associated with lymphoma radiotherapy resistance. These genes are not only expected to be used as potential biomarkers or new targets for therapy but have also demonstrated the advantages of HTS technology in potential target screening [56]. The assessment of the overall condition and prognosis of patients after radiotherapy is another crucial part of the treatment, and it has been a hot topic of research in recent years to indirectly assess the prognosis of patients by monitoring the relevant genes in their peripheral blood-free DNA (cfDNA) using NGS technology. Jae et al. found the value of HPV cfDNA in evaluating treatment response by dynamically monitoring the cfDNA of cervical cancer patients using targeted HTS. They found that HPV cfDNA is valuable for monitoring and predicting treatment response, providing new insights for management and evaluation after radiotherapy [57].

Radiotherapy is an effective cancer treatment, but it still inevitably has some side effects. Most patients tolerate and respond well to radiotherapy after surgery for early-stage breast cancer. However, a proportion of long-term survivors still develop radiotherapy-related complications, with subcutaneous fibrosis and capillary dilatation being the most common cutaneous complications of radiotherapy for breast cancer. In order to identify their susceptibility genes and genotoxicity, Sarah et al. performed targeted HTS on germline DNA samples from 48 breast cancer patients with extreme late-stage cutaneous toxicity phenotypes and identified a total of five single-nucleotide variants in three genes (TP53, ERCC2, and LIG1) with possible effects. This discovery can provide a possible way for radiotherapy to avoid patients susceptible to the side effects and serious consequences of inappropriate radiotherapy58 and promote the development of individualized medication. HTS technology accelerates the discovery of radiotherapy-resistant genes, effectively avoiding ineffective radiotherapy and significantly improving the effectiveness of treatments. However, there are fewer studies on applying HTS to radiotherapy complications, and radiotherapy is mainly used as an adjuvant treatment. Therefore, the influence of chemotherapy or targeted therapy cannot be excluded from the research, and its application as a risk assessment tool still needs to be further explored.

Tumor prognosis

Currently, following surgical intervention and related treatments, tumor patients need to be assessed for treatment and monitored for tumor recurrence through regular serum tumor marker tests and conventional imaging tests. If tumor recurrence can be anticipated at an earlier stage than the traditional examinations, early interventions can be carried out, thus prolonging the survival time of patients. Remaining tiny tumor foci after surgery or radiotherapy treatment are important factors affecting patients' prognosis, but it is more difficult to detect their presence by traditional imaging and serology screening. Fortunately, ctDNA detection based on HTS technology can provide a new idea to solve this problem. Based on this, Jeanne et al. performed ctDNA analysis on stage III colon cancer patients who had undergone chemotherapy and surgery and found that ctDNA analysis in patients undergoing surgery can serve as a marker of prognosis.

In contrast, ctDNA analysis in chemotherapeutic patients could screen out patients who have completed the standard therapy but are still at high risk of recurrence [59]. HTS technology, as an emerging test method, has advantages over traditional serological and imaging tests. Ma et al. assessed ctDNA in breast cancer patients using NGS technology while using the molecular tumor burden index (mTBI) in the samples to monitor tumor burden and found that it may have a higher sensitivity in indicating disease progression and distant metastasis than CT imaging [60].

Although most patients with advanced tumors have lost the opportunity for radical surgical treatment, appropriate radiotherapy or interventional therapy, as well as an assessment of prognosis, are still necessary. By sequencing the RAS gene in ctDNA from 47 plasma samples from 37 patients with RAS-mutated colorectal cancer (CRC) with unresectable metastases, Elena *et al.* found that the RAS-mutated allele score had an independent prognostic value for CRC survival and could be used as a non-invasive decision-making tool in first-line treatment for cancer [61]. Zhao et al. performed targeted capture sequencing on 1,021 genes frequently mutated in unresectable primary HCC cases. The results showed that ctDNA abundance correlated more closely with tumor size than AFP levels. It was also associated with the Barcelona Clinic Liver Cancer (BCLC) staging system. Dynamic changes of ctDNA showed consistent or higher sensitivity compared with imaging in assessing the response to interventions and a high degree of consistency with tumor mutational load of tissue and blood samples [62].

As a focus in the realm, immunotherapies represented by immune-checkpoint inhibitor therapies have revolutionized the treatment of late-stage solid tumors. Immune checkpoint inhibitors and the immunotherapy they represent have revolutionized the treatment of advanced solid tumors as a hotspot in cancer therapy. Valsamo et al. analyzed the clonal dynamics of ctDNA and tumor exogenous TCR parameters during immune checkpoint blockade in non-small cell lung cancer (NSCLC) employing the NGS technology. They assessed the value of liquid biopsy monitoring as a surrogate indicator of treatment response. The research results indicate that ctDNA testing after treatment can enable patients with immune checkpoint blockages and primary drug resistance to be quickly identified for alternative treatment [63].

Because of the side effects and drug resistance that immunotherapy can cause, only a small proportion of patients can benefit from it in the long term, and it is particularly important to provide the necessary monitoring throughout the process[64]. By measuring ctDNA levels and dynamic changes using HTS technology, the prognosis and outcome of immunotherapy can be predicted both before and during treatment to avoid the trauma and misinterpretation that traditional monitoring can cause. How-

ever, it should be noted that monitoring tumors after treatment is a long-term process, and there is still room for improvement in terms of price and variety compared to traditional means. Before HTS can be promoted and applied as a decision-making tool, it is still necessary to carry out comparative experiments on a large scale with traditional means of detection in order to further prove its reliability.

CONCLUSION

As a high-throughput detection technology, HTS can still be applied to large-scale genetic or genomic testing, thus providing a powerful tool for researching the mechanisms of tumor genesis and clinical diagnosis and treatment. As sequencing technology continues to evolve, it is anticipated that the goal of routine screening, prevention, diagnosis, treatment and prognosis of tumors will be achieved through this technology.

ACKNOWLEDGMENTS

The authors thank all the Department of Clinical Laboratory colleagues for their comments on earlier versions of this manuscript.

Funding

This study received funding from the Major Project of Humanities and Social Sciences Research in Anhui Universities (grant no. SK2021ZD0032) and Key Project of Natural Science Research of Higher Education Institutions in Anhui Province (Grant No. 2024AH050739).

Availability of data and materials

Not applicable.

Author's ORCID numbers

- Chonghe Xu (CX): 0009-0001-1377-6946
- Dangui Zhou (DZ): 0000-0003-2805-3553
- Mei Zhu (MZ): 0000-0003-3130-3672

Authors' contributions

CX and DZ wrote the original draft and edited and critically revised the manuscript. MZ substantially contributed to the conception and revision of the work.. All authors read and approved the final manuscript.

Ethics approval and consent to participate

Not applicable.

Patient consent for publication

Not applicable.

Competing interests

The authors have declared that no competing interest exists.

REFERENCES

1. **Siddiqui H, Nederbragt AJ, Lagesen K, Jeansson SL, Jakobsen KS.** Assessing diversity of the female urine microbiota by high throughput sequencing of 16S rDNA amplicons. BMC Microbiol 2011;11:244.
2. **Xiao H, Xiao H, Zhang Y, Guo L, Dou Z, Liu L, Zhu L, Feng W, Liu B, Hu B, Chen T, Liu G, Wen T.** High-throughput sequencing unravels the cell heterogeneity of cerebrospinal fluid in the bacterial meningitis of children. Front Immunol 2022;13:872832.
3. **Novakovic S, Tsui V, Semple T, Martelotto L, McCarthy DJ, Crismani W.** SSNIP-seq: A simple and rapid method for isolation of single-sperm nucleic acid for high-throughput sequencing. PLoS One 2022;17(9):e0275168.
4. **Huang H, Yao T, Wu W, Zhai C, Guan T, Song Y, Sun Y, Xiao C, Liang P, Chen L.** Specific microbes of saliva and vaginal

fluid of Guangdong Han females based on 16S rDNA high-throughput sequencing. Int J Legal Med 2019;133(3):699-710.

5. **Wang P, Wang J, Wang L, Lv J, Shao Y, He D.** High throughput sequencing technology reveals alteration of lower respiratory tract microbiome in severe aspiration pneumonia and its association with inflammation. Infect Genet Evol 2023;116:105533.
6. **Jiang C, Hou X, Gao X, Liu P, Guo X, Hu G, Li Q, Huang C, Li G, Fang W, Mai W, Wu C, Xu Z, Liu P.** The 16S rDNA high-throughput sequencing correlation analysis of milk and gut microbial communities in mastitis Holstein cows. BMC Microbiol 2023;23(1):180.
7. **Li D, Gao G, Li Z, Sun W, Li X, Chen N, Sun J, Yang Y.** Profiling the T-cell receptor repertoire of patient with pleural tuberculosis by high-throughput sequencing. Immunol Lett 2014;162(1 Pt A):170-180.
8. **Yang Y, Muzny DM, Reid JG, Bainbridge MN, Willis A, Ward PA, Braxton A, Beuten J, Xia F, Niu Z, Hardison M, Person R, Bekheirnia MR, Leduc MS, Kirby A, Pham P, Scull J, Wang M, Ding Y, Plon SE, Lupski JR, Beaudet AL, Gibbs RA, Eng CM.** Clinical whole-exome sequencing for the diagnosis of mendelian disorders. N Engl J Med 2013;369(16):1502-1511.
9. **Sun X, Liu X, Zhao Y, Tian G, Wang W.** Detection of Circulating Tumor DNA in Plasma Using Targeted Sequencing. Methods Mol Biol 2023;2695:27-46.
10. **Szász I, Kiss T, Mokánszki A, Koroknai V, Deák J, Patel V, Jámbor K, Ádány R, Balázs M.** Identification of liquid biopsy-based mutations in colorectal cancer by targeted sequencing assays. Mol Cell Probes 2023;67:101888.
11. **Sanger F, Coulson AR.** A rapid method for determining sequences in DNA by primed synthesis with DNA polymerase. J Mol Biol 1975;94(3):441-448.
12. **Park SJ, Saito-Adachi M, Komiyama Y, Nakai K.** Advances, practice, and clinical perspectives in high-throughput sequencing. Oral Dis 2016 Jul;22(5):353-64.
13. **Levy SE, Boone BE.** Next-Generation Sequencing Strategies. Cold Spring Harb Perspect Med 2019;9(7):a025791.
14. **Pareek CS, Smoczynski R, Tretyn A.** Sequencing technologies and genome sequencing. J Appl Genet 2011;52(4):413-435.
15. **Reuter JA, Spacek DV, Snyder MP.** High-throughput sequencing technologies. Mol Cell 2015;58(4):586-597.
16. **Soon WW, Hariharan M, Snyder MP.** High-throughput sequencing for biology and medicine. Mol Syst Biol 2013;9:640.
17. **Slatko BE, Gardner AF, Ausubel FM.** Overview of Next-Generation Sequencing Technologies. Curr Protoc Mol Biol 2018;122(1):e59.
18. **Ronaghi M, Karamohamed S, Pettersson B, Uhlén M, Nyrén P.** Real-time DNA sequencing using detection of pyrophosphate release. Anal Biochem 1996;242(1):84-89.
19. **Churko JM, Mantalas GL, Snyder MP, Wu JC.** Overview of high throughput sequencing technologies to elucidate molecular pathways in cardiovascular diseases. Circ Res 2013;112(12):1613-1623.
20. **Komarova N, Barkova D, Kuznetsov A.** Implementation of High-Throughput Sequencing (HTS) in Aptamer Selection Technology. Int J Mol Sci 2020;21(22):8774.
21. **Fedurco M, Romieu A, Williams S, Lawrence I, Turcatti G.** BTA, a novel reagent for DNA attachment on glass and efficient generation of solid-phase amplified DNA colonies. Nucleic Acids Res 2006;34(3):e22.
22. **Pereira R, Oliveira J, Sousa M.** Bioinformatics and computational tools for Next-generation sequencing analysis in clinical genetics. J Clin Med 2020;9(1):132.
23. **Goldfeder RL, Wall DP, Khoury MJ, Ioannidis JPA, Ashley EA.** Human genome sequencing at the population scale: a primer on high-throughput DNA sequencing and analysis. Am J Epidemiol 2017;186(8):1000-1009.
24. **Wu H, Irizarry RA, Bravo HC.** Intensity normalization improves color calling in SOLiD sequencing. Nat Methods 2010;7(5):336-337.

25. **Mardis ER.** Next-generation DNA sequencing methods. Annu Rev Genomics Hum Genet 2008;9:387-402.
26. **Mardis ER.** The impact of next-generation sequencing technology on genetics. Trends Genet 2008;24(3):133-141.
27. **Ambardar S, Gupta R, Trakroo D, Lal R, Vakhlu J.** High Throughput Sequencing: an overview of sequencing chemistry. Indian J Microbiol 2016 ;56(4):394-404.
28. **Shendure J, Ji H.** Next-generation DNA sequencing. Nat Biotechnol 2008; 26(10): 1135-1145.
29. **Rothberg JM, Hinz W, Rearick TM, Schultz J, Mileski W, Davey M, Leamon JH, Johnson K, Milgrew MJ, Edwards M, Hoon J, Simons JF, Marran D, Myers JW, Davidson JF, Branting A, Nobile JR, Puc BP, Light D, Clark TA, Huber M, Branciforte JT, Stoner IB, Cawley SE, Lyons M, Fu Y, Homer N, Sedova M, Miao X, Reed B, Sabina J, Feierstein E, Schorn M, Alanjary M, Dimalanta E, Dressman D, Kasinskas R, Sokolsky T, Fidanza JA, Namsaraev E, McKernan KJ, Williams A, Roth GT, Bustillo J.** An integrated semiconductor device enabling non-optical genome sequencing. Nature 2011;475(7356):348-352.
30. **Quail MA, Smith M, Coupland P, Otto TD, Harris SR, Connor TR, Bertoni A, Swerdlow HP, Gu Y.** A tale of three next generation sequencing platforms: comparison of Ion Torrent, Pacific Biosciences and Illumina MiSeq sequencers. BMC Genomics 2012;13:341.
31. **McCarthy A.** Third generation DNA sequencing: pacific biosciences' single molecule real time technology. Chem Biol 2010;17(7):675-676.
32. **Athanasopoulou K, Boti MA, Adamopoulos PG, Skourou PC, Scorilas A.** Third-generation sequencing: the spearhead towards the radical transformation of modern genomics. Life (Basel). 2021;12(1):30.
33. **Wang Y, Zhao Y, Bollas A, Wang Y, Au KF.** Nanopore sequencing technology, bioinformatics and applications. Nat Biotechnol 2021;39(11):1348-1365.
34. **Akaçin İ, Ersoy Ş, Doluca O, Güngörmüşler M.** Comparing the significance of the utilization of next generation and third generation sequencing technologies in microbial metagenomics. Microbiol Res 2022;264:127154.
35. **Petersen LM, Martin IW, Moschetti WE, Kershaw CM, Tsongalis GJ.** Third-generation sequencing in the clinical laboratory: exploring the advantages and challenges of Nanopore Sequencing. J Clin Microbiol 2019;58(1):e01315-1319.
36. **Ozsolak F.** Third-generation sequencing techniques and applications to drug discovery. Expert Opin Drug Discov 2012;7(3):231-243.
37. **Liu L, Li Y, Li S, Hu N, He Y, Pong R, Lin D, Lu L, Law M.** Comparison of next-generation sequencing systems. J Biomed Biotechnol 2012;2012:251364.
38. **Bettegowda C, Sausen M, Leary RJ, Kinde I, Wang Y, Agrawal N, Bartlett BR, Wang H, Luber B, Alani RM, Antonarakis ES, Azad NS, Bardelli A, Brem H, Cameron JL, Lee CC, Fecher LA, Gallia GL, Gibbs P, Le D, Giuntoli RL, Goggins M, Hogarty MD, Holdhoff M, Hong SM, Jiao Y, Juhl HH, Kim JJ, Siravegna G, Laheru DA, Lauricella C, Lim M, Lipson EJ, Marie SK, Netto GJ, Oliner KS, Olivi A, Olsson L, Riggins GJ, Sartore-Bianchi A, Schmidt K, Shih lM, Oba-Shinjo SM, Siena S, Theodorescu D, Tie J, Harkins TT, Veronese S, Wang TL, Weingart JD, Wolfgang CL, Wood LD, Xing D, Hruban RH, Wu J, Allen PJ, Schmidt CM, Choti MA, Velculescu VE, Kinzler KW, Vogelstein B, Papadopoulos N, Diaz LA Jr.** Detection of circulating tumor DNA in early- and late-stage human malignancies. Sci Transl Med 2014;6(224):224ra24.
39. **Taylor C, Chacko S, Davey M, Lacroix J, MacPherson A, Finn N, Wajnberg G, Ghosh A, Crapoulet N, Lewis SM, Ouellette RJ.** Peptide-affinity precipitation of extracellular vesicles and cell-free DNA improves sequencing performance for the detection of pathogenic mutations in lung cancer patient plasma. Int J Mol Sci 2020;21(23):9083.
40. **Govind KB, Koppaka D, Dasappa L, Jacob LA, C Babu SM, Lokesh NK, Haleshappa**

RA, Rajeev LK, Saldanha SC, Abhishek A, Asati V, Chethan R, Ramprasad VL. Detection of clinically relevant epidermal growth factor receptor pathway mutations in circulating cell-free tumor DNA using next generation sequencing in squamous cell carcinoma lung. South Asian J Cancer 2019;8(4):247-249.

41. **Yamamoto G, Kikuchi M, Kobayashi S, Arai Y, Fujiyoshi K, Wakatsuki T, Kakuta M, Yamane Y, Iijima Y, Mizutani H, Nakajima Y, Sudo J, Kinoshita H, Kurimoto F, Akiyama H, Uramoto H, Sakai H, Akagi Y, Akagi K.** Routine genetic testing of lung cancer specimens derived from surgery, bronchoscopy and fluid aspiration by next generation sequencing. Int J Oncol 2017;50(5):1579-1589.
42. **Mohan S, Foy V, Ayub M, Leong HS, Schofield P, Sahoo S, Descamps T, Kilerci B, Smith NK, Carter M, Priest L, Zhou C, Carr TH, Miller C, Faivre-Finn C, Blackhall F, Rothwell DG, Dive C, Brady G.** Profiling of circulating free DNA using targeted and genome-wide sequencing in patients with SCLC. J Thorac Oncol 2020;15(2):216-230.
43. **Peng M, Xie Y, Li X, Qian Y, Tu X, Yao X, Cheng F, Xu F, Kong D, He B, Liu C, Cao F, Yang H, Yu F, Xu C, Tian G.** Resectable lung lesions malignancy assessment and cancer detection by ultra-deep sequencing of targeted gene mutations in plasma cell-free DNA. J Med Genet 2019;56(10):647-653.
44. **Beltran H, Romanel A, Conteduca V, Casiraghi N, Sigouros M, Franceschini GM, Orlando F, Fedrizzi T, Ku SY, Dann E, Alonso A, Mosquera JM, Sboner A, Xiang J, Elemento O, Nanus DM, Tagawa ST, Benelli M, Demichelis F.** Circulating tumor DNA profile recognizes transformation to castration-resistant neuroendocrine prostate cancer. J Clin Invest 2020;130(4):1653-1668.
45. **Cai J, Chen L, Zhang Z, Zhang X, Lu X, Liu W, Shi G, Ge Y, Gao P, Yang Y, Ke A, Xiao L, Dong R, Zhu Y, Yang X, Wang J, Zhu T, Yang D, Huang X, Sui C, Qiu S, Shen F, Sun H, Zhou W, Zhou J, Nie J, Zeng C, Stroup EK, Zhang X, Chiu BC, Lau WY, He C, Wang H, Zhang W, Fan J.** Genome-wide mapping of 5-hydroxymethylcytosines in circulating cell-free DNA as a non-invasive approach for early detection of hepatocellular carcinoma. Gut 2019;68(12):2195-2205.
46. **Kotoh Y, Suehiro Y, Saeki I, Hoshida T, Maeda M, Iwamoto T, Matsumoto T, Hidaka I, Ishikawa T, Takami T, Higaki S, Fujii I, Suzuki C, Shindo Y, Tokumitsu Y, Nagano H, Sakaida I, Yamasaki T.** Novel liquid biopsy test based on a sensitive methylated SEPT9 assay for diagnosing hepatocellular carcinoma. Hepatol Commun 2020;4(3):461-470.
47. **Kopetz S, Guthrie KA, Morris VK, Lenz HJ, Magliocco AM, Maru D, Yan Y, Lanman R, Manyam G, Hong DS, Sorokin A, Atreya CE, Diaz LA, Allegra C, Raghav KP, Wang SE, Lieu CH, McDonough SL, Philip PA, Hochster HS.** Randomized trial of irinotecan and cetuximab with or without vemurafenib in BRAF-Mutant metastatic colorectal cancer (SWOG S1406). J Clin Oncol 2021;39(4):285-294.
48. **Zhou Y, Zhang X, Wu X, Zhou Y, Zhang B, Liu X, Wu X, Li Y, Shen L, Li J.** A prospective multicenter phase II study on the efficacy and safety of dasatinib in the treatment of metastatic gastrointestinal stromal tumors failed by imatinib and sunitinib and analysis of NGS in peripheral blood. Cancer Med 2020;9(17):6225-6233.
49. **Grommes C, Tang SS, Wolfe J, Kaley TJ, Daras M, Pentsova EI, Piotrowski AF, Stone J, Lin A, Nolan CP, Manne M, Codega P, Campos C, Viale A, Thomas AA, Berger MF, Hatzoglou V, Reiner AS, Panageas KS, DeAngelis LM, Mellinghoff IK.** Phase 1b trial of an ibrutinib-based combination therapy in recurrent/refractory CNS lymphoma. Blood 2019 ;133(5):436-445.
50. **Hayashi H, Takiguchi Y, Minami H, Akiyoshi K, Segawa Y, Ueda H, Iwamoto Y, Kondoh C, Matsumoto K, Takahashi S, Yasui H, Sawa T, Onozawa Y, Chiba Y, Togashi Y, Fujita Y, Sakai K, Tomida S, Nishio K, Nakagawa K.** Site-specific and targeted

therapy based on molecular profiling by Next-Generation Sequencing for cancer of unknown primary site: a nonrandomized Phase 2 Clinical Trial. JAMA Oncol 2020;6(12):1931-1938.

51. **Radovich M, Jiang G, Hancock BA, Chitambar C, Nanda R, Falkson C, Lynce FC, Gallagher C, Isaacs C, Blaya M, Paplomata E, Walling R, Daily K, Mahtani R, Thompson MA, Graham R, Cooper ME, Pavlick DC, Albacker LA, Gregg J, Solzak JP, Chen YH, Bales CL, Cantor E, Shen F, Storniolo AMV, Badve S, Ballinger TJ, Chang CL, Zhong Y, Savran C, Miller KD, Schneider BP.** Association of Circulating Tumor DNA and Circulating Tumor Cells after neoadjuvant chemotherapy with disease recurrence in patients with Triple-Negative Breast Cancer: preplanned secondary analysis of the BRE12-158 randomized clinical trial. JAMA Oncol 2020;6(9):1410-1415.
52. **Li Y, Guo D, Zhang Y, Wang L, Sun T, Li Z, Zhang X, Wang S, Chen Y, Wu A.** Rapid screening for individualized chemotherapy optimization of colorectal cancer: A novel conditional reprogramming technology-based functional diagnostic assay. Transl Oncol 2021;14(1):100935.
53. **Zhang W, Qi L, Liu Z, He S, Wang CZ, Wu Y, Han L, Liu Z, Fu Z, Tu C, Li Z.** Integrated multiomic analysis and high-throughput screening reveal potential gene targets and synergetic drug combinations for osteosarcoma therapy. MedComm (2020) 2023;4(4):e317.
54. **Cazet AS, Hui MN, Elsworth BL, Wu SZ, Roden D, Chan CL, Skhinas JN, Collot R, Yang J, Harvey K, Johan MZ, Cooper C, Nair R, Herrmann D, McFarland A, Deng N, Ruiz-Borrego M, Rojo F, Trigo JM, Bezares S, Caballero R, Lim E, Timpson P, O'Toole S, Watkins DN, Cox TR, Samuel MS, Martín M, Swarbrick A.** Targeting stromal remodeling and cancer stem cell plasticity overcomes chemoresistance in triple negative breast cancer. Nat Commun 2018;9(1):2897.
55. **Roesel R, Epistolio S, Molinari F, Saletti P, De Dosso S, Valli M, Franzetti-Pellanda A, Deantonio L, Biggiogero M, Spina P, Popeskou SG, Cristaudi A, Mongelli F, Mazzucchelli L, Stefanini FM, Frattini M, Christoforidis D.** A pilot, prospective, observational study to investigate the value of NGS in liquid biopsies to predict tumor response after neoadjuvant chemo-radiotherapy in patients with locally advanced rectal cancer: The LiBReCa Study. Front Oncol 2022;12:900945.
56. **Luo BH, Huang JQ, Huang CY, Tian P, Chen AZ, Wu WH, Ma XM, Yuan YX, Yu L.** Screening of lymphoma radiotherapy-resistant genes with CRISPR Activation Library. Pharmgenomics Pers Med 2023;16:67-80.
57. **Kim JS, Yang S, Jeong K, Kim DY, Kim K, Kang HC.** Plasma cell-free DNA in uterine cervical cancer: therapeutic monitoring and prognostic values after radical radiotherapy. Cancer Res Treat 2023;55(2):659-670.
58. **Cargnin S, Barizzone N, Basagni C, Pisani C, Ferrara E, Masini L, D'Alfonso S, Krengli M, Terrazzino S.** Targeted Next-Generation Sequencing for the identification of genetic predictors of radiation-induced late skin toxicity in breast cancer patients: a preliminary study. J Pers Med 2021;11(10):967.
59. **Tie J, Cohen JD, Wang Y, Christie M, Simons K, Lee M, Wong R, Kosmider S, Ananda S, McKendrick J, Lee B, Cho JH, Faragher I, Jones IT, Ptak J, Schaeffer MJ, Silliman N, Dobbyn L, Li L, Tomasetti C, Papadopoulos N, Kinzler KW, Vogelstein B, Gibbs P.** Circulating Tumor DNA analyses as markers of recurrence risk and benefit of Adjuvant Therapy for Stage III Colon Cancer. JAMA Oncol 2019;5(12):1710-1717.
60. **Ma F, Guan Y, Yi Z, Chang L, Li Q, Chen S, Zhu W, Guan X, Li C, Qian H, Xia X, Yang L, Zhang J, Husain H, Liao Z, Futreal A, Huang J, Yi X, Xu B.** Assessing tumor heterogeneity using ctDNA to predict and monitor therapeutic response in metastatic breast cancer. Int J Cancer 2020;146(5):1359-1368.
61. **Elez E, Chianese C, Sanz-García E, Martinelli E, Noguerido A, Mancuso FM, Caratù G, Matito J, Grasselli J, Car-**

done C, Esposito Abate R, Martini G, Santos C, Macarulla T, Argilés G, Capdevila J, Garcia A, Mulet N, Maiello E, Normanno N, Jones F, Tabernero J, Ciardello F, Salazar R, Vivancos A. Impact of circulating tumor DNA mutant allele fraction on prognosis in RAS-mutant metastatic colorectal cancer. Mol Oncol 2019;13(9):1827-1835.

62. **Zhao W, Qiu L, Liu H, Xu Y, Zhan M, Zhang W, Xin Y, He X, Yang X, Bai J, Xiao J, Guan Y, Li Q, Chang L, Yi X, Li Y, Chen X, Lu L.** Circulating tumor DNA as a potential prognostic and predictive biomarker during interventional therapy of unresectable primary liver cancer. J Gastrointest Oncol 2020;11(5):1065-1077.
63. **Anagnostou V, Forde PM, White JR, Niknafs N, Hruban C, Naidoo J, Marrone K, Sivakumar IKA, Bruhm DC, Rosner S, Phallen J, Leal A, Adleff V, Smith KN, Cottrell TR, Rhymee L, Palsgrove DN, Hann CL, Levy B, Feliciano J, Georgiades C, Verde F, Illei P, Li QK, Gabrielson E, Brock MV, Isbell JM, Sauter JL, Taube J, Scharpf RB, Karchin R, Pardoll DM, Chaft JE, Hellmann MD, Brahmer JR, Velculescu VE.** Dynamics of tumor and immune responses during immune checkpoint blockade in Non-Small Cell Lung Cancer. Cancer Res 2019;79(6):1214-1225.
64. **Zhang Q, Luo J, Wu S, Si H, Gao C, Xu W, Abdullah SE, Higgs BW, Dennis PA, van der Heijden MS, Segal NH, Chaft JE, Hembrough T, Barrett JC, Hellmann MD.** Prognostic and predictive impact of Circulating Tumor DNA in patients with advanced cancers treated with immune checkpoint blockade. Cancer Discov 2020;10(12):1842-1853.

Índice de Autores Vol. 65, Nos. 1-4, 2024

	Págs.
Acosta C	169
Alarcón V	445
Altuner D	83
Alvarado P	294
Álvarez-Nava F	169
An Y	48
Argueta-Figueroa L	387
Balarezo T	169
Baptista T	470
Benítez-Cárdenas OA	454
Bracho V	294
Briceño-Pérez C	462
Bulut S	321
Cai J	5, 37
Cao Y	48
Castro B	462
Castro J	59
Cavallera E	294
Chávez E	169
Chen B	48
Chen F	16
Chen W	48
Coban TA	83
Colmenter LF	253
D´Angelo P	445
Daryanani S	253
de Leon J	470
Dong W	5
Du N	179
Duarte-Inguanzo S	369, 378
Duarte-López A	369, 378
Eblen-Zajjur A	418
Elma B	83
Emir I	220
Evia L	470
Fan N	426
Feria-Madueño A	192
Fernández A	59
Fernández-Lázaro D	230
García JM	445
Gasia J	59
Gil Y	59
GOT Study Group	462
Guanipa J	59
Guizar A	470
Gulaboglu M	321
Guo F	358
Guo L	99
Gutiérrez J	59
Han X	5
Hao J	134
He J	206
Hewett TE	192
Hou Y	426
Hu P	70
Huang L	143
Huang W	48
Hui J	308
Hung A	59
Hurtado O	462
Jaspe R	445
Jia Q	99
Koc Z	321
Kong C	346
Larreal Y	131
Lei M	267
Li G	99
Li L	436
Li Q	48
Li W	308

	Págs.
Li WJ	179
Li X	335
Li Y	5
Lin Li J	143
Lin N	27
Liu CN	179
Liu L	99
Liu S	267
Liu X	426
López-Hidalgo M	418
Loureiro C	445
Lu H	16
Lu N	358
Luengo-Fereira JA	369, 378
Luo C	335
Ma C	436
Ma J	335
Mammadov R	83, 321
Mar Uribe ER	454
Mariel Cárdenas J	454
Mo X	134
Mokhtare B	83
Molero A	109
Monsalve I	445
Mu J	134
Narváez K	169
Ni C	70
Ni Y	70
Núñez-Troconis J	109
Peña I	169
Pilataxi K	169
Pinto-Longart L	418
Poggioli I	418
Pujol FH	445
Qiu Z	37
Quintero González JA	403
Ramírez J	418
Rangel H	445
Regis E	418
Reigosa A	59
Reina J	418
Ríos R	462
Rivas-García JL	387
Rodríguez L	445
Ryder E	1, 265
Sanz B	230
Sañudo B	192
Seco-Calvo J	230
Shen L	16, 155
Shen X	267
Sheng Y	134
Shi C	267
Shi D	335
Silva-De Hoyos LE	387
Song D	279
Soucre N	294
Su C	267
Sulbarán Y	445
Suleyman B	83
Suleyman H	83, 220, 321
Suleyman Z	220
Sun L	436
Tastan TB	321
Torres Hernández EM	454
Torres-Gómez N	387
Unver E	83
Vargas R	131
Vilar J	253
Wang D	279
Wang L	426
Wang M	27
Wang T	426
Wang Y	179
Wang Z	206, 426
Wei L	206
Wu X J	143
Wu Y	426
Wu Z	279

	Págs.
Xia F	37
Xiao J	308
Xu C	476
Xu Q	279
Xu Y	155
Yang H	406
Yang L	27, 335
Yang S	16, 27
Yang Y	426
Yavuzer B	83
Ye M	143
Yeter B	321
Yong Yu C	143
Zambrano JL	445
Zambrano O	369, 378
Zhang G	206
Zhang J	308
Zhen X	134
Zheng X	99
Zhou D	476
Zhou R	267
Zhou S	206
Zhou X	48, 358
Zhu C	346
Zhu M	206, 476
Zúñiga S	253

Investigación Clínica
Vol. 65 Nº 4 / December 2024
Bilingual - Abstracts in Spanish and English

Contents

EDITORIAL

Sixty-fifth anniversary of the Instituto de Investigaciones Clínicas "Dr. Américo Negrette". Icon of science in Zulia.
Quintero J (*E-mail: jequin@gmail.com*) 403
https://doi.org/10.54817/IC.v65n4a00

ORIGINAL PAPERS

Rehabilitation training effect guided by cardiopulmonary fitness assessment on NT-proBNP levels in patients with chronic heart failure. (English)
Yang H (*E-mail: 13943475960@163.com*) 406
https://doi.org/10.54817/IC.v65n4a01

CHA_2DS_2-VASc score as a predictor of stroke severity in patients with atrial fibrillation. (Spanish)
Lopez-Hidalgo M (*E-mail: lopezh9oo@hotmail.com*), Pinto-Longart L, Eblen-Zajjur A, Regis E, Reina JD, Poggioli I, Ramírez JI. 418
https://doi.org/10.54817/IC.v65n4a02

Correlations of serum 25-hydroxy-vitamin D, $CD4^+CD25^+CD127^-$ regulatory T cells and total immunoglobulin E in children with recurrent respiratory tract infections. (English)
Yang Y, Fan N, Liu X, Wang L, Wang Z, Hou Y, Wang T, Wu Y (*E-mail: qudas0@163.com*) 426
https://doi.org/10.54817/IC.v65n4a03

Karyotype analysis of fetus in pregnant women with different indications for amniocentesis. (English)
Ma C, Sun L, Li L (*E-mail: lili_edu.suda@hotmail.com*) 436
https://doi.org/10.54817/IC.v65n4a04

Epidemiological and virological characterization of mpox cases in Venezuela during the multinational 2022-2023 outbreak. (English)
D´Angelo P, Loureiro CL, Jaspe RC, Sulbaran Y, Rodríguez L, Alarcón V, Monsalve I, García JM, Zambrano JL, Rangel HR, Pujol FH (*E-mail: fhpujol@gmail.com*) 445
https://doi.org/10.54817/IC.v65n4a05

CASE REPORT

Finding phleboliths in the oral region: Report of two cases. (Spanish)
Benítez- Cárdenas OA, Torres-Hernández EM, Mar-Uribe ER, Mariel-Cárdenas J. (*E-mail: llairo@yahoo.com.mx*). 454
https://doi.org/10.54817/IC.v65n4a06

Giant ovarian tumors: uncommon ovarian tumors. Report of four cases. (English)
Ríos R, Castro B, Hurtado O, Briceño-Pérez C (*E-mail: cabripe@hotmail.com*), and the GOT Study Group. 462
https://doi.org/10.54817/IC.v65n4a07

Severe necrotic colitis in an adolescent with polypharmacy and high clozapine doses according to his ancestry. (English)
Baptista T (*E-mail: trinobaptista@gmail.com*), de Leon J, Guizar A, Evia L 470
https://doi.org/10.54817/IC.v65n4a08

REVIEW

High throughput sequencing technology and its clinical application in circulating tumor DNA detection in patients with tumors. (English)
Xu C, Zhou D, Zhu M (*E-mail: zhumei@ahmu.edu.cn*) 476
https://doi.org/10.54817/IC.v65n4a09

AUTHOR INDEX. 495

Investigación Clínica
Vol. 65 Nº 4 /Diciembre 2024
Bilingüe - Resúmenes en Español e Inglés

Contenido

EDITORIAL

Sesenta y cinco aniversario del Instituto de Investigaciones Clínicas "Dr. Américo Negrette". Ícono de la ciencia en el Zulia.
Quintero J (*Correo electrónico: jequin@gmail.com*).. 403
https://doi.org/10.54817/IC.v65n4a00

TRABAJOS ORIGINALES

Efecto del entrenamiento de rehabilitación guiado por la evaluación de la aptitud cardiorrespiratoria en los niveles de NT-proBNP en pacientes con insuficiencia cardíaca crónica. (Inglés)
Yang H (*Correo electrónico: 13943475960@163.com*) 406
https://doi.org/10.54817/IC.v65n4a01

Escala CHA_2DS_2-VASc como predictor de severidad de ictus en pacientes con fibrilación auricular. (Español)
Lopez-Hidalgo M (*Correo electrónico: lopezh9oo@hotmail.com*), Pinto-Longart L, Eblen-Zajjur A, Regis E, Reina JD, Poggioli I, Ramírez JI 418
https://doi.org/10.54817/IC.v65n4a02

Las correlaciones séricas de 25-hidroxivitamina D, $CD4^+CD25^+CD127^-$ linfocitos T reguladores e inmunoglobulina E total en niños con infecciones recurrentes del tracto respiratorio. (Inglés)
Yang Y, Fan N, Liu X, Wang L, Wang Z, Hou Y, Wang T, Wu Y (*Correo electrónico: qudas0@163.com*) 426
https://doi.org/10.54817/IC.v65n4a03

Análisis del cariotipo fetal de embarazadas con diferentes indicaciones de amniocentesis. (Inglés)
Ma C, Sun L, Li L (*Correo electrónico: lili_edu.suda@hotmail.com*) 436
https://doi.org/10.54817/IC.v65n4a04

Caracterización epidemiológica y virológica de los casos de mpox en Venezuela durante el brote multinacional 2022-2023. (Inglés)
D´Angelo P, Loureiro CL, Jaspe RC, Sulbaran Y, Rodríguez L, Alarcón V, Monsalve I, García JM, Zambrano JL, Rangel HR, Pujol FH (*Correo electrónico: fhpujol@gmail.com*). . . . 445
https://doi.org/10.54817/IC.v65n4a05

REPORTE DE CASOS

Hallazgo de flebolitos en la región bucal: Reporte de dos casos. (Español)
Benítez-Cárdenas OA, Torres-Hernández EM, Mar-Uribe ER, Mariel-Cárdenas J (*Correo electrónico: llairo@yahoo.com.mx*) 454
https://doi.org/10.54817/IC.v65n4a06

Tumores gigantes de ovario: una rara serie de 4 casos. (Inglés)
Ríos R, Castro B, Hurtado O, Briceño-Pérez C (*Correo electrónico: cabripe@hotmail.com*), y el GOT Study Group. 462
https://doi.org/10.54817/IC.v65n4a07

Severa colitis necrotizante en un adolescente con polifarmacia y dosis elevada de clozapina con relación a su origen étnico. (Inglés)
Baptista T (*Correo electrónico: trinobaptista@gmail.com*), de Leon J, Guizar A, Evia L. 470
https://doi.org/10.54817/IC.v65n4a08

REVISIÓN

Tecnología de secuenciación de alto rendimiento y su aplicación clínica en la detección de ADN tumoral circulante en pacientes oncológicos. (Inglés)
Xu C, Zhou D, Zhu M (*Correo electrónico: zhumei@ahmu.edu.cn*) 476
https://doi.org/10.54817/IC.v65n4a09

ÍNDICE DE AUTORES. 495